UNIVERSITÀ DI SIENA 1240

Dipartimento di Medicina Molecolare e dello Sviluppo

Dottorato in Medicina Molecolare

36° Ciclo

Coordinatore: Prof. Vincenzo Sorrentino

DECODING THE TRANSCRIPTOME: GENE EXPRESSION PROFILES IN ACUTE ISCHEMIC STROKE PATIENTS

Settore scientifico disciplinare: PATOLOGIA CLINICA MED05

Candidata

Giulia Cassioli

Dipartimento di Medicina Sperimentale e clinica,
Università di Firenze

Supervisore

Prof.ssa Betti Giusti

Dipartimento di Medicina Sperimentale e clinica,
Università di Firenze

Co-supervisore

Dr.ssa Elena Sticchi

Dipartimento di Medicina Sperimentale e clinica,
Università di Firenze

Anno accademico di conseguimento del titolo di Dottore di ricerca

2022/2023

Università degli Studi di Siena
Dottorato in Medicina Molecolare
36° Ciclo

Data dell'esame finale
30 maggio 2024

Commissione giudicatrice

Prof.ssa Rossi Daniela

Dr.ssa Vitiello Marianna

Dr.ssa Sticchi Elena

Supplenti
Dr. Amato Rosario

INDEX

CHAPTER 1

ACUTE ISCHEMIC STROKE

Despite making up only 2% of our body weight, our brain is a powerhouse, consuming 20% of our body's energy supply. Its role as the control center is vital, orchestrating complex functions. To sustain this dynamic activity, the brain relies on an intricate network of blood vessels, pumping around 1,100 liters of blood daily, delivering approximately 75 liters of oxygen and 115 grams of sugar. Such demands underscore the critical nature of maintaining a constant and uninterrupted blood supply to the brain.

Strokes, for millennia, were enigmatic events with limited treatment options. Over 2,000 years ago, physicians described this condition in the Hippocratic Corpus, terming it apoplexia, denoting a sudden, violent blow. Treatment approaches were starkly pessimistic, with limited capacity to cure severe strokes and difficulty in treating milder cases. The understanding of strokes was trapped in a historical context where intervention was limited by the available knowledge and resources.

In the pre-seventeenth-century era, the understanding of medical conditions, including strokes, was heavily influenced by the ancient concept of humoral theory. According to this theory, the body's health was believed to be determined by the balance of four bodily fluids or humors: blood, yellow bile, black bile, and phlegm. Any imbalance in these humors was thought to lead to various illnesses, including strokes. This theory, rooted in antiquity, shaped medical thinking for centuries (Storey CE and Pols H, 2010).

The transformative shift in understanding strokes occurred in 1658 when Johann Jacob Wepfer, a pioneering physician practicing in Schaffhausen, Switzerland, conducted postmortem examinations on individuals who had succumbed to strokes. This marked a departure from the traditional humoral theory and laid the foundation for a more nuanced understanding of strokes. Wepfer's groundbreaking work led to the identification of two distinct forms of stroke that continue to be recognized in modern medicine. The majority, almost 85%, was attributed to what he termed an "ischemic insult." In this scenario, a blood clot forms and obstructs a vessel in the brain, resulting in the interruption of blood supply to specific areas of the organ. On the other hand, if the stroke is caused by bleeding within the brain, physicians now refer to it as a hemorrhagic stroke. In the pre-1800 era, strokes were shrouded in mystery, viewed through the lens of the ancient humoral theory. The transformative moment arrived in 1812, marking a seismic shift in the understanding of strokes. Prior to this juncture, strokes were essentially defined by the symptoms they presented. However, a new wave of thought, rooted in the Paris

School of Medicine, introduced a groundbreaking concept, the idea that strokes were not just a collection of symptoms but a result of morphological lesions in the brain.

Jean-André Rochoux, a young physician, played a pivotal role in this revolution. In his 1812 dissertation, he boldly proclaimed, “Apoplexy is a hemorrhage of the brain, by rupture, with more or less serious alteration of its substance.” This was a departure from centuries of symptom-centric definitions, heralding a new era where lesions took center stage. Rochoux's meticulous exposition not only marked a scientific revolution but also laid the foundation for the first modern definition of stroke (Sacco RL et al, 2013).

The 19th century witnessed the coalescence of ideas derived from the anatomico-clinical method. Rochoux's concept of hemorrhage found a counterpart in the idea proposed by another French physician, Léon Rostan, who suggested that strokes could result from the softening of the brain, akin to what we now term ischemic infarction (Sacco RL et al, 2013).

This period saw a refining of these fundamental concepts. Rudolf Virchow, in the mid-19th century, made noteworthy contributions by describing arterial thrombosis and embolism. These were pivotal moments that solidified the understanding of the interplay between blood and arterial walls, laying the groundwork for future advancements. As the 19th century progressed, medicine became inseparable from the natural sciences. A positivistic approach, emphasizing factual knowledge, guided the scientific community. Neurologists, in particular, made substantial contributions between 1850 and 1930, delving into vascular anatomy and clinical-anatomical correlations.

The mid-20th century marked the heyday of pathophysiology, with researchers like Charles Foix, Kapitoline Wolkoff, and Charles Miller-Fisher contributing significantly. This era was characterized by a deepening understanding of the physiological processes underlying vascular lesions and their implications for stroke.

From 1975 onwards, stroke research entered a diversified phase. Investigations expanded into risk factors, stroke registries, randomized trials, databases, and the pursuit of new treatments. This period witnessed the formal emergence of stroke medicine as a subspecialty within neurology.

Notably, the latter part of the 20th century saw unprecedented advancements in technology. Diagnostics, evolving from rudimentary hands-on spinal taps around 1900, burgeoned into sophisticated brain visualizations by the turn of the century. The pace of technological innovation

sometimes outstripped the capacity of doctors' minds to assimilate these rapid changes (Liyuan Pu, 2023).

In essence, the history of stroke is a narrative of evolution. It started with ancient beliefs and symptomatic definitions, transitioned through a revolutionary period that centered on lesions, and culminated in a specialized field within neurology. Each era contributed to the current depth of knowledge, with breakthroughs, refinements, and technological leaps forming the intricate tapestry of stroke medicine. The journey from ancient mysteries to a modern, specialized understanding is a testament to the persistent quest for knowledge and the transformative power of scientific revolutions.

1.1 STROKE EPIDEMIOLOGY

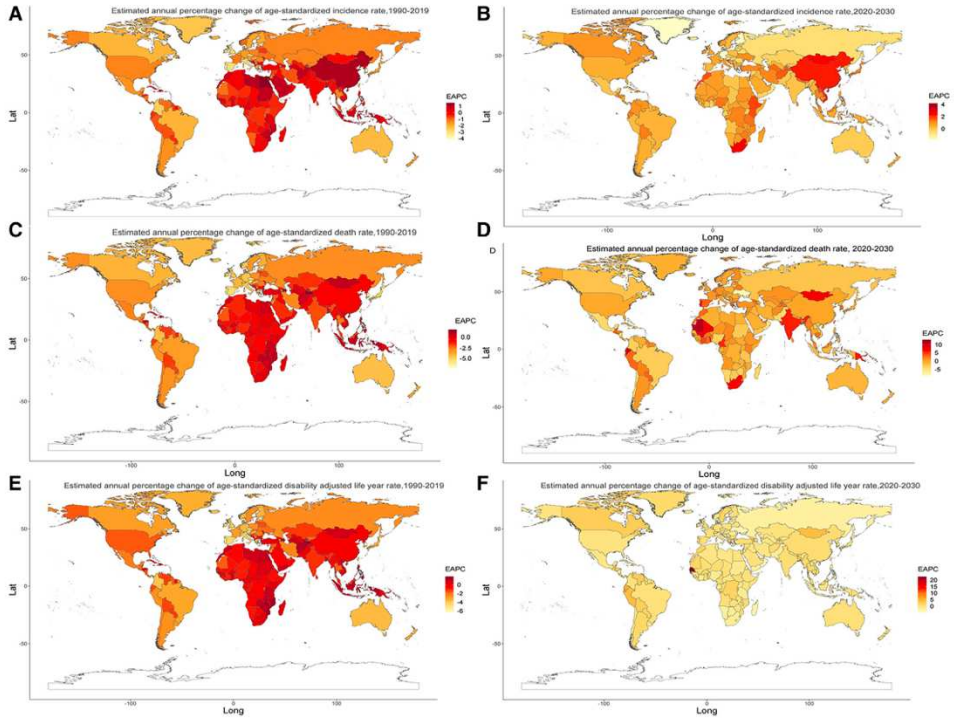

Figure 1: The distribution and the estimated annual percentage changes (EAPCs) in age-standardized incidence rate, death rate, and disability-adjusted life years rate of ischemic stroke at the national level (Pu L et al, 2023)

Studying stroke epidemiology is critical for developing targeted public health interventions, improving healthcare systems, and ultimately reducing the burden of strokes on individuals and societies (Liyuan Pu, 2023).

The alarming prevalence and impact of stroke on a global scale underscore the urgent need for comprehensive awareness, prevention, and healthcare strategies. The statistics from the Global Stroke Factsheet released in 2022 paint a stark picture of the growing burden of stroke worldwide. Stroke has emerged as a leading global health concern, standing as the primary cause of disability and the second leading cause of mortality, accounting for 11.6% of all deaths in 2019. The trajectory of stroke incidence and associated outcomes is particularly concerning, with a 70% increase in stroke cases, a 43% rise in stroke-related deaths, a staggering 102% surge in stroke prevalence, and a 143% increase in Disability Adjusted Life Years (DALY) from 1990 to 2019. Globally, 77.19 million individuals experienced an ischemic stroke in 2019, and 63.48 million DALYs and 3.29 million deaths were attributable to ischemic stroke. Over the last three decades, there has been a notable surge in ischemic stroke cases, deaths, and DALYs worldwide. In 1990, the global numbers stood at 4.07 million cases, 2.05 million deaths, and 40.50 million DALYs, escalating significantly to 7.86 million cases, 3.15 million deaths, and 62.53 million DALYs by 2020.

Projections for 2030 anticipate a further increase in ischemic stroke cases, reaching 9.62 million. The age-standardized rates associated with ischemic stroke provide additional insights. Between 1990 and 2020, there was a consistent decline in the age-standardized incidence, death, and DALY rates per 100,000 population. Projections for 2030, however, paint a nuanced picture. While the age-standardized incidence rate is anticipated to increase to 89.32 per 100,000, there is a simultaneous decline in death and DALY rates to 18.28 and 500.37 per 100,000, respectively. This suggests a complex interplay of factors influencing the overall burden of ischemic strokes (Pu L et al, 2023).

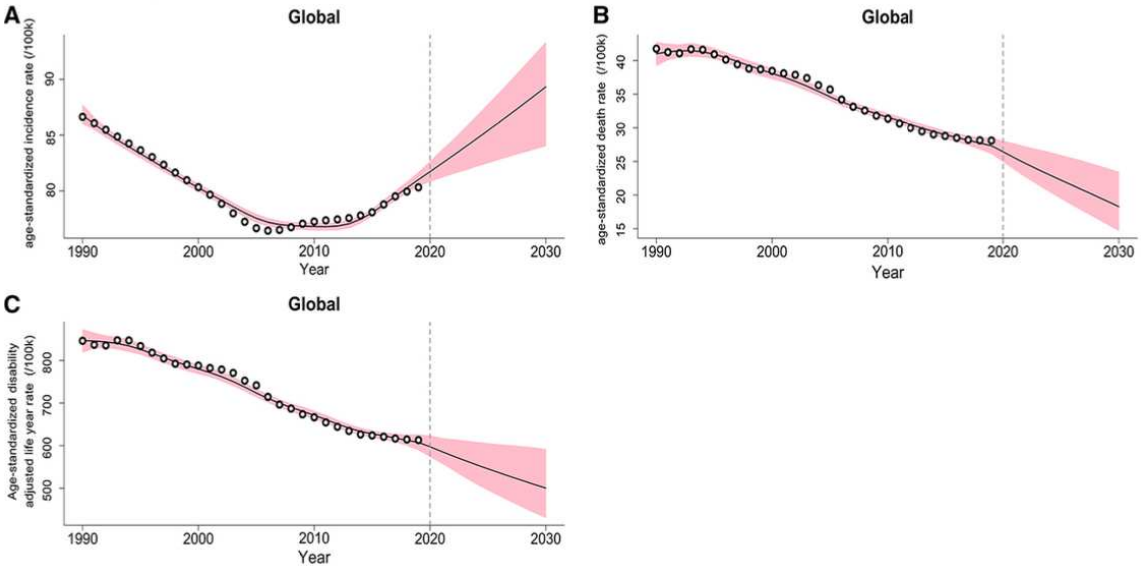

Figure 2: The trends and projections of age-standardized incidence rate, death rate, and disability-adjusted life years rate of ischemic stroke between 1990 and 2030 at the global level (Pu L et al, 2023).

The release of the Global Stroke Factsheet reveals an alarming trend – the lifetime risk of developing a stroke has surged by 50% over the past 17 years. The implication is striking; now, an estimated 1 in 4 individuals is projected to experience a stroke during their lifetime. This shift in lifetime risk emphasizes the urgency of addressing not only the incidence of stroke but also the factors contributing to its increased occurrence.

The most concerning aspect of the data is the disproportionate burden borne by lower and lower-middle-income countries. A staggering 86% of stroke-related deaths and 89% of DALYs are concentrated in these regions. This disproportionate impact not only reflects a health crisis but also highlights the socioeconomic challenges faced by families with limited resources in managing the aftermath of a stroke.

In the past two decades, Europe has witnessed a positive trend with a reduction in the incidence of strokes, especially when age is taken into account. This progress can be attributed to advancements in medical care and treatment, leading to improved recovery rates for individuals who experience strokes.

However, despite these advancements, a new challenge is emerging. The overall number of strokes is expected to rise in Europe due to the aging population. While the relative risk of having a stroke has decreased, the increasing proportion of Europeans over the age of 70 is contributing to a projected 34% increase in the total number of stroke events in the European Union from 613,148 in 2015 to 819,771 in 2035 (King's college report, 2023).

The death rates from strokes vary significantly across European countries, ranging from 30 to 170 deaths per 100,000 of the population. Importantly, the improving rates of survival due to better and quicker treatment mean that more people are living with the consequences of strokes. As a result, the estimated total cost of stroke in Europe, encompassing healthcare and non-healthcare costs, is set to rise from 45 billion euros in 2015.

Despite Europe boasting some of the best stroke care globally, disparities exist. In some regions, public education campaigns to encourage an emergency response to strokes are lacking. Moreover, specialized emergency services for strokes are not uniformly available, leading to variations in the quality of care. Thrombolysis rates, a crucial clot-busting treatment, also show significant discrepancies, ranging from less than 1% to 16% of patients.

One notable concern is the underutilization of stroke units, despite over thirty years of evidence demonstrating their efficacy. Only around 30% of stroke patients receive care in these specialized units, and the proportion varies widely based on geographical location, ranging from less than 10% to over 80%. Inconsistencies persist in the application of guidelines provided by the European Stroke Organization. This lack of uniformity contributes to variations in stroke care quality and outcomes across the continent. A continent-wide, evidence-based system of specialist stroke care is yet to be fully realized.

Access to rehabilitation and long-term support is a significant issue in many parts of Europe. Monitoring and auditing of rehabilitation services are not widespread, and even in regions where audits exist, individuals often receive therapies for brief periods during their hospital stay. Shockingly, two out of every five EU countries lack outpatient therapy services (Wafa Ha et al, 2020).

1.2 STROKE CLASSIFICATION

Stroke classification is a crucial aspect of understanding and managing strokes. Based on the fundamental cerebrovascular issue driving the event, whether it involves the obstruction or breakage of a blood vessel in the brain, the classification is determined as either ischemic or hemorrhagic stroke.

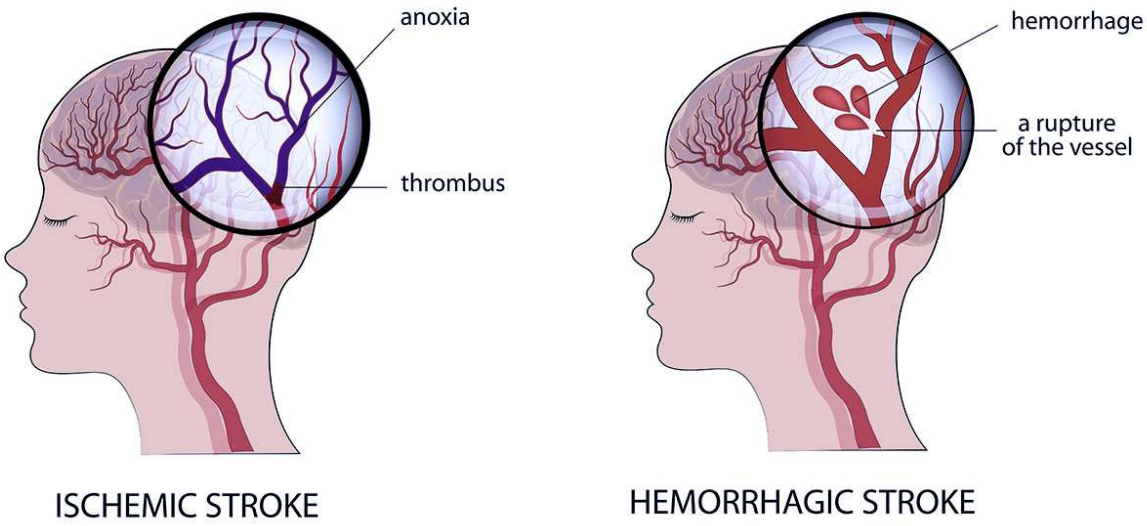

Figure 3: Stroke classification: Ischemic and Hemorragic stroke (Covenant Health Cumberland)

A) ISCHEMIC STROKE

Ischemic stroke, constituting approximately 87% of all stroke cases, stands as a complex and critical manifestation within the spectrum of cerebrovascular events. Its essence lies in the abrupt interruption of blood flow to specific regions of the brain, sparking a cascade of neurobiological consequences.

Analogous to a myocardial infarction in the heart, an ischemic stroke, often referred to as a "brain attack," transpires when there is an acute disruption in blood supply to the brain. This interruption precipitates a state of ischemia, characterized by insufficient oxygen and glucose delivery to neurons and other cerebral cells. Within minutes, this oxygen deprivation results in the demise of millions of neurons, accompanied by inflammatory responses, edema, and additional processes that perpetuate damage over hours to days following the initial insult.

The brain receives blood from four main arteries: two internal carotid arteries (ICAs) and two vertebral arteries (VAs). The ICA ascends vertically in the neck, extending from the common

carotid bifurcation to the base of the skull, entering through the carotid canal. Branching off into several vessels, such as the posterior communicating artery, it terminates at the bifurcation into the anterior and middle cerebral arteries. The two VAs originate from the subclavian arteries, entering the skull through the foramen magnum, and unite to form the basilar artery (BA). Extending from the pontomedullary junction to the pons-midbrain junction, the BA bifurcates into the right and left posterior cerebral arteries (PCAs).

The circle of Willis, comprising both intracranial ICAs, both anterior cerebral arteries (ACAs), the anterior communicating artery connecting the left and right ACAs, the BA, both PCAs, and both posterior communicating arteries, forms at the base of the brain. This circle provides crucial collateral circulation in case of ICA or BA occlusion. The ACA supplies the medial surface of the cerebrum and the upper border of the frontal and parietal lobes. The MCA covers the majority of the brain hemisphere, including the lateral surface and deep structures of the frontal and parietal lobes. The vertebrobasilar system, including the PCA, supplies various regions such as the upper spinal cord, brain stem, labyrinth, cochlea, cerebellum, subthalamus, part of the thalamus, and the temporooccipital lobes.

Ischemic strokes are often heralded by identifiable symptoms or warning signs, encompassing:

- Diminished strength or sensation on one side of the body
- Speech and language difficulties
- Alterations in vision or balance

Typically, these episodes manifest during the night or early morning hours. The onset of symptoms is characterized by a gradual development over a few minutes or a progressive worsening over the course of hours. Recognizing these indicators is pivotal for prompt medical attention, as early intervention significantly improves the chances of mitigating the impact of an ischemic stroke.

The primary etiological factor behind ischemic strokes is the formation of obstructive blood clots. These clots, or thrombi, can manifest either as a thrombus, forming within the wall of a blood vessel and impeding normal blood flow, or as an embolus, breaking free from the vessel wall and traversing the bloodstream to cause obstruction at distant cerebral sites. A subset of ischemic strokes, known as cardioembolic strokes, emanates from clots originating in the heart, often associated with conditions such as atrial fibrillation, heart failure, stenosis, or post-myocardial infarction scenarios.

Chronic atherosclerosis, characterized by the accumulation of fatty deposits (plaque) and cellular debris within blood vessel walls, stands as another contributor to ischemic strokes. As atherosclerotic plaques burgeon, they induce the narrowing of blood vessels (stenosis) and activate clotting mechanisms. Post-ischemic stroke, the affected brain region typically exhibits an irreversibly damaged core alongside a surrounding area termed the ischemic penumbra—a region at risk but salvageable through timely reperfusion.

In the realm of ischemic events, the transient ischemic attack (TIA) serves as a forewarning—a brief episode mirroring stroke symptoms that spontaneously resolve within 24 hours. Despite its transient nature, a TIA should not be dismissed lightly, as it unveils a 10 to 20 percent risk of subsequent stroke within 90 days. In many cases, TIAs result from unstable clots, necessitating prompt intervention to mitigate the potential for a more permanent cerebral blockage.

B) HEMORRHAGIC STROKE

A hemorrhagic stroke, constituting a formidable subset of cerebrovascular events, unfurls a narrative marked by the rupture of blood vessels within the intricate canvas of the brain. Unlike its ischemic counterpart, which revolves around blocked blood flow, a hemorrhagic stroke manifests when vessels succumb to rupture, unleashing a cascade of neurological consequences.

The manifestations of a hemorrhagic stroke typically arise abruptly and frequently encompass:

- Intense headache
- Nausea and vomiting
- Partial or complete loss of consciousness
- Seizure, aphasia, and hemianopia

These symptoms necessitate immediate attention, as their sudden onset indicates a critical medical condition.

The saga of hemorrhagic strokes commences with intracerebral hemorrhage (ICH), where blood vessels rupture within the cerebral parenchyma. This rupture may be instigated by various factors, including chronic hypertension and cerebral amyloid angiopathy, which weaken the structural integrity of blood vessel walls. Conditions that impair blood clotting, or the use of blood-thinning medications like warfarin, further amplify the vulnerability to bleeding events.

Structural anomalies also come into play, with arteriovenous malformations (AVMs) emerging as intricate entities. AVMs constitute a tangled network of thin-walled cerebral blood vessels,

potentially present from birth in a fraction of the population, contributing to the predisposition for intracerebral hemorrhage.

Venturing into the realm of subarachnoid hemorrhage (SAH), the rupture occurs in the subarachnoid space, a fluid-filled domain between layers of connective tissue enveloping the brain. The heralding sign often takes the form of a thunderclap headache, an abrupt onset of severe head pain devoid of an apparent cause. This rupture may transpire within an AVM or, more commonly, at a site where a blood vessel has weakened and bulged, forming an aneurysm. Aneurysms, structural anomalies that can be hereditary and affect up to one percent of the population, pose a distinct risk. The size, shape, location, and individual's age, coupled with the habit of smoking, intertwine to influence the likelihood of an aneurysm rupture. The meticulous understanding of these risk factors guides physicians in advising whether asymptomatic aneurysms warrant intervention.

In the aftermath of a hemorrhagic stroke, a profound departure from the norm occurs. Neural tissue, typically shielded by the blood-brain barrier, is suddenly exposed to an influx of red and white blood cells and large molecules. This breach unleashes a hematoma, an accumulation of blood, that exerts pressure on delicate neural structures, impairs normal blood flow, and induces cerebral damage through compression.

The predominant locations for hemorrhage are the basal ganglia (50%), cerebral lobes (10% to 20%), the thalamus (15%), pons and brain stem (10% to 20%), and the cerebellum (10%) (Chen S et al, 2014). The presence of a hematoma disrupts normal neural and glial function, instigating oligemia, neurotransmitter release, mitochondrial dysfunction, and cellular swelling. Furthermore, thrombin activation prompts microglia, inciting inflammation, and edema (Magrid-Bernstein J et al, 2022).

Primary injury ensues from the compression of brain tissue by the hematoma, culminating in elevated intracranial pressure (ICP). Contributing to secondary injury are factors like inflammation, blood-brain barrier (BBB) disruption, edema, heightened production of free radicals such as reactive oxygen species (ROS), glutamate-induced excitotoxicity, and the release of hemoglobin and iron from the clot.

Typically, hematoma enlargement transpires within 3 to 12 hours, with one-third of cases experiencing rapid expansion within 3 hours. Perihematomal edema intensifies within 24 hours, reaching its zenith around 5 to 6 days and lingering for up to 14 days. An encircling area of hypoperfusion characterizes the hematoma. Deterioration in ICH is influenced by factors such as

hematoma expansion, intraventricular hemorrhage, perihematomal edema, and inflammation (Chen S et al, 2014). In the context of a cerebellar hematoma, hydrocephalus may manifest due to the compression of the fourth ventricle in the early stages. SAH can be classified as either perimesencephalic or non-perimesencephalic SAH. Perimesencephalic SAH predominantly involves bleeding in the interpeduncular cistern. Physical exertion, particularly the Valsalva maneuver, leading to increased intrathoracic and intracranial venous pressure, serves as a predisposing factor for perimesencephalic non-aneurysmal SAH (PM-SAH). Non-perimesencephalic SAH (NPM-SAH) is characterized by diffuse blood distribution (Coelho LG et al, 2016).

Treatment strategies for hemorrhagic stroke present a multifaceted landscape with varying opinions and ongoing trials seeking optimal management approaches. Noteworthy trials such as Antihypertensive Treatment in Acute Cerebral Hemorrhage (ATACH), Intensive Blood Pressure Reduction in Acute Cerebral Hemorrhage Trial (INTERACT), Factor VIIa for Acute Hemorrhagic Stroke Treatment (FAST), and Surgical Trial in Intracerebral Hemorrhage (STICH) underscore the complexity of the field (Lapchak PA et al, 2007).

- Blood Pressure (BP) Management is a crucial facet of hemorrhagic stroke care. Gradual BP reduction to 150/90 mmHg, employing agents like beta-blockers (labetalol, esmolol), ACE inhibitors (enalapril), calcium channel blockers (nicardipine), or hydralazine, is recommended. Regular BP monitoring, as per the American Stroke Association (ASA) guidelines, aids in tailoring interventions based on patient presentation (Ojaghihaghighi S et al, 2017).
- Managing Raised Intracranial Pressure (ICP) involves elevating the head of the bed, employing osmotic agents (mannitol, hypertonic saline), and, if necessary, hyperventilation and sedation. Continuous monitoring of ICP is recommended for specific patient groups to maintain cerebral perfusion pressure within the optimal range (Hemphill JC et al, 2015).
- Hemostatic Therapy aims to reduce hematoma progression, particularly crucial for reversing coagulopathy in patients on anticoagulants. Various agents, including vitamin K, prothrombin complex concentrates (PCCs), recombinant activated factor VII (rFVIIa), and fresh frozen plasma (FFP), are utilized, with a tailored approach based on individual patient characteristics (Ojaghihaghighi S et al, 2017).
- Antiepileptic Therapy is considered for patients prone to seizures, with continuous EEG monitoring for those with decreased consciousness levels. ASA guidelines advise against

prophylactic anticonvulsant medication, emphasizing the importance of tailored interventions (Gigliotti MJ et al, 2022).

- Surgery, while a controversial topic, may be considered in specific cases. The STICH trial demonstrated no overall benefit from early surgery, but certain subsets, such as lobar hemorrhages with mild clinical deficits, may benefit. Emergency surgical evacuation is indicated for cerebellar hemorrhages with hydrocephalus or brainstem compression, guided by individual patient criteria (Schlunk F et al, 2022).
- Cerebroprotection strategies, encompassing anti-inflammatory and antioxidant agents, are explored to mitigate secondary injury effects. Citicoline, pioglitazone, and nimodipine are among the substances investigated for their neuroprotective potential (Laskowitz DT et al, 2010).
- General care involves a holistic approach, addressing complications such as dysphagia, cardiac issues, kidney injury, and infections. Multidisciplinary rehabilitation plays a pivotal role in minimizing disability, emphasizing the importance of comprehensive medical, nursing, and rehabilitation care (Hemphill JC et al, 2015).

1.3 RISK FACTORS

Addressing and alleviating the burden of stroke in the population necessitates a comprehensive understanding of both modifiable and non-modifiable risk factors, along with demonstrating the effectiveness of risk reduction strategies. Modifiable risk factors encompass elements like diet and comorbid conditions, while non-modifiable factors include age and race. Additionally, risk factors can be categorized as short-term triggers (infectious events, sepsis, stress), intermediate-term factors (hypertension, hyperlipidemia), and long-term factors (sex, ethnicity). It's noteworthy that risk factors for stroke in younger individuals may differ from those in older patients.

Efficiently estimating an individual's stroke risk, especially concerning the occurrence of a first stroke event, plays a crucial role in primary care. This involves assessing a person's unique combination of risk factors. Many patients express a desire to be informed about their stroke risk, highlighting the significance of incorporating risk assessments into routine healthcare practices. By identifying and addressing modifiable risk factors and educating individuals about their specific stroke risk profile, healthcare providers can contribute significantly to preventive efforts and promote overall cardiovascular health.

A) NON-MODIFIABLE STROKE RISK FACTORS

Non-modifiable risk factors (also called risk markers) for stroke include age, sex, ethnicity, and genetics.

- Age: Stroke is predominantly a disease of aging, and the risk increases significantly with advancing age. The incidence of stroke doubles for each decade after the age of 55. While the mean age for incident ischemic stroke is around 69.2 years, there's a concerning trend showing an increase in the incidence of stroke among individuals aged 20-54. This shift may partly be attributed to changes in diagnostic testing, enhancing sensitivity for detecting stroke in those with minor symptoms.
- Sex: The relationship between sex and stroke risk is nuanced and age-dependent. At younger ages, women have an equal or higher risk of stroke compared to men, which may be influenced by factors such as pregnancy, the post-partum state, and the use of hormonal contraceptives. However, at older ages, the relative risk is slightly higher for men. Overall, more strokes occur in women due to their longer lifespan.

- Ethnicity: Racial disparities in stroke incidence are well-documented. African Americans face twice the risk of incident stroke compared to their white counterparts, with higher mortality associated with stroke. Hispanic/Latino Americans also exhibit an increased risk of stroke in certain cohorts, and American Indians have a higher incidence compared to non-Hispanic whites. These disparities are influenced by a range of factors, including a higher prevalence of stroke risk factors among specific ethnic groups.
- Genetics: Genetic factors are non-modifiable contributors to stroke risk. A family history of stroke increases the likelihood of experiencing a stroke. These genetic risks vary based on age, sex, and race. While the specific genetic factors and heritability will be discussed in more detail in the genetics section below, it's important to note that genetic influences play a role in an individual's susceptibility to stroke.

Understanding these non-modifiable risk factors is crucial for tailoring preventive interventions and healthcare strategies. Recognizing the complexities of these factors helps healthcare providers identify at-risk populations, implement targeted screening measures, and develop interventions that consider the unique characteristics of different demographic groups.

B) MODIFIABLE STROKE RISK FACTORS

The significance of modifiable risk factors cannot be overstated, as implementing strategies to decrease these factors holds the potential to lower the risk of stroke. Early recognition and adjustment of these risk elements are crucial. Modifiable risk factors can be categorized into medical conditions and behavioral aspects. Established risk factors like hypertension, diabetes, hyperlipidemia, and smoking have long been recognized for their role in causing strokes. Meanwhile, ongoing research actively explores new or emerging risk factors.

- Hypertension: The impact of hypertension on stroke risk cannot be overstated. The relationship is not only strong but also linear and continuous. The INTERSTROKE study highlights hypertension as the predominant risk factor, attributing to more than half of the strokes in the studied population. The age-related increase in blood pressure underscores the importance of hypertension control across the lifespan. As individuals age, the risk of hypertension rises, contributing to an elevated lifetime risk of stroke. While there have been improvements in awareness and treatment, hypertension remains undertreated in the community. This emphasizes the need for heightened efforts in hypertension control, not only through medication but also lifestyle modifications. Recent studies suggesting that

intraindividual variability in blood pressure measurements is associated with stroke risk add a layer of complexity. This variability, beyond mean blood pressure, may indicate a lack of cardiovascular homeostasis, prompting consideration for tailored treatment strategies.

- Diabetes: Diabetes stands as an independent risk factor for stroke, doubling the risk for individuals with the condition. Moreover, stroke accounts for a significant proportion of deaths in diabetics, indicating the severity of the association. With approximately 8% of Americans having diabetes and nearly half of those over 65 being pre-diabetic, the scale of the issue is substantial. The duration of diabetes further compounds the risk, emphasizing the need for early intervention and management. The revelation that combined behavioral modification and medical therapy are more effective in reducing stroke risk in diabetics compared to glycemic control alone underscores the multifaceted nature of diabetes management in stroke prevention.
- Atrial Fibrillation and Atrial Cardiopathy: Atrial fibrillation's increasing incidence over the past three decades signify a growing concern. The assumption that AF's association with stroke solely results from thrombus formation faces challenges. The recognition of other supraventricular tachycardias, without fibrillation, contributing to stroke risk broadens our understanding. Genetic mutations associated with AF and their link to strokes before AF onset add complexity.
- Dyslipidemia: Dyslipidemia's relationship with stroke risk is intricate. Increased total cholesterol is associated with an increased risk of ischemic stroke, while elevated HDL cholesterol is linked to a decreased risk. The varying associations of cholesterol levels with different stroke subtypes highlight the need for subtype-specific considerations in stroke prevention strategies. The use of statins in reducing overall and ischemic stroke risk, while potentially increasing the risk of intracerebral hemorrhage in certain patients, necessitates a nuanced, individualized approach in treatment decisions.
- Sedentary Behavior, Diet/Nutrition, Obesity, and Metabolic Syndrome: Physical inactivity's contribution to stroke risk emphasizes the holistic impact of lifestyle on health. The benefits extend beyond stroke prevention to include reductions in blood pressure, diabetes, and excess body weight. The impact of diet on stroke risk, including the influence of salt, potassium, and adherence to a Mediterranean diet, underscores the importance of dietary considerations in preventive strategies. The multi-faceted link between obesity and stroke risk, mediated by associations with hypertension and diabetes, prompts a comprehensive

approach that goes beyond weight reduction to address metabolic health. While Metabolic Syndrome is associated with an increased risk of cardiovascular disease, its relationship with stroke requires further elucidation. The cumulative effect of its components on stroke risk suggests a need for integrated preventive measures.

- Alcohol Consumption, Substance Abuse, and Smoking: The J-shaped relationship between alcohol consumption and ischemic stroke risk, with protective effects at moderate levels and increased risk at heavy levels, illustrates the dual nature of alcohol's impact. The association between illicit substance abuse and both ischemic and hemorrhagic strokes signifies the need for awareness and intervention in substance abuse prevention. Smoking's pervasive influence on stroke risk, with a dose-response relationship, establishes it as a major, modifiable risk factor. The rapid reduction in risk post-smoking cessation highlights the potential for impactful interventions.
- Inflammation and Infection: The association of inflammatory biomarkers, especially C-reactive protein, with ischemic stroke, emphasizes the inflammatory nature of atherosclerosis. The potential direct contribution of CRP to stroke risk prompts further exploration. Chronic exposure to common infections and acute infections acting as triggers for stroke add infectious components to the risk landscape. The association between infectious burden and stroke risk, as well as other health outcomes, requires ongoing investigation. The modestly increased risk of both ischemic and hemorrhagic strokes in individuals with HIV infection raises questions about the interplay between infection, immunosuppression, and vascular health. The multifactorial nature of this risk necessitates a comprehensive understanding for effective prevention.

1.4 PATHOPHYSIOLOGY AND SIGNALING PATHWAYS INVOLVED IN AIS

Our contemporary comprehension of stroke pathophysiology surpasses the mere consequences of localized blood circulation impairment. The intricate mechanisms governing brain damage in strokes involve a multitude of highly complex processes that culminate in infarct maturation. Given the brain's intense requirement for oxygen and glucose, a disruption in circulation promptly triggers a depletion of these vital substrates within minutes. Simultaneously, the accumulation of toxic metabolites occurs. This sequence of events sets the stage for an energy deficit in the affected tissue, leading to functional or even structural damage to the cells. The extent and duration of this energy deficit determine the severity of the resultant impairment. The occurrences within the ischemic area are intricate and adhere to a predictable temporal and spatial pattern. Shortly after the onset of the perfusion deficit, the primary mechanisms of damage involve excitotoxicity, the generation of reactive oxygen/nitrogen species, tissue acidosis, and peri-infarct depolarizations. Inflammation and programmed cell death follow. Simultaneously, protective mechanisms are activated, mitigating the damage. Models of ischemic tolerance offer insight into these mechanisms, and the concept of the ischemic penumbra, crucial for comprehending these processes, will be detailed below.

Beyond the acute events triggered by the focal perfusion deficit in the brain, considerations of neuronal plasticity and regeneration have become significant concepts over a more prolonged timescale. Research in these domains focuses on spontaneous and therapeutically induced neuroneogenesis, the homing of blood-derived cells into the brain, and their transdifferentiation or fusion with parenchymal cells, consequently leading to cell replacement therapies.

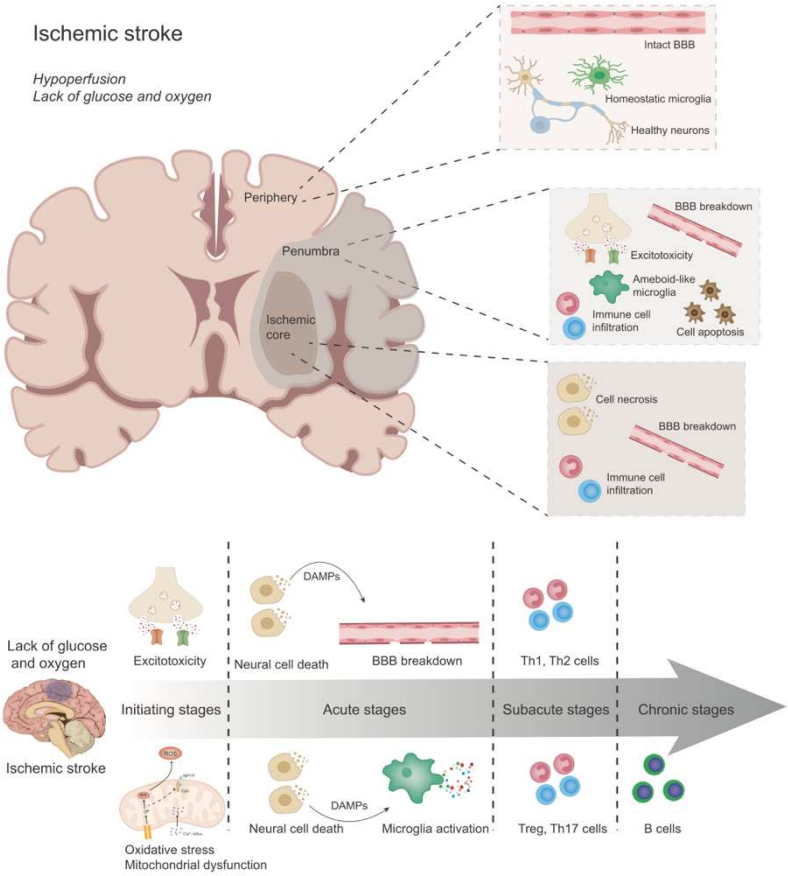

Figure 4: Spatial and temporal relationships of the pathophysiology in ischemic stroke. BBB Blood-brain barrier, DAMPs Damage-associated molecular patterns, Th1 T-helper cell 1, Th2 T helper cell 2,(Sig Transduction and Targeted Therapy, 2022)

The notion of the ischemic penumbra, introduced by Astrup in 1981, distinguishes two tissue areas in the ischemic brain—the infarction core and the surrounding zone known as the (ischemic) penumbra. Contrary to immediate cell death in the ischemic core, it is now widely acknowledged that not all brain cells perish immediately after an ischemic stroke. Instead, cell death progresses in a defined spatial and temporal continuum, particularly in the perilesional penumbra.

The ischemic core, formed almost immediately after vessel occlusion, represents an area where cells are fated to die regardless of therapeutic interventions unless swift restoration of blood flow occurs. The substantial reduction of blood flow in the ischemic core results in the breakdown of cellular metabolism, energy supply, ion homeostasis, and subsequent loss of cellular integrity. This leads to cell death within minutes, marked by the evolution of necrosis in cells and tissues.

Collaterals maintain residual circulation in the surrounding penumbra. Although functionally silent, this tissue remains metabolically active and, therefore, salvageable. However, the disruption of cellular homeostasis in the penumbra initiates slow cell death, gradually expanding the lesion, and the once viable brain tissue transforms into infarcted tissue. In the penumbra, apoptotic and inflammatory signaling cascades play crucial roles. In the early stages of a stroke, the penumbra can constitute up to 50% of the volume that eventually becomes infarcted.

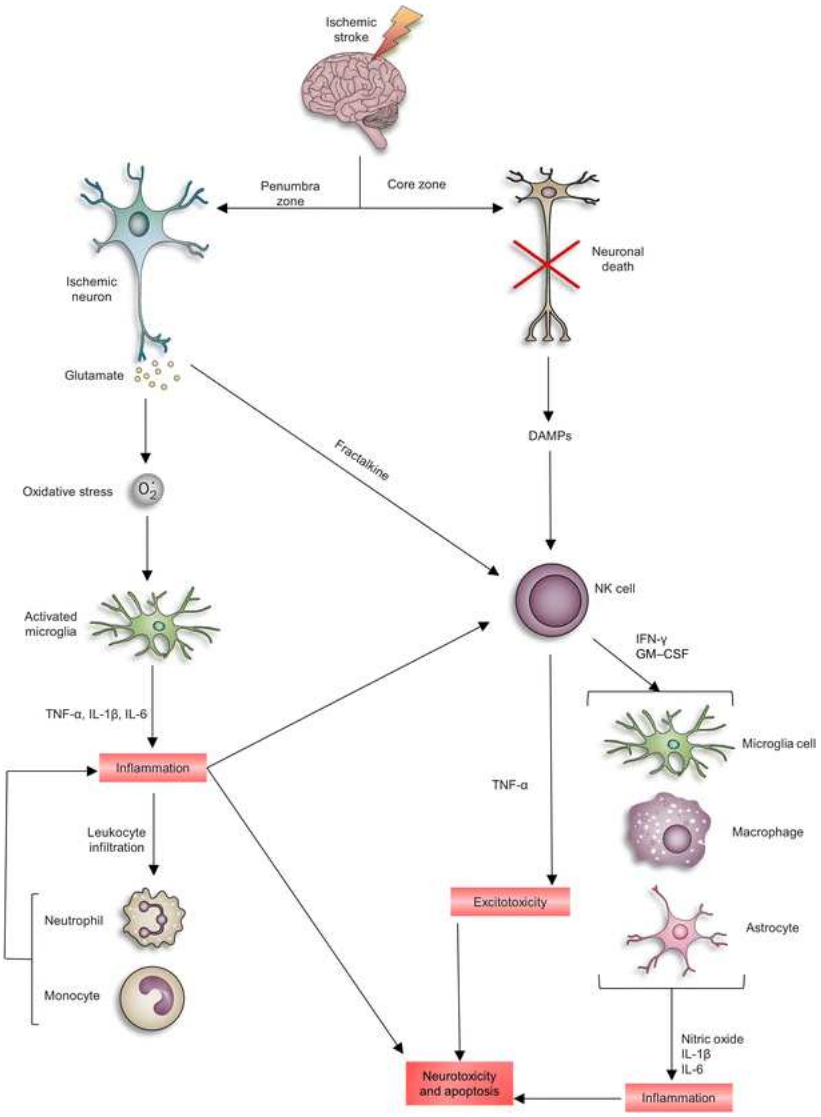

Figure 5: Mechanisms activate after an ischemic stroke event. Modified

As we said before, initially, damage caused by reduced blood supply (ischemic injury) results from a lack of energy, elevated levels of intracellular calcium, and the release of excitatory amino acids leading to excitotoxicity. This triggers downstream mechanisms of ischemic harm, such as the generation of free radicals and peroxynitrite, activation of calpain, phospholipases, and poly-ADP-ribose polymerase. Simultaneously, pathways that lead to programmed cell death (apoptosis) are

set in motion. Peri-infarct depolarization waves further disrupt the energy balance of neurons in the surrounding vulnerable area (penumbra). Additionally, inflammation plays a role in advancing tissue damage. Subsequent stages of cell death may involve enduring alterations in large molecules and other essential metabolites.

A) NEUROINFLAMMATION AND DAMAGE OF THE BLOOD–BRAIN BARRIER

The integrity of the Blood–Brain Barrier (BBB) relies on an intact cellular matrix composed of endothelial cells and astrocytes. Cerebral ischemia damages the cellular matrix, disrupts intercellular interactions, and impairs signal transduction. Matrix metalloproteases (MMPs), particularly MMP2 and MMP9, are implicated in BBB damage after cerebral ischemia. The expression levels of MMPs correlate with the severity of BBB damage, the risk of hemorrhagic transformation, and the extent of neuronal damage. MMPs contribute to the destruction of the basal lamina, allowing leukocyte immigration and leading to vasogenic edema. Inhibiting MMPs genetically or pharmacologically not only reduces BBB damage but also diminishes infarct volume.

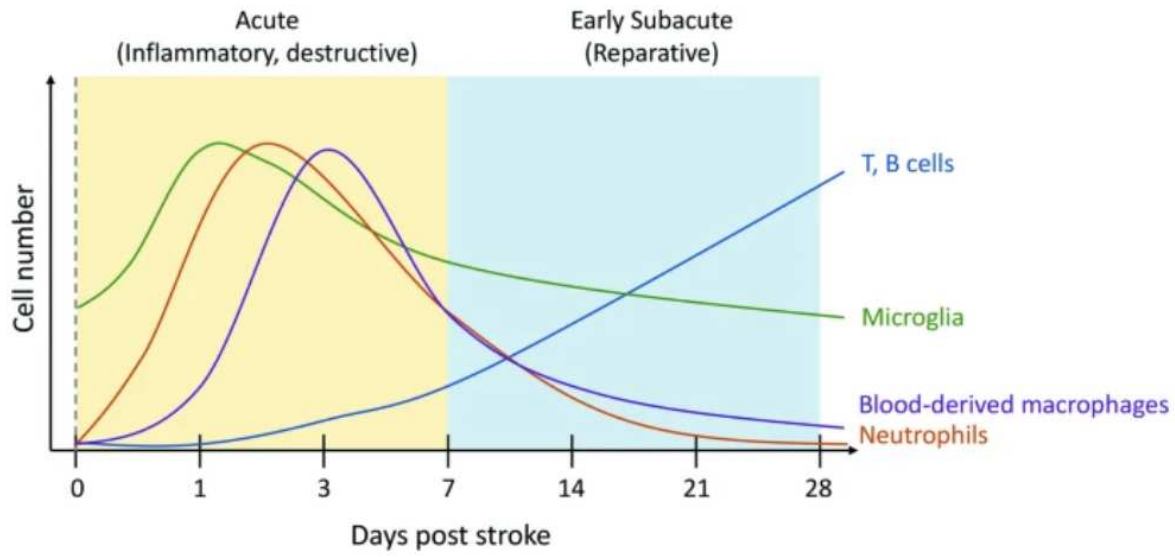

Figure 6: Expansion of leukocyte populations in the brain during ischemic stroke. In the acute stage of ischemic stroke, microglia in the brain proliferate and peripheral immune populations infiltrate the brain parenchyma. In the early subacute stage, innate immune population numbers in the brain decrease, while T and B cell numbers continue increasing until at least 28 days post-stroke (Inflammatory response after ischemic stroke, 2022)

In ischemic stroke, inflammation plays a crucial role and occurs throughout various stages of the condition. Neuroinflammation is initiated when damaged or dead cells release molecules known as DAMPs (Damage-Associated Molecular Patterns), which include substances like adenosine, heat shock proteins, high mobility group box 1, and interleukin-33. These DAMPs are then

recognized by specific immune cells, triggering a cascade of signaling pathways. Throughout the inflammatory process, different types of immune cells, such as microglia, macrophages, and T lymphocytes, become activated. Additionally, the production of inflammatory cytokines, interferons, and chemokines, including monocyte chemoattractant protein-1 (MCP-1), is stimulated. This heightened immune response leads to the upregulation of adhesion molecules, facilitating the attachment of leukocytes to vascular surfaces and promoting the infiltration of immune cells into affected areas.

The increased levels of pro-inflammatory cytokines also contribute to the breakdown of the blood-brain barrier (BBB) by activating endothelial cells and pericytes. This process results in the release of specific markers like von Willebrand factor and nerve growth factor. The compromised BBB leads to cerebral edema, accompanied by the expression of astrocytic aquaporin 4. Various factors, including MCP-1, von Willebrand factor, nerve growth factor, and aquaporin 4, collectively contribute to immune cell adhesion to vascular walls and subsequent infiltration into the central nervous system. This process ultimately exacerbates BBB breakdown and cellular edema in ischemic stroke.

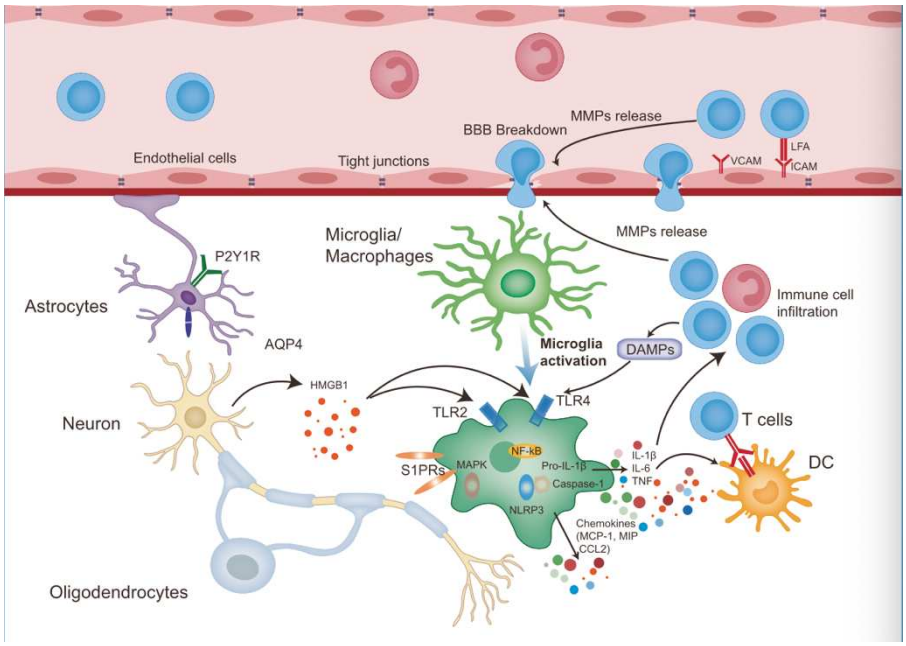

Figure 7: Breakdown of BBB by activation of pro-inflammatory cytokines

In ischemic stroke, multiple interconnected signaling pathways contribute to neuroinflammation and the breakdown of the blood-brain barrier (BBB), collectively influencing the pathophysiology of cerebral ischemia.

- Cytokine- and Chemokine-Induced Signaling Pathways:

Microglia, the main resident immune cells in the brain, play a pivotal role in ischemic stroke-induced neuroinflammation. They release both pro-inflammatory cytokines (IL-1β, IL-6, TNF-α) and anti-inflammatory cytokines (IL-1R antagonist (IL-1Ra), IL-10). These cytokines form a complex signaling network, with TNF-α being extensively studied.

TNF, extensively studied in ischemic stroke, comprises a soluble form (solTNF) and a transmembrane form (tmTNF). Both types of signal through distinct receptors, TNFR1 and TNFR2. The solTNF-TNFR1 signal is linked to pro-inflammatory effects and activation of cell death pathways, while TNFR2 promotes cell growth and regeneration. Recognizing the pivotal regulatory role of TNF signals in inflammation and neurological processes suggests their involvement in ischemic stroke pathophysiology. Genome-wide studies have identified a TNF gene polymorphism enhancing stroke susceptibility, emphasizing the importance of TNF/TNFR1 in stroke etiopathogenesis. Elevated TNF levels during cerebral ischemia contribute to neuronal plasticity. Microglia, predominantly secreting TNF, protects against cerebral ischemia. Myeloid cell-specific TNF knockout mice exhibit larger infarct volumes and severe deficits. Removing solTNF in mice reportedly alleviates symptoms and pathology, suggesting potential benefits in cerebral ischemic injuries by eliminating solTNF and retaining tmTNF. Overall, the diverse forms of TNF play varying roles in ischemic stroke, underscoring TNF's significance in the disease.

The IL-1 family forms a vast and intricate network of multifaceted pro-inflammatory cytokines closely involved in the regulation of immune cells and inflammatory processes. Among the IL-1 family members, namely IL-1α, IL-1β, and IL-1Rα, detailed studies have been conducted regarding their relevance to ischemic stroke. An association has been identified between a polymorphism in the IL-1A gene and an increased susceptibility to stroke, while conversely, a polymorphism in the IL-1B gene appears to lower the risk of stroke.

In the context of cerebral ischemia, the expression of IL-1α is significantly heightened. IL-1α derived from platelets contributes to neurovascular inflammation and induces the infiltration of neutrophils into ischemic lesions. The secretion of IL-1β, primarily by microglia and

macrophages, impacts neurons, glial cells, and the vasculature. Notably, IL-1β levels are markedly elevated in the cerebrospinal fluid at days 2 and 3 post-stroke, suggesting a potential predictive value in understanding stroke pathophysiology.

Experimental ischemic stroke models involving IL-1α/β knockout mice reveal a reduction in infarct volumes, indicating that the IL-1 family exacerbates stroke pathology. Conversely, the administration of IL-1β worsens outcomes in mice subjected to ischemic stroke. Overall, the IL-1 family plays a detrimental role in the pathophysiology of cerebral ischemic stroke and emerges as a potential therapeutic target for intervention.

IL-6, another crucial member of pro-inflammatory interleukins, is secreted by various cells, including monocytes, neurons, and glial cells. The signaling pathways of IL-6 can be categorized into classic signaling, which involves IL-6R and gp130, and trans-signaling, where IL-6 is associated with soluble IL-6R (sIL-6R). Classic signaling is considered neuroprotective, contributing to the maintenance of neuronal homeostasis, while trans-signaling is linked to IL-6-induced pro-inflammatory outcomes.

During cerebral ischemia, IL-6 levels are elevated, showing a correlation with infarct volumes and survival rates. Interestingly, IL-6 levels appear to be upregulated by IL-1β. Notably, brain-derived IL-6 is found to promote neurogenesis after a stroke, suggesting a potential neuroprotective effect that contributes to long-term functional recovery. Despite limited studies focusing on the role of IL-6 in ischemic stroke, its diverse and pleiotropic effects warrant further investigation.

In contrast to the pro-inflammatory cytokines mentioned earlier, IL-10 is primarily released by type-2 helper T cells and functions as an anti-inflammatory cytokine. Its role is to reduce inflammation and limit cellular apoptosis. There is an association between IL-10 gene polymorphism and the risk of stroke subtypes. In experimental ischemic stroke models, transgenic mice with enhanced IL-10 expression exhibited reduced infarct volumes and decreased cellular apoptosis.

Clinical studies further support the significance of IL-10 in ischemic stroke outcomes. Low levels of IL-10 correlate with poor stroke outcomes, worse neurological deficits, and excessive inflammatory reactions. These findings suggest that the anti-inflammatory properties of IL-10 could serve as a valuable indicator for the diagnosis and prognosis of ischemic stroke.

Chemokines, a group of small signaling proteins, contribute to the inflammatory processes in ischemic stroke alongside cytokines. Immediately after cerebral ischemia, pro-inflammatory

cytokines like TNF-α and IL-1β induce the secretion of chemokines, including MCP-1, fractalkine, macrophage inflammatory protein 1, microglial response factor-1, and cytokine-induced neutrophil chemoattractant. The chemokine-chemokine ligand 2 (CCL2) and its corresponding receptor, CCR2, play a role in regulating the inflammatory response in ischemia, possibly by facilitating immune cell recruitment and adhesion to cerebral endothelial cells. CCL2 expression is heightened in the ischemic penumbra, cerebrospinal fluid, and serum after ischemia or ischemia-reperfusion. Enhanced CCL2 expression correlates positively with infarct area and lesion enlargement, exacerbating ischemic injury in mice. Ischemic damage increases MCP-1 mRNA (CCL2) expression, worsening ischemic brain injury with an abundance of inflammatory cell infiltration in experimental ischemic stroke models. These findings highlight the detrimental role of CCL2/CCR2 signaling pathways in ischemic stroke.

Beyond CCL2, other chemokines contribute to the pathogenesis of ischemic stroke. For example, CCL3 is upregulated in experimental ischemic stroke models, and external administration of CCL3 exacerbates ischemia-induced injuries. Similarly, another chemokine, CCL5, regulates ischemia/reperfusion (I/R) injuries in experimental ischemic stroke models. Clinical studies show increased plasma CCL5 levels in symptomatic patients compared to asymptomatic ones. Additionally, CXC chemokines, part of the CC chemokine family, play crucial roles in ischemic stroke pathogenesis. ELR+ CXC chemokines, including CXCL1, CXCL2, and CXCL8, directly attract neutrophils toward ischemic brain regions, while ELR− CXC chemokines, including CXCL10, CXCL12, and CXCL16, mainly induce Th1-cell infiltration in post-ischemic inflammation.

- HMGB1/TLR and NF-κB Signaling Pathways:

The High-mobility group box protein 1 (HMGB1)/Toll-like receptor (TLR) and NF-κB signaling pathways play a crucial role in neuroinflammation during ischemic stroke. Various immune cells and their cellular products, associated with oxidative stress and necrosis, activate the innate immune system, likely through the Toll-like receptor (TLR) signaling pathway. TLRs, expressed on both the cell surface and intracellular space, regulate numerous immune cell functions and status. TLR signaling pathways can be categorized into two major downstream adaptor proteins: myeloid differentiation primary response 88 (MyD88)-dependent and

adapter-inducing interferon-β-dependent pathways. Both TLR signaling pathways activate NF-κB, triggering the release of pro-inflammatory cytokines.

Interestingly, TLRs exhibit a double-edged sword effect in ischemic stroke. In cases of relatively moderate ischemic injury, TLR2 and TLR4/NF-κB signaling pathways are inhibited, while interferon regulatory factor 3 signaling is enhanced, exerting neuroprotective effects on ischemia. Pretreatment with TLR2, TLR3, TLR4, TLR7, or TLR9 agonists alleviates symptoms and pathological damage in various ischemic stroke models. Administration of lipopolysaccharide (LPS) before ischemic insult protects against cerebral ischemia, possibly by modulating the TLR4 signaling pathway and inhibiting NF-κB after ischemic stroke attack. In contrast, elevated levels of plasma LPS appear to promote TLR4 expression, leading to the release of inflammatory cytokines, larger infarct volumes, and more severe functional deficits in rat cerebral ischemia models. These seemingly contradictory results suggest that LPS modulation of TLR4 response possibly depends on whether activation occurs before or after ischemic insult.

A key component in the TLR-related signaling pathway is HMGB1, significantly elevated in the brain, particularly in microglia, astrocytes, and blood vessel cells, closely associated with neuroinflammation and cellular stress in stroke. As a major ligand for TLRs, extracellular HMGB1 interacts with TLR2 or TLR4, subsequently activating NF-κB to elicit pro-inflammatory reactions. Moreover, the release of HMGB1 activates TLR4, enhancing IL-1β production through Nod-like receptor protein 3 (NLRP3) inflammasome activation. Furthermore, HMGB1 enhances the secretion of several pro-inflammatory cytokines, including inducible NOS, cytochrome c oxidase subunit 2, IL-1β, and TNF-α, promoting neuronal cell death during ischemia. These findings suggest that HMGB1/TLR signals induce both inflammatory reactions and cell death signaling pathways in ischemic stroke, potentially aggravating ischemic injury.

- MAPK Signaling Pathway:

The Mitogen-Activated Protein Kinase (MAPK) signaling pathway, consisting of three main effectors—ERK1/2, JNK, and p38—plays a significant role in inflammation and blood-brain barrier (BBB) dysfunction. Stress-activated protein kinases, namely JNK, p38 MAPK, and ERK, exert detrimental effects during cerebral ischemia. The MAPK signaling pathway becomes activated shortly after the onset of ischemic injury, with p38 MAPK specifically regulating the expression of various pro-inflammatory cytokines.

Activation of the p38/MAPK/AR-related signaling pathway has been observed to promote the microglial pro-inflammatory phenotype in cerebral ischemia. Additionally, activation of MAPK/ERK signaling leads to the stimulation of metalloproteinase (MMP) expression, potentially exacerbating BBB damage in ischemic stroke and further enhancing the expression of pro-inflammatory factors. Similarly, BBB damage induced by cerebral ischemia associated with a high-salt diet has been linked to the p38/MAPK/SGK1 signaling pathway.

These findings suggest that MAPK-related signaling pathways play a role in exacerbating ischemic brain injury, potentially by enhancing neuroinflammatory processes and contributing to BBB dysfunction.

- MMPs and BBB Dysfunction:

MMPs play a crucial role in the function and structure of the BBB in both human and animal stroke models. The increased production of MMPs and myeloperoxidase in ischemic stroke contributes to BBB breakdown. Specifically, MMP9 is implicated in inducing proteolysis of the BBB basal lamina. Clinical studies have identified baseline MMP9 as an important indicator of BBB disruption in ischemic stroke, correlating with the hyperintense acute reperfusion injury marker used in magnetic resonance imaging. Hypothermia followed by rapid rewarming has been shown to increase BBB permeability in ischemic stroke, accompanied by elevated MMP9 expression levels and damage to tight junctions. Elevated levels of MMP12 have been observed in rat cerebral ischemic stroke models, and suppressing MMP12 has been found to alleviate symptoms induced by ischemia. Additionally, MMP2 may be involved in the pathophysiology of ischemic stroke, potentially interacting with VEGF signaling. The latter is likely implicated in the initial stages of ischemic stroke, where hypoxic preconditioning exacerbates BBB injury and brain edema. Moreover, recovery from BBB damage in acute cerebral ischemia is associated with both the MMP2 and VEGF pathways, suggesting a close connection between MMP2 and VEGF in this context.

- S1PR-Related Signaling Pathways:

Sphingosine-1-phosphate receptors (S1PRs) constitute a group of G protein-coupled receptors that are abundant in microglia and are believed to regulate inflammatory responses in ischemic stroke. In vitro studies have demonstrated that the addition of sphingosine-1-phosphate (S1P) to microglia exposed to oxygen-glucose deprivation/reperfusion exacerbates

hypoxia-induced neuronal apoptosis. In experimental ischemic stroke models, sphingosine kinase 1 phosphorylates sphingosine to generate S1P, which binds to S1PR3, imparting a pro-inflammatory phenotype to microglia. Sphingosine kinase 1 has been shown to increase the brain infarct volume and worsen neurological symptoms by upregulating the expression of pro-inflammatory cytokines. Intriguingly, the S1PR agonist fingolimod has recently been reported to shift microglia from a pro-inflammatory to an alternatively activated phenotype in a chronic hypo-perfused ischemic stroke model in mice. Therefore, further exploration is needed to understand the detailed pro-inflammatory mechanisms of S1PRs in ischemic stroke.

- Inflammasome Activation:

Inflammasomes are large multiprotein complexes known to mediate neuroinflammation and contribute to neural cell death in ischemic stroke. Both in vivo and in vitro model studies suggest that the NLRP3 inflammasome plays a pivotal role in microglia-associated neuroinflammation in ischemic stroke, potentially influencing the microglial phenotype. These effects may be associated with the activation of the NF-κB signaling pathway. Additionally, NLRP1 has been implicated in cerebral ischemic injuries, and inhibiting its activity has been shown to alleviate neuroinflammation in ischemic conditions. Consequently, the activation of inflammasomes, whether through NLRP1 or NLRP3, contributes to the pathogenesis of ischemic stroke and could be explored as a potential therapeutic target against cerebral ischemia.

- Microglial Phagocytosis and Complement Activation:

Microglia serve as the primary phagocytes in the central nervous system, responsible for clearing myelin debris and pruning synapses. In experimental ischemic stroke models, microglia have been observed to phagocytose tissue debris, contributing to tissue repair and neuronal network reconstruction. However, conflicting studies suggest that excessive microglial engulfment may exacerbate brain injuries induced by cerebral ischemia. Therefore, microglial phagocytosis appears to play both beneficial and detrimental roles in ischemic stroke.

Microglia can engulf various dying cells and debris, involving multiple signaling pathways. For instance, stressed neurons in ischemic stroke express TMEM16F, inducing neurons to expose

phospholipid phosphatidylserine (PS), a signal that promotes phagocytosis. Knockdown of TMEM16F hindered microglial phagocytosis of viable neurons in the penumbra after experimental ischemic stroke. Additionally, the triggering receptor expressed on myeloid cells (TREM2) signaling pathways are implicated in microglial phagocytosis in ischemic stroke. Deficiency in TREM2 dampens microglial phagocytosis of neurons, worsening ischemic brain injuries, highlighting the neuroprotective role of Trem2 in ischemic stroke.

Complement components, such as C1q and C3, are integral to the complement system and contribute to the regulation of dying cell clearance. Upon activation, C3 is cleaved into C3a and C3b, with C3b and its receptor, CR3, working together to regulate the clearance of dying cells. C1q, a major component of the C1 complex, enhances microglial clearance of apoptotic cells in ischemic stroke. After ischemic stroke, complement activation directs microglial phagocytosis of both synapses and neurons, ultimately contributing to cognitive decline. The complement system's activation, involving various signaling pathways, interacts closely with microglial phagocytosis and may significantly influence the pathologies of ischemic stroke.

B) CELL DEATH MECHANISMS AFTER STROKE

The precise timing and cellular pathways triggering cell death after a stroke are not entirely clear. However, it is widely acknowledged that mechanisms promoting cell death are activated post-stroke. The pathways culminating in cell demise include:

- Necrosis: Characterized by ischemic or edematous cell changes, necrosis is a form of cell death resulting from the breakdown of cellular metabolism and energy supply. It leads to structural alterations in cells.
- Apoptosis: Exhibits various features, including morphological changes like apoptotic bodies, biochemical indicators like DNA laddering, and activation of caspases (proteases responsible for cell destruction). This form of programmed cell death occurs hours after the onset of a stroke.
- Autophagocytosis: Involves the cell engulfing its own components, a process that can contribute to cell death. The exact role and timing of autophagy in stroke-induced cell death remain subjects of ongoing research.

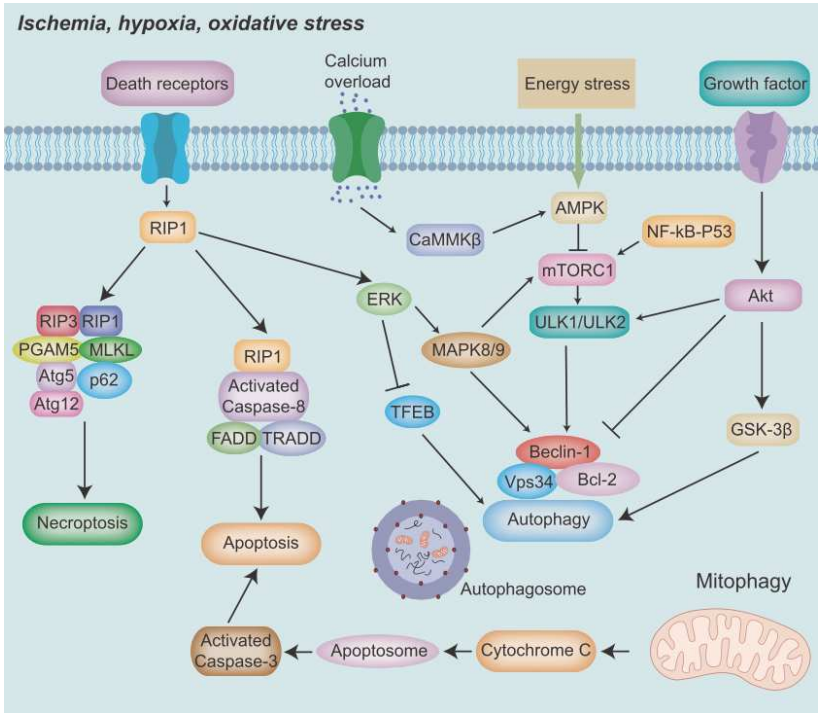

Figure 8: Cell death signaling pathways involved in ischemic stroke. GSK3β Glycogen synthase kinase-3β; Bcl-2 B-cell lymphoma-2; ERK Ras/extracellular signal-regulated kinase; CAMKs Ca2+/calmodulin-dependent protein kinases; MAPK Mitogen-activated protein kinase, TNF Tumor necrosis factor; mTOR mammalian target of rapamycin; AMPK 5'-AMP-activated protein kinase; FADD Fas-associating protein with a novel death domain; TRADD TNFRSF1A Associated Via Death Domain; RIPK Receptor-interacting protein kinase; MLKL Mixed lineage kinase domain-like protein; RIP1 Receptor interaction protein 1; RIP3 Receptor interaction protein 3; PGAM5 Phosphoglycerate Mutase Family Member 5; MLKL mixed lineage kinase domain like pseudokinase; Atg5 Autophagy related 5; Atg12 Autophagy related 12; TFEB Transcription factor EB; ULK1 Unc-51 Like Autophagy Activating Kinase 1; AMPK 5'-AMP-activated protein kinase; mTOR mammalian target of rapamycin; Apaf-1 Apoptotic peptidase activating factor 1 (Sig Transduction and Targeted Therapy, 2022)

The principal pathways related to autophagy in AIS are:

- mTOR-related signaling pathways:

mTOR, or mammalian target of rapamycin, is a serine/threonine protein kinase found in two primary forms: mTORC1 (rapamycin-sensitive) and mTORC2 (rapamycin-insensitive). mTORC1 is responsible for cell growth and cell cycle progression, while mTORC2 contributes to cellular skeleton formation. mTOR serves as a key regulator of the initial phase of autophagy, sensing changes in signaling within the cell. Normally, mTOR limits autophagy by inhibiting the phosphorylation of the Atg1/ULK1 protease complex.

During ischemic stroke, mTOR interacts with multiple components of signaling pathways that regulate autophagy, including PI3K/Akt, AMPK, and MAPK. Akt, a protein involved in various biological processes, can influence cellular autophagy through several signaling pathways, with PI3K/Akt/mTOR being the most significant. The PI3K/Akt signaling pathway has been suggested to exert a neuroprotective effect in ischemic stroke, possibly by regulating mTORC and, consequently, autophagy in both mouse middle cerebral artery occlusion (MCAO) models and primary neurons treated with oxygen-glucose deprivation (OGD) in vitro. Another study found that inhibiting mTOR with rapamycin activated the PI3K/Akt signaling pathway and, in turn, autophagy, providing protection against hypoxia in neonatal rats. Interestingly, homocysteine appears to have a neurotoxic effect, potentially due to excessive autophagy following the downregulation of PI3K/Akt/mTOR signaling in neural stem cells, indicating the dual role of autophagy in ischemic stroke.

AMPK (AMP-activated protein kinase) belongs to the serine/threonine kinase family and acts as a crucial endogenous defense factor against cerebral ischemia. During cerebral ischemia or hypoxia, the energy deficiency leads to an elevated AMP/ATP ratio, triggering the phosphorylation of AMPK. This activation of AMPK, in turn, stimulates autophagy to enhance energy production. In animal experimental ischemic stroke models, studies have demonstrated that protective autophagy can be induced by regulating the AMPK/mTOR signaling pathway, thereby mitigating cerebral ischemic injury. Several factors, both downstream and upstream, contribute to AMPK activity in both in vivo experimental ischemic stroke models and in vitro. Mechanistically, AMPK inhibits mTORC1 activity by phosphorylating and stimulating the TSC1/TSC2 complex during ischemia, promoting autophagy. Additionally, Ca2+ overload during ischemic stroke can activate AMPK via

calcium/calmodulin-dependent protein kinase beta, activating autophagy through the AMPK/mTOR pathway. Cytosolic p53 is another molecule that plays a role, inhibiting autophagosome formation while activated p53 promotes AMPKβ expression and inhibits mTOR expression to enhance autophagy.

MAPK is another crucial regulator of autophagy associated with ischemic stroke. MAPKs act as upstream regulators of mTORC1, influencing autophagy through the MAPK/mTOR signaling pathway. Studies have shown that autophagy protects against experimental cerebral ischemic injury through the induction of an Akt-independent MAPK/mTOR signaling pathway, wherein ERK negatively regulates mTORC1. However, contrasting findings are suggesting that ERK might negatively control autophagy by activating mTOR, contributing to neuronal survival after ischemic stroke injuries. The MAPK/ERK signaling pathway family appears to have a dual role in regulating mTOR in ischemic stroke, and further research is needed to understand the exact mechanisms involved.

- Beclin1/Bcl2 signaling pathway:

Beclin1 plays a crucial role in the early stages of autophagy, and its expression can be upregulated during local cerebral ischemia, inducing autophagy-like cell death. This suggests the involvement of the Beclin1/Bcl2 signaling pathway in the regulation of autophagy in ischemic stroke. Researchers have found that Bcl2 phosphorylation, triggered by cerebral ischemia in rats, disrupts the Beclin1-Bcl2 complex, leading to distal ischemic conditional autophagy that alleviates mitochondrial damage.

Furthermore, the expression of peroxisome proliferator-activated receptor γ (PPAR-γ) increases during experimental cerebral ischemic injury. Activated PPAR-γ has been shown to inhibit Beclin1-mediated autophagy, possibly by upregulating the expression of Bcl2/BclXL. This indicates that both detrimental and neuroprotective factors can influence Beclin1-Bcl2 signal activities, subsequently impacting autophagy in the context of ischemic stroke. The modulation of this signaling pathway represents a potential avenue for therapeutic interventions in ischemic stroke.

- Other autophagy pathways:

Under ischemic conditions, cellular stressors such as the accumulation of misfolded proteins and disruption of Ca2+ homeostasis activate the unfolded protein response (UPR), which is a cellular mechanism aimed at restoring endoplasmic reticulum (ER) homeostasis. The UPR has been implicated in the regulation of autophagy, some key points related to the UPR and autophagy in the context of ischemic stroke are:

1. UPR-Mediated Autophagy Promotion: The UPR has been shown to promote autophagy through several pathways:

- The PERK (protein kinase RNA-like ER kinase)/eIF2 (eukaryotic initiation factor 2) pathway is one of the UPR branches that can stimulate autophagy.

- The IRE1 (inositol-requiring enzyme 1)/TRAF2 (tumor necrosis factor receptor-associated factor 2)/JNK (c-Jun N-terminal kinase) pathway is another UPR branch involved in autophagy regulation.

2. Activating Transcription Factor 6 (ATF6) and Autophagy: ATF6, another mediator of the UPR signaling pathway, has been suggested to influence autophagy, but the specific mechanisms through which ATF6 may regulate autophagy in the context of ischemic stroke need further investigation.

3. Role of Rab7 in Autophagy Regulation: Rab7, a small GTPase associated with lysosomes, plays a role in regulating autophagy during cerebral ischemia. Rab7 facilitates the fusion of autophagosomes with lysosomes, contributing to autophagosome maturation, lysosome formation, and the maintenance of lysosomal function.

Programmed cell death, specifically apoptosis, is a process triggered by a cascade of events in response to acute damage to the central nervous system, such as ischemic injury. In the ischemic core of an infarction, neuronal and glial cells typically undergo rapid necrotic cell death within a matter of minutes or hours. On the other hand, apoptosis predominantly occurs in the penumbral region, initiating hours after the onset of ischemia and potentially lasting for days. Apoptosis is characterized by the activation of caspases, which are proteases catalyzing the breakdown of cellular components and molecules. Experimental stroke studies often lack definitive morphological criteria for apoptosis, but molecular, biochemical, and pharmacological criteria for defining apoptotic cell death are met in ischemic neuronal death. The brain's induction and regulation of apoptosis mostly rely on mechanisms common to other tissues.

In terms of apoptosis routes, the most commonly identified pathways are:

- Apoptosis by the extrinsic/death receptor pathway:

The activation of the extrinsic apoptotic pathway is initiated by the binding of specific ligands, such as TNF-α, FasL, and TRAIL, to their respective death receptors—TNF-α receptor 1, Fas/CD95/APO1, and TRAIL-R—located on the cell surface. In the context of an ischemic stroke, the interaction between these ligands and death receptors triggers the recruitment of death domain adaptor proteins, namely FADD and TRADD. This recruitment forms a complex that binds to procaspase-8, setting off a series of downstream events that culminate in the activation of caspase-8.

Upon activation, caspase-8 plays a pivotal role in initiating apoptotic processes. It can directly activate downstream effector caspases through proteolytic cleavage. Alternatively, caspase-8 can indirectly activate effector caspases by cleaving BH3-interacting domain (BID) to its truncated form. This truncated BID subsequently mediates apoptotic cell death through the mitochondria-dependent pathway.

Furthermore, in the context of ischemic injury, neurons and glial cells release TNF-α, leading to an increase in both Fas mRNA and protein levels. These elevated Fas levels serve as stimuli for the extrinsic apoptotic pathway, contributing to the initiation of programmed cell death, particularly in neurons.

- Apoptosis by the intrinsic/mitochondrial pathway:

The intrinsic pathway, also known as the mitochondrial pathway, constitutes a receptor-independent signaling cascade that profoundly impacts mitochondrial energy metabolism. This pathway is activated in response to apoptotic stimuli, such as excessive Ca2+ accumulation and oxidative stress, leading to mitochondrial-mediated cell death. Under conditions of oxygen and glucose deficiency, a decrease in ATP levels causes cellular depolarization and the release of excessive glutamate. These events further intensify Ca2+ influx, contributing to the initiation of the intrinsic apoptotic pathway. Ca2+ overload activates calpain, which, in conjunction with caspase-8 in the death receptor pathway, cleaves Bcl2-interacting BID into its truncated active form. The truncated BID interacts with pro-apoptotic members of the Bcl2 family, forming dimers that induce the opening of the mitochondrial permeability transition pore (MPTP). This sequence of events results in the

release of various pro-apoptotic factors, including cytochrome c, endonuclease G, and AIF. These factors, in turn, contribute to the formation of the apoptosome by binding to apoptotic protease activating factor-1.

Once the apoptosome is formed, procaspase-9 undergoes activation to caspase-9, initiating the activation of downstream effector caspases such as caspase-3, caspase-6, and caspase-7. These activated effector caspases play a crucial role in promoting apoptosis in neuronal cells through the intrinsic pathway.

- p53-mediated apoptotic pathway:

In addition to the extrinsic and intrinsic apoptotic pathways, ischemic stroke triggers another programmed cell death mechanism primarily governed by p53. The tumor suppressor p53 becomes activated specifically in the ischemic regions of the brain, where it plays a significant role in promoting neuronal apoptosis. Upon activation, p53 translocates to the nucleus and binds to its specific DNA sites, initiating the apoptotic cascade in ischemic brain cells. Various detrimental signals can activate p53, including DNA damage, which induces p53 phosphorylation, and hypoxia and oxidative stress, which upregulate p53 protein levels. Additionally, upstream cascade proteins like JNKs, p38, DAPK, ASK1, and Notch contribute mechanistically to p53 activation, collectively leading to cellular apoptosis in ischemic stroke. The apoptotic process induced by p53 encompasses the activation of downstream genes and molecules, notably the pro-apoptotic genes Bax, Noxa, p53AIP1, and PUMA. These genes act directly on mitochondria to instigate apoptosis. Subsequently, p53 engages the intrinsic apoptotic pathway, resulting in the release of pro-apoptotic factors, the formation of an apoptosome, activation of effector caspases, and the induction of neuronal apoptosis. Additionally, p53 mediates apoptosis by regulating the expression of paternally expressed 3 and impeding cell survival signaling. Collectively, these intricate processes contribute to the initiation and progression of p53-mediated apoptosis in the context of ischemic stroke.

- Notch signaling pathways in apoptosis:

Notch signaling pathways, with Notch1 being a crucial component, play pivotal roles in various biological processes within the central nervous system. The activation of Notch1, along with other signaling pathways such as NF-κB and p53, contributes significantly to neuronal death processes. Studies have indicated a close association between p53, Pin1, Notch, and NICD in

the context of ischemic stroke. As a key mediator of apoptosis, p53 becomes activated in response to damaging factors like hypoxia. The collaboration between Notch and p53 emerges as a critical factor in neuronal apoptosis during ischemic stroke, involving the stabilization of p53 and the transcriptional regulation of p53 and NICD target genes. Pin1, an isomerase influencing p53 transactivation, is implicated in the pathogenesis of ischemic stroke, linking with Notch signaling and contributing to ischemic stroke-induced neuronal death and neurological deficits. Moreover, research suggests significant roles for Notch in modulating NF-κB-related cell death pathways. For instance, the down-regulation of NICD levels by γ-secretase inhibitors has been shown to protect against ischemic stroke damages, potentially through the regulation of NF-κB-related signals. Simultaneously, these inhibitors block Notch signals and alleviate microglial activation, revealing interactions between Notch and NF-κB pathways in both neurons and microglia during cerebral ischemia. Additionally, ischemic stroke has been associated with increased HIF-1α expression levels, which can directly bind with NICD and NF-κB. Inhibition of both γ-secretase/Notch and HIF-1α significantly reduces cell apoptosis, while enhanced expression of NICD and HIF-1α increases NF-κB levels. These findings highlight the intricate interactions among NICD, p53, HIF-1α, and NF-κB, emphasizing their close association with neuronal death processes, particularly neuronal apoptosis in ischemic stroke.

Necrosis or necroptosis is a notable consequence of cerebral ischemia. In the aftermath of a stroke, the reduced cerebral blood flow in the infarct area triggers the necrotic demise of resident neurons, primarily driven by a decrease in ATP levels during ischemia. Recent research has shed light on necrosis as a regulated process involving various signaling pathways, with TNF-α playing a pivotal role. Downstream signaling pathways, including receptor-interacting protein kinases (RIPK1 and RIPK3) and mixed lineage kinase domain-like pathways, are crucially controlled by TNFα.

In response to cerebral ischemic damage, the formation of a complex involving TRADD, RIPK1, and ubiquitin 3 ligases is initiated by the interaction of TNF-α with its TNFR1 receptor. This activation of Complex IIb, occurring in both ischemia and hypoxia, leads to the phosphorylation and association of RIPK1 and RIPK3. Within this complex, mixed lineage kinase domain-like is activated by RIPK3, ultimately resulting in cell death. Simultaneously, a cascade of inflammatory reactions, including the secretion of pro-inflammatory cytokines, amplifies necrotic damage, exacerbating ischemic brain injuries.

Other mechanisms of cell death are Pyroptosis and Ferroptosis.

Pyroptosis, predominantly observed in the ischemic penumbra, is another cell death pathway that potentially induces pro-inflammatory pathways in ischemic stroke. During pyroptosis, cells undergo swelling, and cellular organelles are released, triggering inflammation. Caspase-1 is activated, forming inflammasomes and contributing to pyroptotic cell death, accompanied by the secretion of inflammatory factors such as IL-1β and IL-18.

Ferroptosis, a less discussed but significant cell death pathway, is regulated by peroxidation and requires sufficient accessible iron. In ischemic brain regions, heightened cellular excitotoxicity reduces GPX4 activity and diminishes GSH production, leading to the accumulation of excessive ferric ions and inducing ferroptotic cell death. Additionally, the damaged blood-brain barrier facilitates the transfer of iron into neuronal cells, further enhancing ferroptosis. From another perspective, ferroptosis is closely associated with oxidative stress, involving signaling pathways such as calcium-related signals, ATF4, and Keap1-Nrf2. Despite being less frequently discussed, ferroptosis may play a substantial role in the pathogenesis of ischemic stroke, with various signaling pathways potentially participating.

C) PERI-INFARCT DEPOLARIZATION

Anoxic depolarizations within the central region of the infarct result from a lack of oxygen in both neurons and non-neuronal cells, leading to the release of glutamate, other excitatory amino acids, and potassium. This causes sustained depolarization of cells, ultimately leading to their demise. In the adjacent penumbra, cells may undergo repolarization, but this comes at the expense of high energy consumption. Following depolarization, the extracellular release of neurotransmitters and potassium triggers repetitive waves known as peri-infarct depolarizations (PIDs). Typically originating from the core of the lesion, these PIDs propagate outward in a wave-like manner for at least 6–8 hours at a frequency of 1–4 events per hour.

Evidence from both ischemic animal models and human studies indicates that PIDs significantly contribute to tissue damage following a stroke. The total number and frequency of PIDs are closely correlated with the final lesion volume and cellular damage. It has been demonstrated that the propagation of each depolarization actively promotes the immediate expansion of the ischemic lesion from the core to the periphery. Moreover, interventions targeting the reduction of PIDs, such as blocking NMDA or AMPA receptors, have been shown to preserve tissue.

Subsequent repolarization, a process dependent on energy, can further exacerbate the growth of the ischemic lesion, causing lethal damage to metabolically compromised cells within the penumbra.

D) EXCITOTOXICITY

Following focal ischemia, the brain parenchyma experiences a severe shortage of oxygen and glucose, crucial sources of energy produced through oxidative phosphorylation. This local energy deficit triggers the depolarization of neurons and glia, leading to the activation of voltage-gated calcium channels and the release of excitotoxic amino acids into the extracellular matrix. While glutamate is typically rapidly re-uptaken under normal conditions, its binding to ionotropic N-methyl-D-aspartate (NMDA) and α-amino-3-hydroxy-5-methyl-4-isoxazolepropionic acid (AMPA) receptors, following release, induces excessive calcium influx into neurons. Elevated intracellular calcium serves as a universal second and third messenger, initiating a cascade of downstream events involving phospholipases, lipases, kinases, endonucleases and proteases that degrade essential membranes and proteins crucial for cellular integrity. Despite their involvement in causing excitotoxicity in ischemic stroke, NMDARs exhibit a dual role, acting as a double-edged sword. Both functional and structural studies have uncovered that when NMDARs have the GluN2B subunit, their activation triggers excitotoxicity leading to neuronal apoptosis during ischemic stroke. On the other hand, NMDARs with the GluN2A subunit activation exert a neuroprotective effect. The distinction between synaptic and extra-synaptic NMDARs also plays a crucial role, as it is hypothesized that synaptic NMDARs support neuronal survival, while extra-synaptic NMDARs have detrimental effects on neuronal activity. This analogy extends to the GluN2A-containing NMDARs, which are neuroprotective, versus the GluN2B-containing NMDARs, which contribute to excitotoxicity. This dual effect of NMDARs showcases their complex regulation of signaling pathways, influencing both neuroprotective and detrimental outcomes in the context of ischemic stroke.

Mitochondrial outer membrane depolarization (MOMP) and subsequent cell death are triggered by the overload of intracellular calcium. Furthermore, sodium and chloride enter neurons through channels for monovalent ions (for example the AMPA receptor), accompanied by the passive entry of water, resulting in intracellular "cytotoxic" edema. Significant imbalances of other ions, including the release of large amounts of stored zinc from vesicles in excitatory neurons upon depolarization, contribute to excitotoxic cell death.

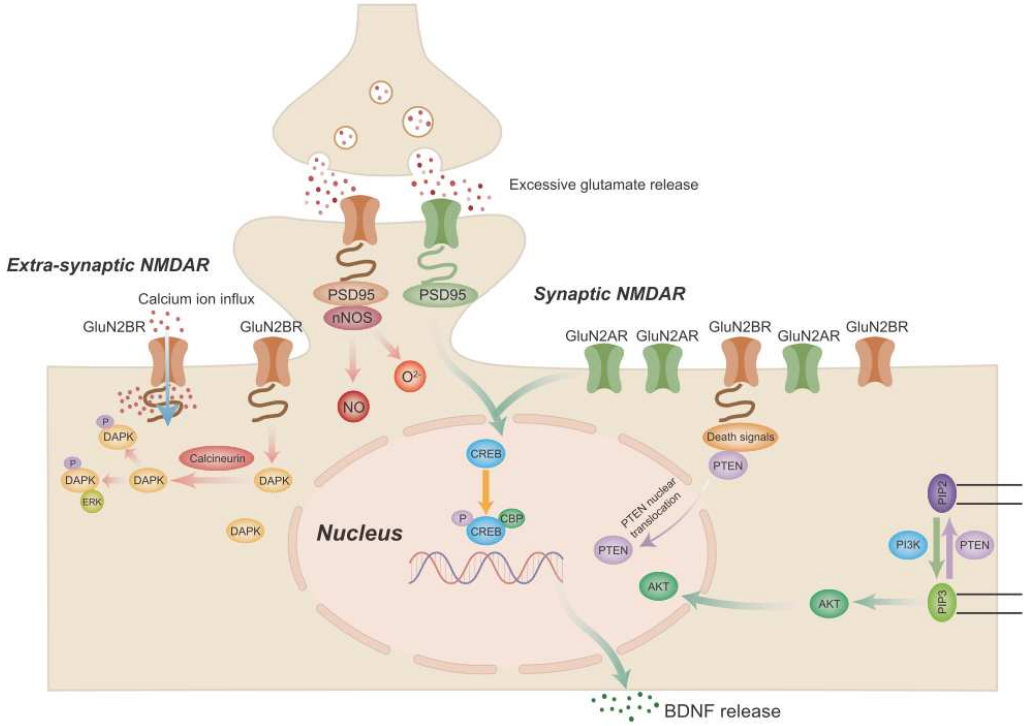

Figure 9: Excitotoxicity and signaling pathways involved in ischemic stroke. NMDAR N-methyl-D-aspartate receptors, PI3K Phosphatidylinositol 3 kinase, BDNF Brain-derived neurotrophic factor, CREB cAMP-response element-binding protein PTEN Phosphate and tension homology deleted on chromosome ten, PIP3 plasma membrane intrinsic protein 3, DAPK1 Death-associated protein kinase 1, PSD95 Postsynaptic density protein 95, nNOS Neuronal nitric oxide synthase (Sig Transduction and Targeted Therapy, 2022)

Prominent among the pathways mainly involved in the excitotoxicity process are:

- Phosphatidylinositol 3-kinase (PI3K)-Akt signaling pathway:

Stimulation of synaptic NMDARs (N-methyl-D-aspartate receptors) activates the pro-survival PI3K/Akt signaling pathway, leading to a neuroprotective effect. PI3K (phosphoinositide 3-kinase) is an intracellular kinase that is classified into three categories (I, II, and III) based on its structure and substrate specificity. In neurons, activation of the PI3K/Akt signaling pathway by NMDAR occurs through the involvement of Ca2+ and calmodulin, which recruit

phosphoinositide-dependent protein kinase 1. Additionally, Ca2+ triggers tyrosine phosphorylation of insulin receptor substrate 1, reinforcing NMDAR-induced Akt activation. This process has been reported to have a protective effect on ischemic stroke, both in in vitro neurons during hypoxia and in vivo against ischemic neuronal death. Inhibition of the PI3K/Akt signaling pathway has been shown to exacerbate ischemia-induced neuronal death in experimental stroke animals.

The neuroprotective effect of Akt is mechanistically linked to the phosphorylation and inactivation of various downstream targets. These targets include glycogen synthase kinase 3 beta (GSK3β), pro-apoptotic B-cell lymphoma 2 (Bcl2)-associated BAD, c-Jun N-terminal kinase (JNK)/p38 activator ASK1, and apoptotic p53. These effects are not limited to neurons but also extend to other types of neural cells, suggesting a broader role in inhibiting synaptic excitotoxicity and exerting neuroprotective effects in the context of ischemic stroke.

- Brain-derived neurotrophic factor (BDNF) and cAMP-response element-binding protein (CREB)-related gene products:

The activation of synaptic NMDARs (N-methyl-D-aspartate receptors) and subsequent Ca2+ influx stimulate the Ras/extracellular signal-regulated kinase (ERK) signaling pathway and nuclear Ca2+/calmodulin-dependent protein kinases. This activation leads to the phosphorylation and activation of CREB (cAMP response element-binding protein). Working in conjunction with NMDAR and BDNF (brain-derived neurotrophic factor), CREB promotes the expression of numerous pro-neuronal survival genes. BDNF production in the brain relies on Ca2+ influx through NMDAR, and synaptic NMDARs specifically enhance BDNF gene expression. On the other hand, extra-synaptic NMDARs inhibit CREB-mediated BDNF expression.

In experimental ischemic stroke models, BDNF is released into the brain and provides protection against ischemia-induced injury through the activation of neuronal GluN2A-NMDAR. These findings highlight the contributions of BDNF and, to some extent, the upstream CREB signaling pathway in the neuroprotective effects associated with synaptic excitotoxicity in cerebral ischemia.

- Phosphatase and tensin homolog (PTEN) signaling pathway:

Extra-synaptic NMDARs (N-methyl-D-aspartate receptors) are associated with signaling pathways linked to cell death and often produce effects that oppose those triggered by synaptic NMDARs. When activated by Ca2+ influx through NMDARs, PTEN (phosphatase and tensin homolog) is recruited to GluN2B-NMDARs. The direct interaction between PTEN and the GluN1 subunit of GluN2B-NMDARs enhances current flow through the channel, strengthening the connections between PTEN and the neuronal death signaling complex. Simultaneously, the excitotoxic stimulation of NMDARs leads to PTEN nuclear translocation, significantly reducing the phosphorylation of phosphatidylinositol-trisphosphate and Akt, consequently inhibiting PI3K/Akt signaling.

In contrast to the protective effect of PI3K/Akt signaling, PTEN signaling may decrease cell survival and induce neuronal death. Downregulating PTEN expression has been shown to inhibit extra-synaptic NMDAR currents and protect neurons from experimental ischemic injury. This evidence suggests a detrimental role of PTEN in ischemic stroke, largely mediated by the regulation of extra-synaptic NMDAR activities.

- Death-associated protein kinase 1 (DAPK1) signaling pathway:

DAPK1 (Death-Associated Protein Kinase 1) is a Ca2+/calmodulin-dependent serine/threonine-protein kinase, and its phosphorylation is involved in apoptotic cell death. In the context of ischemic stroke, DAPK1 plays a role in excitotoxicity. During ischemia, overactivation of NMDARs leads to Ca2+ influx, activation of Ca2+/calmodulin, and stimulation of calcineurin phosphatase. This activation of calcineurin subsequently dephosphorylates and activates DAPK1. Activated DAPK1 is then transferred to the GluN2B subunit of NMDARs, exacerbating ischemic injury.

Preventing the interaction between GluN2B and DAPK1 has been shown to attenuate neuronal excitotoxicity in mouse ischemic stroke models and downregulate NMDAR currents in vitro. Additionally, NMDAR-regulated calcineurin activation contributes to DAPK1 activation. Inhibiting NMDAR or calcineurin prevents DAPK1 dephosphorylation. Inhibition of DAPK1 has demonstrated protective effects against ischemic injury both in cultured neurons and in vivo. This suggests that potential treatments for ischemic stroke could involve targeting and inhibiting DAPK1. Notably, the pro-survival signaling factor ERK serves as a downstream effector of DAPK1, and the interaction between DAPK1 and ERK may block the

neuroprotective effect of ERK in experimental ischemic stroke, possibly by retaining ERK in neuronal cytoplasm.

- Postsynaptic density protein-95 (PSD95)/neuronal nitric oxide synthase (nNOS) signaling pathways and excitotoxicity-induced cell death:

Neuronal NMDARs (N-methyl-D-aspartate receptors) contribute to nitric oxide (NO) production, a process associated with calcium/calmodulin and regulated by neuronal nitric oxide synthase (nNOS). The subunits of NMDARs bind directly to PSD95 (postsynaptic density protein 95), a protein composed of three PDZ domains. The interaction between PSD95, NMDAR, and nNOS enhances Ca2+ influx, a key feature of excitotoxicity. PSD95/nNOS signaling is thought to play a pivotal role in ischemic stroke, as demonstrated by the improvement in neurological deficits observed in animals with cerebral ischemia when nNOS activity was inhibited pharmacologically or genetically. During cerebral ischemia, there is an increased interaction between NMDARs, PSD95, and nNOS in neurons, further exacerbating brain injuries in experimental ischemic stroke. These findings underscore the importance of the PSD95/nNOS complex in mediating excitotoxicity in ischemic stroke and contributing to the neurotoxic effects of extra-synaptic NMDARs.

E) OXIDATIVE AND NITROSATIVE STRESS

As a result of ischemia, especially following reperfusion, reactive oxygen species (ROS) like superoxide, hydrogen peroxide, and hydroxyl radical are produced. These ROS are pivotal mediators of tissue damage not only in the brain but also in other organs experiencing reperfusion injury, such as the heart or kidneys. Free radicals generated during this process can react with various cellular components (carbohydrates, amino acids, DNA, and phospholipids), causing direct structural damage. Moreover, free radicals initiate a detrimental cycle in the mitochondria, hindering the electron transport chain, leading to excessive production of superoxide, and activating mitochondrial permeability transition (mPT) along with the induction of mitochondrial outer membrane permeabilization (MOMP). Apart from impeding ATP production due to the loss of mitochondrial potential, mPT results in mitochondrial swelling and the release of proapoptotic molecules.

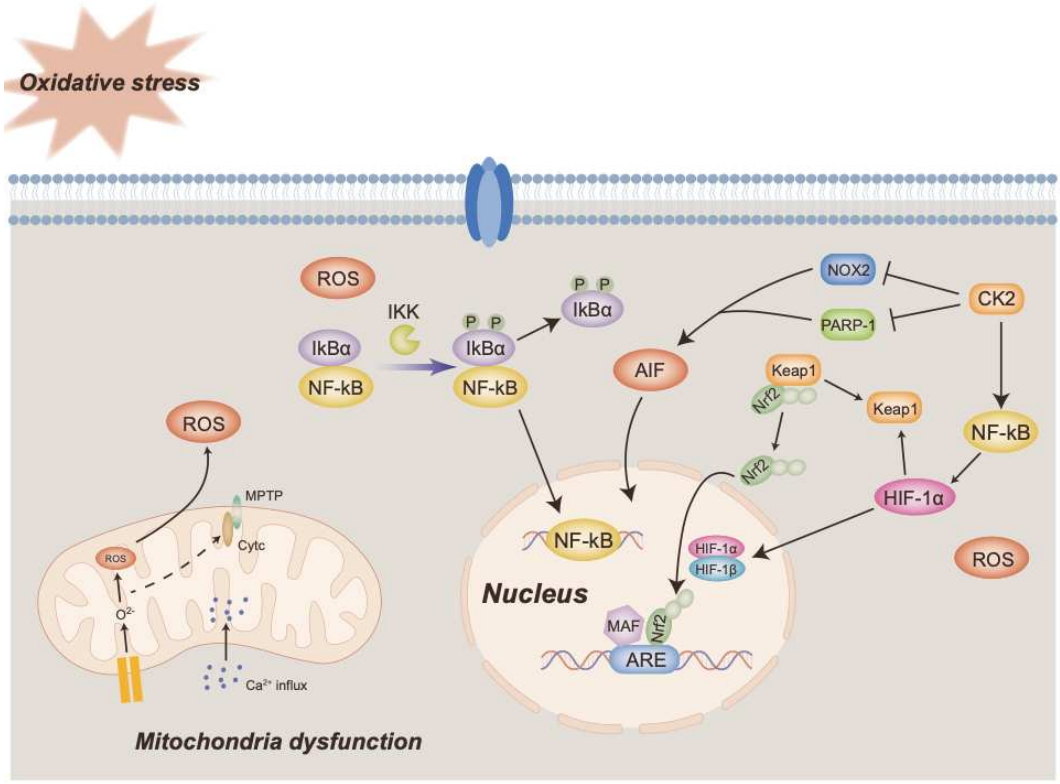

Figure 10: Oxidative stress and mitochondrial dysfunctions and signaling pathways involved in ischemic stroke. MPTP mitochondrial permeability transition pore, ROS Reactive oxygen species, ATP Adenosine triphosphate, HIF-1 Hypoxia-induced factor, Nrf2 Nuclear factor E2-related factor 2, ARE Antioxidant response element, CK2 Casein kinase 2, PARP-1 Poly ADP-ribose polymerase 1, AIF Apoptosis-inducing factor, PINK1 PTEN induced putative kinase 1, NF-kB Necrosis factor-kB (Sig Transduction and Targeted Therapy, 2022)

Oxidative stress is intricately linked to excitotoxicity, energy depletion, and ionic imbalances, all of which contribute significantly to tissue damage. Endogenous scavengers of ROS, such as superoxide dismutase (SOD) or glutathione, can mitigate injuries caused by oxidative stress, but they are insufficient to counteract damage resulting from focal ischemia. Studies in mice that overexpress SOD have demonstrated reduced injury following focal occlusion, supporting interventions that enhance endogenous ROS scavenging mechanisms as potential therapeutic targets after ischemic stroke.

In addition to oxidative stress, nitrosative stress plays a role in tissue damage. Nitric oxide (NO), synthesized from l-arginine by various isoforms of NO synthase (NOS I, NOS II, and NOS III), can be both beneficial and harmful during brain ischemia, depending on the timing and location of its production. Under conditions of increased oxidative stress, NO reacts with superoxide anions to produce the highly reactive and cytotoxic peroxynitrite. In models of focal cerebral ischemia, inhibiting inducible NO synthase (iNOS) has favorable outcomes, even when treatment is initiated 24 hours after inducing ischemia. Compared to the constitutively expressed isoforms of NO

synthase (eNOS and nNOS), iNOS produces larger amounts of cytotoxic NO. Blocking both iNOS and cyclooxygenase-2 (COX-2) remains effective in preventing damage even with delayed treatment (6–24 hours after ischemia onset) in rodent stroke models, suggesting these enzymes as promising targets for novel therapeutic strategies.

Prominent among the pathways mainly involved in the oxidative stress process are:

- Hypoxia-inducible factor (HIF) signaling pathway:

Hypoxia-inducible factor 1 (HIF-1) is a key transcription factor activated during cerebral ischemia and hypoxia, consisting of two subunits: HIF-1α and HIF-1β. HIF-1 plays a crucial role in enhancing the expression of glycolysis-associated genes under hypoxic conditions, enabling cells and tissues to adapt to low oxygen levels. Additionally, HIF-1α expression is strongly correlated with reactive oxygen species (ROS) levels, as the abundance of ROS stabilizes HIF-1α chains during hypoxia. In a positive feedback loop, the lack of oxygen and glucose due to ischemia may enhance HIF-1 expression, leading to oxidative stress and further stimulating HIF-1 activity.

Contrary to its potential role in promoting oxidative stress, some studies suggest that HIF-1α may also have protective functions, particularly in the regulation of energy metabolism, especially in neurons. Depletion of HIF-1α has been shown to result in excessive ROS, reduced glycolytic metabolism, and cell death in mouse embryo fibroblasts. Additionally, HIF-1α activation may benefit cellular homeostasis by maintaining redox equilibrium. Knockout of HIF-1α disrupts redox homeostasis and glucose metabolism in cell lines cultured under oxygen-glucose deprivation.

In summary, the role of HIF signaling in oxidative stress remains a subject of debate. While there are indications that HIF-1α activation may be associated with ROS production and oxidative stress, it is also suggested that HIF-1α may have protective effects on cellular homeostasis and redox equilibrium.

- Nuclear factor E2-related factor 2 (Nrf2) signaling pathway:

Nrf2 (nuclear factor erythroid 2-related factor 2) is a key regulator of cellular redox homeostasis and acts as a defense mechanism against oxidative stress. Activation of Nrf2 is protective against cerebral ischemic damage. In its resting state, Nrf2 is bound to Keap1 (Kelch-like ECH-associated protein 1), its specific cytoplasmic receptor. Under conditions of

electrophilic or oxidative stress, the structure of Keap1 changes, leading to the uncoupling of Nrf2 from Keap1. This uncoupling allows Nrf2 to translocate into the nucleus, where it binds to antioxidant response elements (ARE) and promotes the expression of various anti-inflammatory proteins, antioxidant enzymes, and growth factors.

In the context of ischemic stroke, elevated levels of reactive oxygen species (ROS) induce Nrf2 accumulation in the nucleus, where it contributes to the maintenance of normal mitochondrial function. The beneficial role of Nrf2 in mitochondria is suggested, as insufficient Nrf2 is associated with neuronal mitochondrial depolarization, ATP depletion, and impaired respiratory function.

Several downstream signaling pathways, including PI3K/Akt, ERK/mitogen-activated protein kinase (MAPK), and nuclear factor kappa beta (NF-κB), are involved in mediating the antioxidant effects of Nrf2 during ischemia. The neuroprotective PI3K/Akt pathway induces the nuclear translocation of Nrf2, stimulating the production of various antioxidants. Similarly, the ERK/MAPK signaling pathway during ischemia is associated with various neuroprotective processes, including preventing apoptosis and enhancing Nrf2 phosphorylation and translocation. The interactions between NRF2 and NF-κB signaling pathways are noteworthy. NRF2 deletion results in increased inflammation and high levels of NF-κB, while elevated NRF2 expression inhibits NF-κB-regulated pro-inflammatory and immune responses. This highlights the neuroprotective effects of NRF2 against NF-κB-induced inflammatory responses in cerebral ischemia.

Nrf2 plays a crucial role in protecting against oxidative stress and mitochondrial dysfunction in ischemic brain injuries, potentially through the regulation of various downstream signaling pathways.

- Casein kinase 2 (CK2) signaling pathway:

CK2 (Casein kinase 2) is an important oncogenic kinase with a role in counteracting ROS (reactive oxygen species) accumulation. CK2 exerts a protective effect against oxidative stress through various mechanisms:

1. Inhibition of NADPH oxidase: CK2 inhibits NADPH oxidase, a source of ROS, by regulating Rac1, a GTPase that significantly activates NADPH oxidase. This regulation may occur through interactions with other subunits and linking cytosolic subunits with the cell membrane.

2. Phosphorylation of Janus kinase and STAT3: CK2 phosphorylates Janus kinase and STAT3, enabling ROS detoxification by superoxide dismutase 2 (SOD2).

3. Activation of HIF-1α and NF-κB: CK2 activates HIF-1α and phosphorylates NF-κB, promoting the release of vascular endothelial growth factor (VEGF) and angiogenic proteins under hypoxic conditions.

However, there are contrasting findings regarding CK2 in the context of ischemic stroke:

- CK2 inhibition in the ischemic region may contribute to poly (ADP-ribose) polymerase 1 accumulation, leading to the release of mitochondrial cytochrome c and apoptosis-inducing factor (AIF), ultimately activating downstream apoptotic events.
- CK2 has been shown to activate ROS-generating NADPH oxidase isoform 2 in experimental ischemic stroke models, inducing AIF release into the mitochondria, DNA damage, and apoptosis.
- CK2 activation of cyclin-dependent kinase 5 and AKT/GSK3β in ischemia/reperfusion injuries may have detrimental effects. Inhibition of cyclin-dependent kinase 5 reportedly alleviates cerebral ischemic stroke-induced damage.

The dual role of CK2 in promoting protective mechanisms against oxidative stress while potentially contributing to apoptosis suggests a complex involvement in ischemic stroke.

- Mitophagy and related signaling pathways:

Mitophagy is a cellular process crucial for maintaining cellular homeostasis, and it acts as a protective strategy in various central nervous system diseases, including ischemic stroke. Several signaling pathways are implicated in mitophagy during ischemia-reperfusion:

1. PINK1/Parkin pathway: In the reperfusion stage, increased levels of the free radical $ONOO^-$ lead to the recruitment of dynamin-related protein 1 (Drp1) to the mitochondria, initiating PINK1/Parkin-associated mitophagy. Elevated reactive oxygen species (ROS) levels also upregulate Parkin, which is recruited by PINK1, further enhancing mitophagy. PINK1-regulated mitophagy is mechanistically associated with the opening of the mitochondrial permeability transition pore (MPTP).

2. Bcl2-interacting protein 3 (Bnip3) pathway: Elevated ROS levels induce upregulation of Bnip3, which can independently induce mitophagy. Bnip3-induced mitophagy is suggested to be independent of MPTP.

The activated mitophagy pathway aims to alleviate oxidative stress-induced cell injuries by promoting the degradation of damaged mitochondria. Enhanced mitophagy has been shown to have a potential role in ameliorating reactive oxygen species (ROS) accumulation in cerebral ischemic stroke.

F) TISSUE ACIDOSIS

Acidosis induced by ischemia plays a crucial role in mediating damage during focal cerebral ischemia. While acid-sensing ion channels (ASICs) have been identified as contributors to acidotic damage in cerebral ischemia, the mechanisms underlying acidosis remain unclear. Traditionally, it has been proposed that acidosis in cerebral ischemia is initiated by the accumulation of lactate. Hypoxia induces anaerobic glycolysis, leading to lactate production, and the "lactate-acidosis hypothesis" has been commonly invoked to explain the glucose "paradox" observed in cerebral ischemia. This paradox stems from experimental evidence indicating that elevated glucose levels exacerbate tissue damage, despite the crucial role of glucose in neuronal energy production. Acidosis disrupts intracellular protein synthesis and promotes the generation of various free oxygen radicals, thereby increasing tissue damage.

However, the role of acidosis in the pathophysiology of stroke is intricate and not fully comprehended, and the validity of the lactate-acidosis hypothesis has been scrutinized. Specifically, acidosis has the ability to block NMDA receptors, thereby exhibiting anti-excitotoxic effects. Moreover, it has been suggested that the reported detrimental effects of induced hyperglycemia in stroke models may be an experimental artifact, potentially stemming from the significant release of glucocorticoids following glucose infusion. The multifaceted nature of acidosis in stroke pathophysiology underscores the need for further research to unravel its intricate mechanisms and implications.

1.5 ETIOLOGIC CLASSIFICATION OF AIS AND STROKE SCALES

Accurately pinpointing the cause of ischemic stroke (IS) is vital for timely therapeutic interventions to address the root issue and prevent recurrent cerebral ischemic events. This task, however, poses challenges and relies on a combination of clinical features, imaging techniques, and various diagnostic exams. The Trial of ORG 10172 in Acute Stroke Treatment (TOAST), a placebo-controlled, randomized, blinded study of the low-molecular-weight heparinoid given to patients within 24 hours after stroke, stands out as a widely adopted method for classifying stroke etiology, systematically categorizing clinical data based on different mechanisms of formation. Introduced in 1993, the TOAST classification system proposed by the investigators divided ischemic stroke into five distinct etiological subtypes. This classification, rooted in clinical features and diagnostic study results, has become the gold standard for establishing ischemic stroke etiology. Not only has it been employed in clinical trials, but it has also served as a blueprint for genetic and epidemiological studies. Building upon TOAST, the criteria were refined in the SSS-TOAST system. Here, each original subtype was further categorized as "evident," "probable," or "possible," based on varying levels of diagnostic evidence. Despite the widespread use of TOAST, ongoing enhancements led to the development of a computerized version known as Causative Classification Systems (CCS). In 2009, the Atherosclerosis Small Vessel Disease Cardiac Source Other Causes (ASCO) system was introduced, demonstrating improved precision in identifying a wide range of causes and addressing diagnostic challenges more effectively. These classification systems, including CCS and ASCO, play a pivotal role in defining stroke subtypes and optimizing the efficiency of data in clinical studies. Notably, they reduce the number of patients classified as having undetermined causes and enhance subtype assignment compared to TOAST. The significance of classifying stroke subtypes extends beyond daily clinical practice, proving valuable in genetic research for clinical studies.

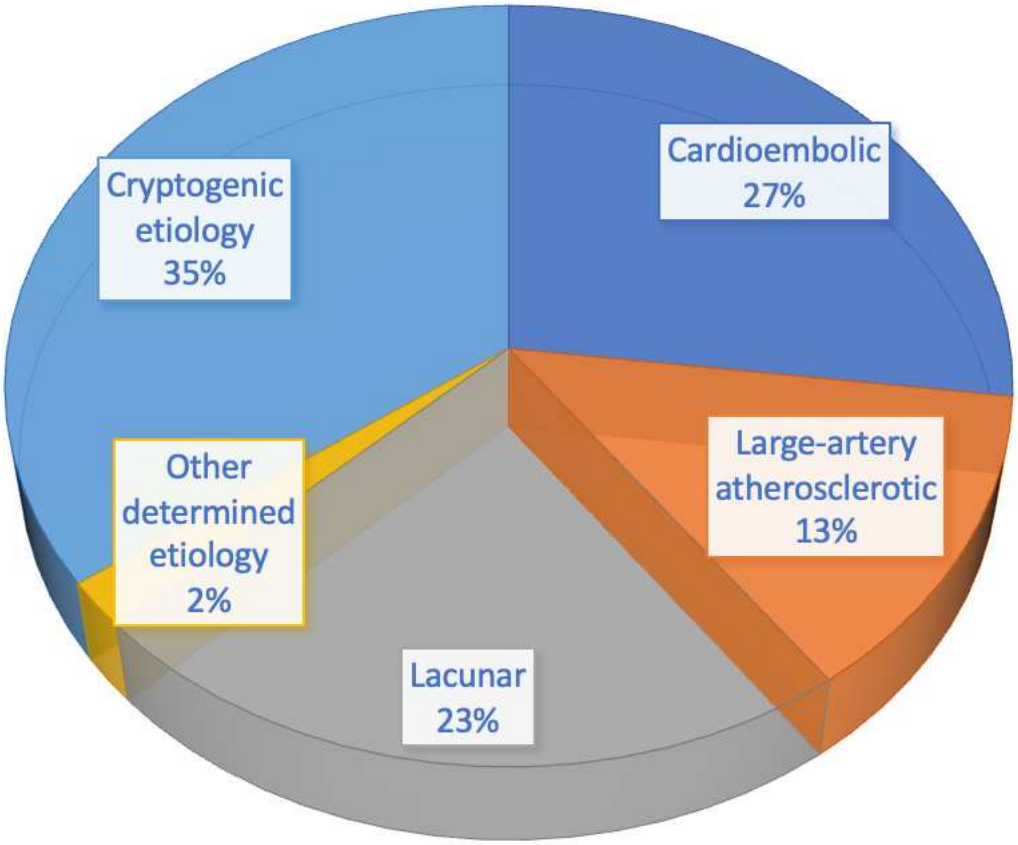

Figure 11: Trial of ORG 10172 in Acute Stroke Treatment (TOAST) classification of stroke subtypes

The TOAST system categorizes ischemic stroke into five specific groups:

1. Large-artery atherosclerosis (embolus/thrombosis): Characterized by the presence of significant (>50%) stenosis or occlusion in a major brain artery or branch cortical artery due to atherosclerosis.

2. Cardioembolism (high-risk/medium-risk): Characterized by arterial occlusions presumed to be caused by emboli originating in the heart. Divided into high-risk and medium-risk based on the relative propensity for embolism from identified cardiac sources.

3. Small-vessel occlusion (lacune): Strokes labeled as lacunar infarcts, characterized by traditional lacunar syndromes without evidence of cerebral cortical dysfunction.

4. Stroke of other determined etiology: Caused by rare conditions such as nonatherosclerotic vasculopathies, hypercoagulable states, or hematologic disorders.

5. Stroke of undetermined etiology:

- When the cause cannot be confidently determined.
- When no cause is found despite a cursory evaluation.
- When there are two or more potential causes, making a final diagnosis challenging.

Stroke underscores the importance of employing clinical rating scales not only for diagnostic and therapeutic purposes but also for assessing prognosis and guiding care decisions. These scales aid in the measurement of acute disability, functional outcomes, and overall quality of life, all of which significantly impact the trajectory of stroke recovery.

1. Acute Neurological Deficit Scales in Stroke

    - National Institutes of Health Stroke Scale (NIHSS): This scale, validated for use in various stroke-related contexts, serves multiple purposes. It assesses stroke severity, providing a numerical measure of neurological deficits based on a standardized examination. Comprising 11 items, the NIHSS covers aspects such as consciousness, visual fields, facial muscle activity, limb strength, coordination, language skills, and neglect. Its versatility extends to applications in telemedicine and remote evaluations, proving reliable and valid in different clinical settings. The NIHSS is particularly valuable for monitoring acute stroke patients' neurological status, aiding in quick and accurate assessments. Its predictive value extends to long-term outcomes, offering insights into the potential trajectory of poststroke recovery. However, it is essential to recognize the limitations of the NIHSS, such as its potential oversight of detailed cranial nerve assessments and its tendency to underestimate the severity of certain types of strokes, especially those in the vertebrobasilar arterial system.
    - Glasgow Coma Scale (GCS): This scale primarily assesses trauma severity in the acute phase, evaluating the patient's level of consciousness and coma severity. The GCS score ranges from 3 (indicating severe coma) to 15 (reflecting full consciousness). While it is commonly utilized in hospitals and intensive care units, the GCS has its limitations. For instance, it may struggle to provide accurate assessments in cases where patients cannot offer verbal responses or open their eyes, such as those with facial lesions or those who are intubated. To address this, alternative scales like the Swedish Reaction Level Scale may be employed.

2. Functional Outcome Measurement Scales in Stroke

- Barthel index (BI): The BI is a scale designed to assess 10 key aspects of activity related to self-care and patient mobility. It assigns a normal score of 100, with lower scores indicating varying degrees of dependence. BI relies on observations of patients engaging in various activities, including assessments of bowel and bladder continence. The scale demonstrates high reliability among observers and when obtained through telephone interviews. While it provides valuable insights into patients' abilities and predicts outcomes, it has limitations. BI may be less accurate in self-reported scores, especially in patients with cognitive dysfunction, severe diseases, or those over 75 years old. It moderately aligns with infarct volume but does not evaluate aspects such as cognitive level, language, visual function, emotional disability, and pain.
- Modified Rankin Scale (mRS): The mRS is another scale used to assess residual disability in stroke patients. Categorically defined with five degrees, ranging from 0 (no symptoms) to 5 (severe disability), the mRS assigns scores based on the assistance needed for varying levels of autonomy. It proves valid in assessing residual disability, with well-documented interobserver and intraobserver reliability. The mRS correlates modestly with infarct volumes. While offering a quick evaluation of stroke outcomes and activities in a social context, it includes items related to cognitive function, language, visual function, and pain. However, its limitation lies in the potential overestimation of clinical conditions in cases where a small cerebral infarct causes severe disability or a major infarction result in mild disabilities.
- Functional Independence Measure (FIM): The FIM serves as a disability measure, complementing BI and mRS in functional outcome studies of stroke. It consists of 18 items grouped into physical and cognitive characteristics, evaluating dimensions such as nutrition, personal cleanliness, communication, social interactions, problem-solving, and memory. Each item is scored on a scale from 1 (completely dependent) to 7 (completely independent). The FIM boasts high interobserver agreement, even when administered by telephone. While it provides a detailed evaluation of functional abilities, it requires a more complex learning process compared to other scales.
- Stroke Impact Scale (SIS): The SIS, developed for patients and caregivers, measures the quality of life in stroke survivors. With several versions and ongoing refinements, the latest version (SIS-16) evaluates disability levels 1–3 months after stroke. Similar to BI, SIS-

16 shows greater sensitivity in detecting different levels of disability. However, it relies on self-reporting or proxy use, posing limitations in aphasic patients or those in denial. Proxy responses may differ from direct patient responses, sometimes overestimating clinical severity. Currently, the SIS is not widely used in clinical settings.

1.6 TREATMENT STRATEGIES OF AIS

While advancements have been made in understanding the pathophysiological mechanisms of stroke and improving protocols for early diagnosis and treatment, certain clinical challenges persist. In the context of AIS management, various imaging techniques, such as computed tomography (CT) and magnetic resonance imaging (MRI), are routinely employed. Notably, the assessment of MRI mismatch between diffusion-weighted imaging (DWI) and fluid-attenuated inversion recovery (FLAIR), along with CT perfusion (CTP) imaging, enables the differentiation between core and penumbra regions.

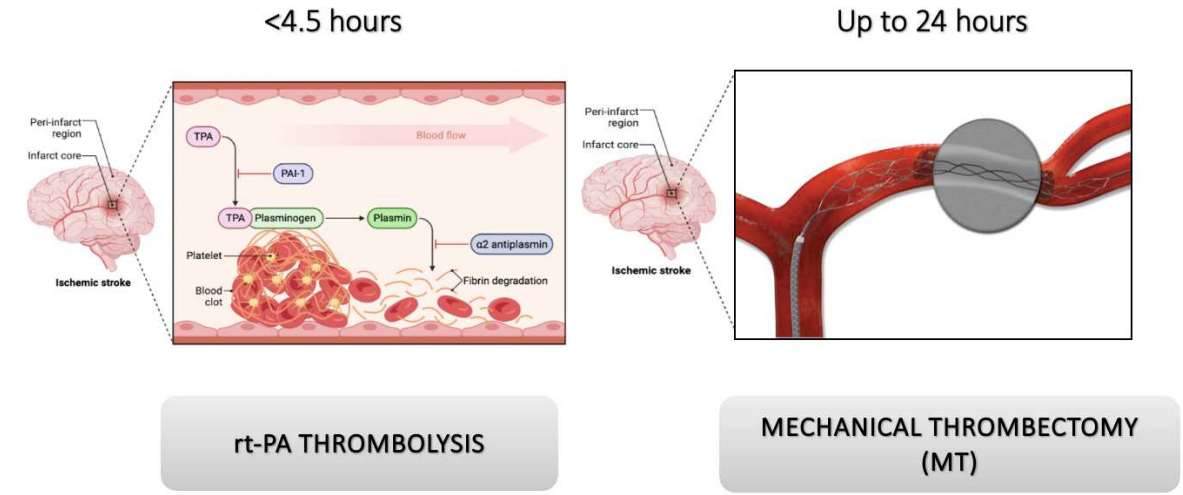

Figure 12: Treatment strategies of Acute Ischemic stroke (Biorender)

These advanced neuroimaging modalities play a crucial role in extending the time window for treatment decisions, particularly in selecting patients who could benefit from both intravenous thrombolysis (IVT) and endovascular treatment (EVT) reperfusion strategies. This extension is significant for patients presenting beyond the conventional 4.5–6 hour time window or those with an unknown or wake-up onset time.

The primary objective of therapeutic strategies for stroke is to achieve revascularization, limit secondary neuronal injury, and minimize long-term disability and stroke-related mortality. Currently, two approved therapies focus on reperfusing the ischemic region. The first is IVT using tissue-type plasminogen activator (tPA), commonly known as alteplase. The second approach involves a minimally invasive procedure called mechanical thrombectomy (MT), particularly using EVT with stent-retrievers. EVT has shown effectiveness in opening occluded proximal blood

vessels, enhancing functional outcomes in patients with large vessel occlusions (LVO) by removing the clot.

Another avenue in acute ischemic stroke therapy has aimed to disrupt the ischemic cascade, historically referred to as neuroprotection. Previous attempts in clinical trials to develop such neuroprotective treatments were largely unsuccessful. The term "cytoprotection" is now more appropriate for new approaches, as they should target components of the neurovascular unit beyond neurons. Future clinical trials are likely to favor therapies with multiple mechanisms of action due to the intricate nature of the ischemic cascade and the multitude of cellular targets involved.

1- INTRAVENOUS THROMBOLYSIS:

In the treatment of acute ischemic stroke, IVT is a critical intervention that has witnessed a significant shift in its approach over the past five years. This shift moves beyond a strict time window, embracing a tissue clock approach and exploring new thrombolytic drugs. Alteplase, a recombinant tPA (rtPA), has been the standard IVT drug approved by the U.S. Food and Drug Administration (FDA) for treating acute ischemic stroke within three hours of symptom onset since 1996. Employing recombinant DNA technology, Alteplase is produced as a glycosylated single chain. It is a serine protease that is found naturally in vascular endothelium, which catalyzes the production of plasmin, an active proteolytic enzyme, by cleaving the arginine-valine bond of plasminogen (Korninger C et al, 1981). It demonstrates remarkable thrombus specificity, boasting a 400-fold increase in proteolytic activity within a thrombus. This heightened activity leads to an acceleration of fibrinolysis, making it a potent thrombolytic agent. Upon intravenous administration, Alteplase initially remains relatively inactive in the circulatory system. However, its transformation into an active state occurs when it binds to fibrin, triggering the conversion of plasminogen to plasmin. This enzymatic cascade results in the dissolution of the fibrin clot, a pivotal step in restoring blood flow to ischemic regions of the brain. The pivotal NINDS trial in 1995 played a foundational role in establishing Alteplase's efficacy. This trial, encompassing 624 patients, showcased a 30% increase in favorable outcomes at three months, emphasizing minimal or no disability. However, this positive outcome was juxtaposed with a 6.4% risk of symptomatic intracranial hemorrhage (sICH), marking a crucial consideration in Alteplase administration. Over time, efforts to extend the treatment window have been underway. The ECASSIII study pushed the temporal boundaries to 4.5 hours from symptom onset, albeit with modest results. Meta-

analyses consolidated findings from various thrombolysis studies, reinforcing the overall efficacy of Alteplase, with adjusted odds ratios indicating a significant positive impact. As stroke management evolves, the International Stroke Trial (IST-III) added substantial weight to the efficacy of thrombolysis, particularly for patients over 80 years old. The consideration of age as a factor in treatment response underscores the nuanced nature of stroke intervention. Beyond its immediate thrombolytic effects, Alteplase's broader impact becomes evident when considering its pleiotropic role. In addition to its role in clot dissolution, endogenous tissue plasminogen activator (tPA), of which Alteplase is a synthetic variant, participates in the dynamic remodeling of the extracellular matrix. This multifaceted role extends to the intricate processes shaping the central and peripheral nervous systems.

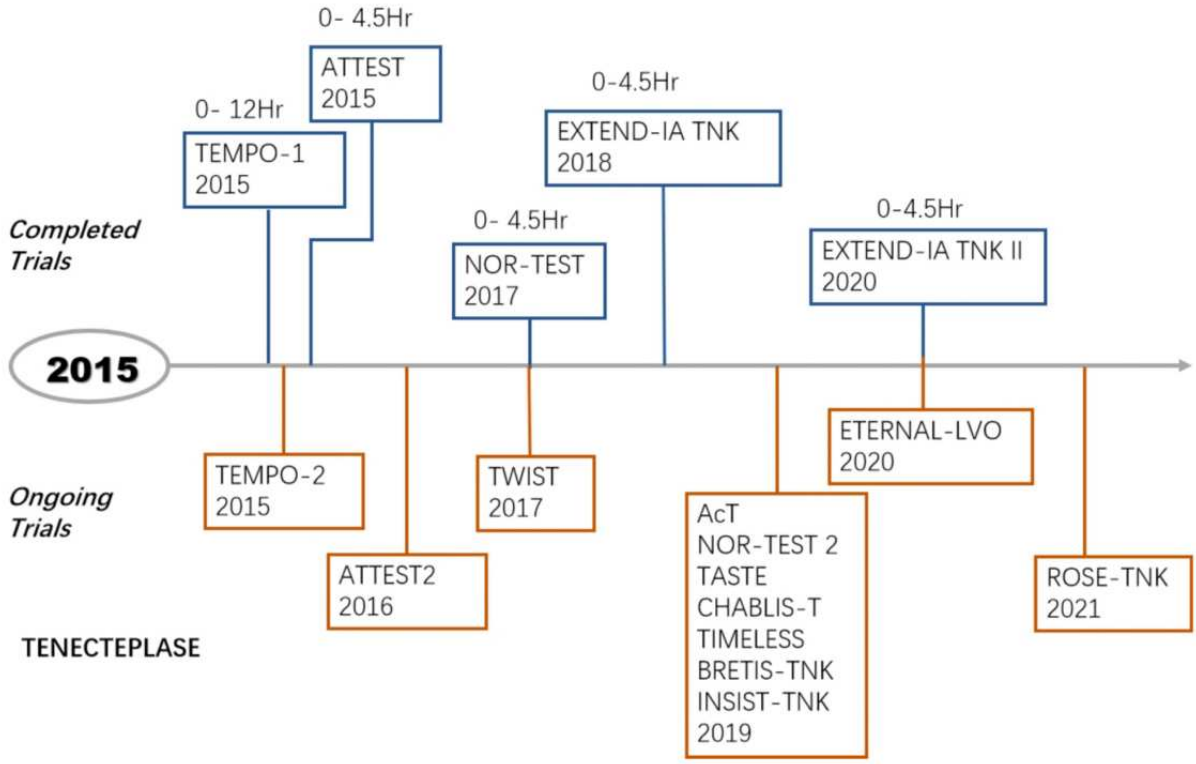

Figure 13: History of tenecteplase trials in acute ischemic stroke from 2015 Circulation Research. 2022;130:1230–1251. DOI: 10.1161/CIRCRESAHA.121.319948.

Tenecteplase (TNK) has garnered significant interest as a potential alternative to or replacement for alteplase in stroke thrombolysis. TNK, a genetically modified variant of alteplase, offers theoretical and practical advantages, including a longer half-life, greater fibrin specificity, and tolerance to plasminogen activator inhibitor-1. Unlike alteplase, TNK allows for a bolus injection without the need for a one-hour infusion. Various studies have explored TNK's effectiveness in comparison to alteplase, indicating its potential benefits, especially in patients with LVO. While

the NOR-TEST trial did not show TNK's superiority over alteplase in mild stroke patients, further research is underway, including the ongoing NOR-TEST 2 trial. The EXTEND-IA TNK study demonstrated TNK's increased rate of successful recanalization before thrombectomy compared to alteplase, supporting the potential use of TNK in conjunction with mechanical thrombectomy. The optimal dose for TNK, particularly in bridging therapy, is still under investigation, and ongoing trials like TEMPO-2 are expected to provide more insights. Current evidence suggests that TNK may serve as an alternative to alteplase in acute ischemic stroke, particularly in patients eligible for MT. Ongoing and future trials, such as TASTE, ATTEST2, and AcT, will likely contribute further evidence regarding TNK's efficacy and safety in acute ischemic stroke. Imaging-based trials, including TWIST, CHABLIS-T, TIMELESS, ETERNAL-LVO, and ROSE-TNK, are exploring TNK's utility in the extended time window beyond 4.5 hours after symptom onset. While the 2019 American Heart Association/American Stroke Association guidelines acknowledge the potential use of TNK over alteplase in certain cases, further investigations and regulatory approvals are needed for TNK's broader acceptance in acute ischemic stroke treatment. Presently, TNK is FDA-approved for myocardial ischemia and is under continued evaluation for acute ischemic stroke.

Staphylokinase, first isolated and purified in 1948, emerged as a thrombolytic drug with high fibrin-selectivity. However, early experiences with patients suffering from acute myocardial infarction revealed a significant drawback—many patients developed neutralizing antibodies against it, hindering further research on this agent. In response, a new thrombolytic drug, non-immunogenic staphylokinase, was developed. This modified recombinant staphylokinase boasts low immunogenicity, high thrombolytic activity, and specificity to fibrin. The FRIDA trial, conducted in 385 patients, aimed to compare non-immunogenic staphylokinase with alteplase in treating acute ischemic stroke occurring 4.5 hours after symptom onset in Russia. The results indicated that non-immunogenic staphylokinase was non-inferior to alteplase concerning favorable functional outcomes, with a comparable rate of symptomatic intracerebral hemorrhage (sICH). Despite the trial facing challenges due to a relatively wide noninferiority margin, a small sample size, and a lack of phase 2 trial data specific to acute ischemic stroke, it represents a significant step forward. More trials are necessary to delve deeper into the potential superiority of non-immunogenic staphylokinase when compared to alteplase.

2- MECHANICAL THROMBECTOMY:

Thrombectomy is a mechanical interventional procedure designed to remove a blood clot or thrombus from a blood vessel, typically under image guidance and using endovascular devices. While it is most commonly associated with AIS, thrombectomy is also employed as a procedure for clot removal in acute myocardial infarction (MI) and pulmonary embolism (PE). The procedure of mechanical thrombectomy involves the use of various techniques, primarily utilizing catheter-based therapies. The three main approaches are:

- Stent-Retrieval: In stent-retrieval thrombectomy, a catheter with a stent at its tip is navigated through the blood vessels to the site of the clot. The stent is then deployed, capturing, and trapping the clot within its mesh. The catheter with the stent and the trapped clot is then carefully withdrawn, removing the clot from the blood vessel.
- Direct Aspiration: This technique involves using a catheter with a suction or aspiration device at its tip to directly aspirate, or suck out, the clot from the blood vessel. The catheter is advanced to the location of the clot, and the suction force is applied to remove the thrombus.
- Combination Approach: In some cases, a combination of stent-retrieval and direct aspiration techniques may be employed to optimize clot removal. This hybrid approach aims to enhance the effectiveness of the thrombectomy procedure.

Overall, MT has become a crucial intervention in the management of various thrombotic conditions, offering a minimally invasive and effective means of clot removal in specific clinical scenarios. The choice of technique depends on the characteristics of the clot, the location within the vascular system, and the patient's clinical condition (Shibin M et al, 2023).

A meta-analysis of five major randomized controlled trials (MR CLEAN, ESCAPE, REVASCAT, SWIFT PRIME, and EXTEND-IA) had collectively examined the efficacy of endovascular treatment (EVT) for AIS associated with LVO in the MCA and ICA. The primary focus was on interventions within 6 hours of symptom onset. The meta-analysis revealed that EVT significantly reduced disability at 90 days compared to medical management, with an adjusted common odds ratio (OR) of 2.49 (95% CI, 1.76–3.53; $P<0.0001$). The number needed to treat (NNT) to achieve a meaningful reduction in disability was 2.6. The benefits of EVT extended to various subgroups, including patients aged 80 or older, those randomized more than 5 hours after symptom onset, and

individuals ineligible for iv-tPA. Importantly, mortality at 90 days and the risk of sICH did not differ significantly between the EVT and control groups. Subsequent trials, DAWN and DEFUSE 3, challenged the conventional time window for revascularization by extending it up to 24 hours after symptom onset. DAWN compared the use of a specific stent-retriever within a 6- to 24-hour time window, demonstrating improved functional independence at 90 days (49% vs. 13% in control). DEFUSE 3 enrolled patients within the 6- to 16-hour time window, achieving significantly higher rates of complete recanalization and functional independence with EVT. The AURORA meta-analysis challenged the distinction between DEFUSE 3 (6–16 hours) and DAWN (6–24 hours), suggesting it might be unnecessary. Thrombectomy beyond 6 hours post-symptom onset was beneficial over medical management, with an unadjusted common OR of 2.42 (95% CI, 1.76–3.33; P<0.0001). The EVT effect was stronger in patients randomized within 12 to 24 hours. Ongoing trials like DIRECT ANGIO and WE-TRUST aim to optimize workflow and reduce time to treatment by directly transferring patients to catheter labs, bypassing conventional emergency department routes. This approach, using newer angiography systems, has shown promising results in reducing the time from symptom onset to recanalization. Studies like ASTER and COMPASS explored alternative thrombectomy strategies, specifically direct aspiration as a first-pass technique. Results indicated non-inferior functional outcomes with direct aspiration compared to stent-retriever thrombectomy. Achieving early and complete revascularization with a single pass is critical for favorable functional outcomes. Understanding clot characteristics, such as density and susceptibility to fracture, plays a vital role in achieving a first-pass effect during thrombectomy. Balloon guide catheters have shown efficacy in inducing flow arrest and reversal during EVT, leading to higher rates of functional independence. Ongoing trials are investigating the value of thrombectomy in various patient populations, including those presenting within a 4.5-hour time window, with large core volume infarct, and in specific occlusion sites. Limitations of current studies include small sample sizes, selection bias, and variations in EVT modalities.

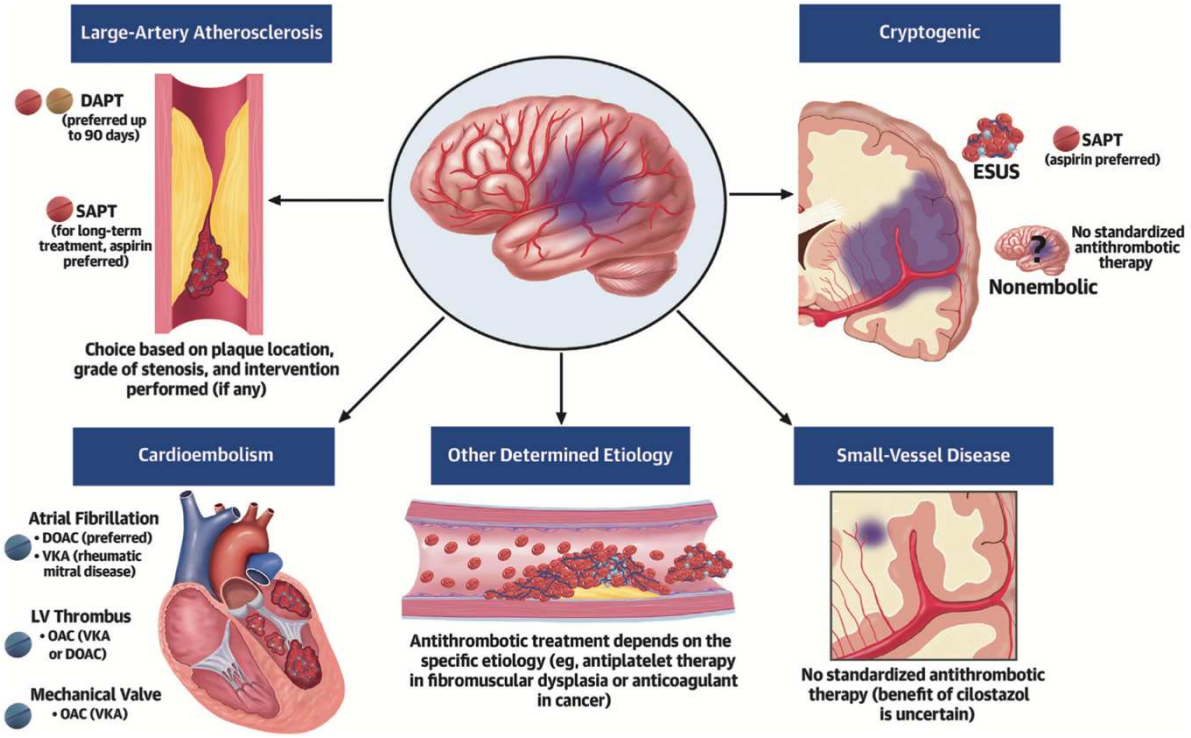

Figure 14: Different therapeutic strategies based on AIS etiology, (Greco A, J am Coll Cardiol, 2023)

Choosing the most effective antithrombotic therapy for preventing primary and secondary ischemic strokes involves a thorough assessment of the risks and benefits associated with these treatments. The selection between antiplatelet and anticoagulant regimens for secondary prevention is heavily influenced by the underlying cause of the stroke. In general, managing ischemic stroke requires a personalized approach, taking into consideration the unique clinical characteristics, comorbidities, and preferences of each individual. Survivors of ischemic stroke face a notable risk of recurrence, with variations based on ethnicity, sex, and stroke subtype. Over the past six decades, the rates of recurrent ischemic strokes and major vascular events have markedly decreased, primarily due to improved blood pressure control and the use of antithrombotic agents, which play a pivotal role in both primary and secondary prevention. Selecting the appropriate antithrombotic agent involves identifying modifiable risk factors for stroke and understanding the pathophysiology of the initial ischemic injury. Antiplatelet therapy is typically favored in cases involving large-artery atherosclerosis and small-vessel disease, where there is likely arterial plaque disruption or endothelial injury. Conversely, anticoagulation is recommended in conditions characterized by blood stasis (AF) or hypercoagulable states (thrombophilia) that often lead to the formation of red thrombi. It's crucial to note that while antithrombotic therapies offer protection against ischemic events, they come with an elevated

risk of bleeding. Balancing this tradeoff requires considering various factors, including the overlap in risk factors for ischemic and bleeding events, as well as the potential for hemorrhagic transformation of ischemic stroke. Consequently, the pharmacological management of this condition is intricate and poses challenges.

- MANAGEMENT OF LAA STROKES:

LAA refers to the presence of atheromatous plaques in either the intracranial arteries (specifically the anterior cerebral, middle cerebral, and basilar arteries) or the extracranial arteries (namely the carotid and vertebral arteries), leading to stenosis of 50% or more, or complete vessel occlusion. The prevention and management of strokes of this nature primarily rely on antithrombotic therapy, involving a diverse range of drugs (including antiplatelet and anticoagulant agents), combinations, and durations.

PRIMARY PREVENTION: The potential advantages of using aspirin for the primary prevention of ischemic stroke must be carefully weighed against the risk of bleeding. Other strategies for preventing adverse cardiovascular events, including ischemic stroke, were compared with aspirin in trials involving individuals at high risk and patients with manifestations of atherosclerotic vascular disease, including cerebrovascular disease. In the CAPRIE (Clopidogrel Versus Aspirin in Patients at Risk of Ischemic Events) trial, the benefit of clopidogrel compared with aspirin was less pronounced in patients without a previous history of ischemic events. Significant reductions in stroke were observed with the addition of clopidogrel to aspirin in the CHARISMA (Clopidogrel for High Atherothrombotic Risk and Ischemic Stabilization, Management and Avoidance) trial and with the addition of low-dose rivaroxaban in COMPASS.

SECONDARY PREVENTION: Initial studies focusing on antiplatelet strategies for AIS primarily emphasized aspirin monotherapy, yielding mixed results in two large trials. However, a pooled analysis demonstrated a 30% reduction in recurrent stroke with in-hospital initiation of aspirin. In the CAPRIE trial, where a third of patients experienced an ischemic stroke within the previous 6 months, clopidogrel did not show superiority to aspirin in this subgroup. The SOCRATES trial, comparing ticagrelor with aspirin in 13,199 patients with nonsevere AIS or high-risk transient ischemic attack (TIA), showed no apparent benefit. Small Japanese trials on low-dose prasugrel also failed to demonstrate significant benefits. Dipyridamole and

cilostazol, though investigated, showed positive evidence with limited adoption in clinical practice. Numerous trials explored dual antiplatelet therapy (DAPT) with aspirin and clopidogrel, resulting in mixed outcomes. The MATCH trial, involving 7,599 high-risk patients, did not associate DAPT with a reduction in ischemic events compared with aspirin alone, increasing the risk of bleeding. However, DAPT's evidence is more compelling in acute minor stroke or high-risk TIA, although these trials included populations beyond large-artery atherosclerosis. The CHANCE trial, involving 5,170 Chinese patients, demonstrated a significant reduction in stroke incidence with DAPT without an increase in severe bleeding. The POINT trial, halted prematurely due to excess major bleeding, showed a 25% reduction in ischemic events at 90 days with DAPT. Temporal trends indicate that DAPT's benefit is most prominent in the initial 3 weeks following an ischemic stroke. Discrepancies between trials may reflect differences in population, loading dose of clopidogrel, and DAPT duration. DAPT with aspirin and ticagrelor was also considered in the THALES trial, reducing the composite of ischemic stroke or death by 21% at 30 days but with increased severe bleeding. The CHANCE-2 trial, involving 11,255 Chinese patients with minor stroke or TIA carrying cytochrome P450 2C19 loss-of-function alleles, showed a 23% reduction in stroke risk with ticagrelor-based DAPT, accompanied by an increase in bleeding without differences in severe or moderate bleeding. Aspirin and cilostazol combination trials were mainly impaired by methodological limitations. The CSPS.com trial, involving 1,879 Japanese patients, showed a 51% reduction in stroke risk with cilostazol-based DAPT compared with aspirin or clopidogrel monotherapy, without increased severe or life-threatening bleeding. Aspirin and dipyridamole combination trials showed mixed results. While better than placebo in recent ischemic stroke, noninferiority to clopidogrel could not be demonstrated. Clinical use has been limited due to severe headaches, leading to dipyridamole discontinuation. The combination of clopidogrel and dipyridamole, tested in diabetic patients with peripheral artery disease, showed significant reductions in ischemic events and stroke or TIA compared with clopidogrel alone. The TARDIS trial, involving 3,096 patients with acute ischemic stroke or TIA, was stopped prematurely due to increased major bleeding without differences in recurrent ischemic stroke or TIA. Treatment recommendations consider antiplatelet therapy a fundamental component for large-artery atherosclerosis-related strokes. As per American guidelines, aspirin is recommended within 24 to 48 hours for patients not eligible for thrombolysis, whereas it is delayed until 24 hours later for those treated with intravenous alteplase. Conversely,

ticagrelor and triple antiplatelet therapy with aspirin, clopidogrel, and dipyridamole are not recommended. For minor non-cardioembolic ischemic stroke, DAPT with aspirin and clopidogrel is recommended within 24 hours and continued for 21 to 90 days. DAPT with aspirin and clopidogrel should be considered for 3 months in patients with recent stroke or TIA and a 70% to 99% intracranial artery stenosis. DAPT with aspirin and ticagrelor may be considered for 30 days in patients with acute minor stroke or high-risk TIA and a 30% or greater intracranial artery stenosis. European guidelines recommend aspirin, dipyridamole plus aspirin, or clopidogrel alone in patients with non-cardioembolic ischemic stroke or TIA. Guidelines from the European Stroke Organization on TIA management recommend short-term DAPT with aspirin and clopidogrel in high-risk patients, whereas DAPT is not recommended over antiplatelet monotherapy in those at low risk.

- MANAGEMENT OF CE STROKES:

CE stroke occurs when cerebral blood flow is obstructed by a clot or debris originating from the heart. Predisposing conditions leading to blood stasis and clot formation in the heart chambers include atrial fibrillation, heart failure, the presence of mechanical prostheses, infective endocarditis, and paradoxical embolism through a patent foramen ovale. Antithrombotic therapy is crucial for both primary and secondary prevention in certain causes of cardioembolic stroke, and surgical or device interventions may also be considered based on the underlying etiology.

PRIMARY PREVENTION: Atrial fibrillation is the most common high-risk condition for ischemic stroke and necessitates anticoagulation unless contraindicated. Aspirin monotherapy is ineffective, and dual antiplatelet therapy (DAPT) with aspirin and clopidogrel has limited efficacy. Vitamin K antagonists (VKAs) like warfarin have traditionally been the mainstay of anticoagulant therapy for atrial fibrillation patients with additional stroke risk factors. However, their need for frequent monitoring and dose adjustments has resulted in low patient adherence and underuse. Direct oral anticoagulants (DOACs), including dabigatran, rivaroxaban, apixaban, and edoxaban, have emerged as safer and more convenient options due to their rapid onset and offset of action, fewer interactions, and fixed-dose administration without routine monitoring. DOACs have demonstrated safety and efficacy comparable to warfarin in preventing stroke and systemic embolism in patients with nonvalvular atrial

fibrillation. While DOACs have been associated with a reduction in ischemic stroke or systemic embolism, hemorrhagic stroke, and all-cause mortality compared with warfarin, they are also linked to a higher risk of gastrointestinal bleeding. For patients with contraindications to oral anticoagulation, DAPT reduces the risk of stroke but increases major bleeding and intracranial hemorrhage. Left atrial appendage occlusion may be considered as a valid alternative. Factor XI inhibitors, such as asundexian, have shown promise in reducing bleeding rates compared with apixaban. Ongoing trials, like OCEANIC-AF, aim to further evaluate the efficacy and safety of asundexian compared to apixaban. Patients with heart failure, particularly those with a thrombus in the left heart chambers, are at risk for cardioembolic stroke. Warfarin has shown significant stroke reduction compared with antiplatelet therapy in these patients with sinus rhythm. However, low-dose rivaroxaban did not prove more effective than placebo in preventing ischemic events in the COMMANDER-HF trial. Routine anticoagulation is not recommended for primary prevention in heart failure patients in sinus rhythm due to the increased risk of bleeding. Patients with mechanical heart valves require lifelong treatment with VKAs, with an INR target between 2.5 and 3.5, depending on prosthesis thrombogenicity. The risk of thromboembolism is highest in the first 6 months, and VKA administration should start immediately. Antiplatelet therapy may be considered in patients at very high risk of thromboembolism. For those with mitral or tricuspid bioprosthetic valves without another indication for oral anticoagulation, VKA therapy for 3 months is recommended. Aspirin is an alternative for aortic surgical bioprostheses and is the standard of care after transcatheter aortic valve implantation in patients not requiring anticoagulation. DOACs are not inferior to VKA in reducing major adverse cardiovascular events in patients with bioprosthetic valves and a baseline indication for anticoagulation. In cases of infective endocarditis, stroke can result from vegetation fragments migrating into the cerebral circulation. Antibiotic therapy is a fundamental part of treatment, and cardiac surgery is recommended for high-risk embolism patients. There is currently no evidence supporting the use of antiplatelet therapy post-diagnosis of infective endocarditis, and limited data exist on the effects of oral anticoagulants. Paradoxical embolization through a patent foramen ovale accounts for a significant proportion of cryptogenic cardioembolic strokes. Neither medical therapy nor percutaneous closure is generally recommended for primary prevention in this scenario.

SECONDARY PREVENTION: The treatment effects of Direct Oral Anticoagulants (DOACs) remain consistent across subgroups, indicating their efficacy in both primary and secondary

prevention, especially in patients with atrial fibrillation. The optimal timing to initiate DOACs after an acute stroke in atrial fibrillation patients is uncertain and depends on factors like the risk of hemorrhagic transformation, infarct size, and other considerations. A randomized trial demonstrated noninferiority in early initiation (within 4 days) compared to delayed start (between 5 and 10 days). Guidelines recommend initiating oral anticoagulation between 2 and 14 days (Class 2b) or beyond 14 days (Class 2a) based on low and high risk, respectively. Considering infarct size, the ELAN trial compared early to late initiation, revealing similar efficacy and safety for both strategies. For secondary stroke prevention in patients with heart failure, there is no specific evidence, and general strategies for preventing recurrent cardioembolism should be applied, such as anticoagulation in the presence of atrial fibrillation. The addition of antiplatelet therapy may be considered in patients with an ischemic stroke despite an adequate International Normalized Ratio (INR). In cases of ischemic stroke related to endocarditis, the decision to undergo cardiac surgery depends on a comprehensive evaluation of neurological damage, cardiac function, and the extent of infective endocarditis.

- MANAGEMENT OF CRYPTOGENIC STROKES:

The term "cryptogenic" refers to ischemic strokes whose origin remains unknown despite thorough diagnostic evaluations. Approximately half of cryptogenic strokes are classified as embolic strokes of undetermined source (ESUS), indicating embolic events without a clear origin even after diagnostic work-up. ESUS is a heterogeneous condition, and while covert atrial fibrillation was initially considered its primary cause, recent research has identified other potential sources of embolism. These include atrial cardiopathy, non-stenotic plaques, hypercoagulability associated with malignancy, and aortic arch atherosclerosis. This diversity has prompted investigations into alternative antithrombotic therapies for secondary prevention, involving both anticoagulant and antiplatelet drugs. However, four randomized clinical trials of DOACs in ESUS (NAVIGATE ESUS, RE-SPECT ESUS, ATTICUS, and ARCADIA) did not demonstrate a significant benefit of anticoagulation over aspirin. These trials were terminated prematurely or showed futility due to concerns about major bleeding, intracranial hemorrhage, and the absence of clear benefits in preventing recurrent ischemic stroke. The NAVIGATE ESUS trial, comparing rivaroxaban and aspirin, was terminated prematurely due to higher rates of major bleeding and intracranial hemorrhage with rivaroxaban, without a clear

benefit in preventing recurrent ischemic stroke. Similarly, the RE-SPECT ESUS trial, comparing dabigatran and aspirin, did not show the superiority of dabigatran over aspirin, although event curves started to diverge in favor of dabigatran after 450 days. The ATTICUS trial, comparing apixaban and aspirin, was terminated prematurely for futility. The trial enrolled an enriched ESUS population with additional risk factors for cardiac thromboembolism. Continuous cardiac monitoring detected subclinical episodes of atrial fibrillation in 26% of the study population. Patients found to have atrial fibrillation in the aspirin arm were switched to receive apixaban, potentially contributing to the neutral result. In the ARCADIA trial, comparing apixaban and aspirin in patients with ESUS and evidence of atrial cardiopathy, there were no differences in terms of stroke recurrence, death, and intracranial hemorrhage. The trial was stopped prematurely for futility. Based on these results, anticoagulation therapy cannot be generally recommended for the secondary prevention of stroke in unselected patients with ESUS. Exploratory analyses have suggested potential age-related differences in treatment effects, with anticoagulation possibly working better in older patients with multiple concomitant embolic sources.

- MANAGEMENT OF SVD STROKES:

Strokes from SVD are characterized by small subcortical infarcts resulting from the occlusion of small deep perforating arterioles. The pathogenesis, often linked to lipohyalinosis, is not fully understood. Hypertension is a crucial risk factor for small-vessel disease strokes, and interventions to control blood pressure and other modifiable risk factors are essential for reducing further events and cognitive impairment. Evidence for antithrombotic therapy in strokes from small-vessel disease is primarily derived from subgroup analyses of trials with heterogeneous stroke populations, with limited dedicated trials. The SPS3 (Secondary Prevention of Small Subcortical Strokes) trial, which added clopidogrel to aspirin in patients with recent small-vessel disease strokes, did not reduce recurrent strokes and was associated with more bleeding and death. The LACI-2 (Lacunar Intervention-2) trial investigated the role of cilostazol and isosorbide mononitrate in small-vessel disease strokes, showing improved clinical outcomes with both drugs. Anticoagulation has been discouraged due to an association with cerebral microbleeds in small-vessel disease, making patients prone to bleeding with anticoagulants. The evidence supporting antiplatelet therapy, especially aspirin, is strong, with conflicting results for dipyridamole. Cilostazol has shown promising effects in

small-vessel disease due to its action on endothelial function and mild antiplatelet effects. Network meta-analyses have indicated that cilostazol is the most effective agent for strokes from small-vessel disease. DAPT, including aspirin and clopidogrel, failed to show a reduction in recurrent ischemic strokes in small-vessel disease and was associated with increased major bleeding compared to aspirin alone.

- MANAGEMENT OF STROKES OF OTHER DETERMINED ETIOLOGY:

Strokes of other determined etiology encompass a highly heterogeneous category, involving various conditions that can potentially cause ischemic strokes. There is no standardized strategy for antithrombotic prevention in this stroke subtype, and treatment should be tailored based on the specific underlying etiology. The approach to antithrombotic prevention varies depending on the identified etiology. For certain conditions like moyamoya disease, several hypercoagulable states, fibromuscular dysplasia, or carotid web, antiplatelet therapy is recommended. On the other hand, conditions such as several congenital heart diseases, cancer, or antiphospholipid syndrome may necessitate anticoagulation for secondary prevention of ischemic strokes. Extracranial carotid or vertebral dissections represent a relatively common cause of strokes in young adults. The CADISS (Cervical Artery Dissection in Stroke Study) trial compared 3-month antiplatelet and anticoagulant regimens in patients with acute extracranial dissection. The study demonstrated substantial equipoise between the two approaches. Accordingly, current guidelines recommend either aspirin or VKA for the first 3 months after an extracranial dissection, with a Class 2a recommendation. This implies that either option is reasonable and may be considered based on individual patient factors and preferences.

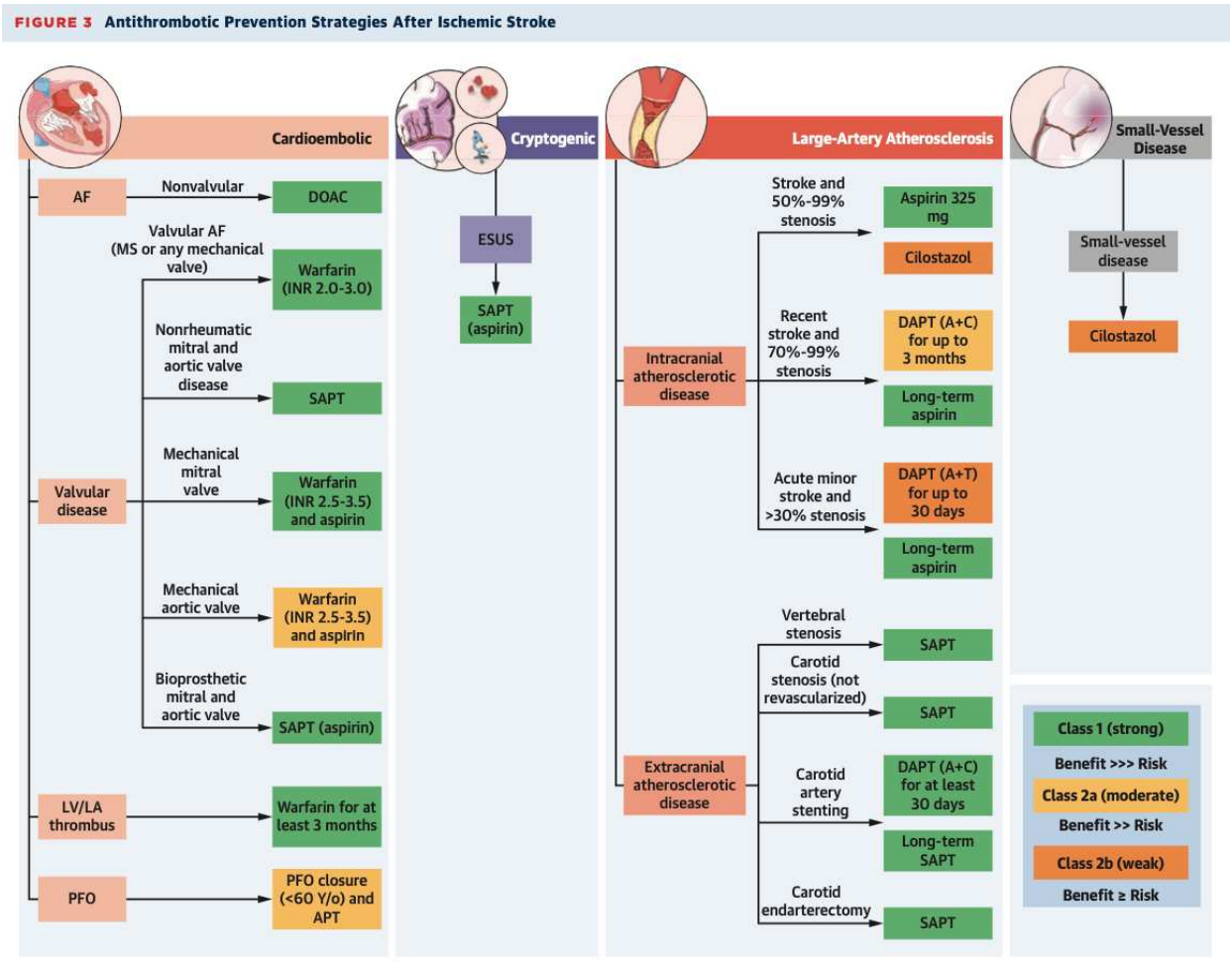

Figure 15: : Different therapeutic strategies based on AIS etiology, (Greco A, J am Coll Cardiol, 2023)

CHAPTER 2

ANATOMY OF CEREBRAL THROMBUS

The therapeutic approach to AIS centers on restoring blood flow through the dissolution or mechanical extraction of the obstructive blood clot. The introduction of mechanical thrombectomy (MT) has facilitated the histological assessment of occlusive clots, commonly referred to as cerebral thrombi. This development has spurred extensive research endeavors aimed at comprehensively characterizing the histological components of these clots and investigating their associations with clinical manifestations (LaGrange DD et al, 2023). Alterations in clot configuration are of significant interest due to their associations with the risk of myocardial infarction (MI), acute ischemic stroke, and venous thromboembolism (VTE). Recent reviews have extensively documented the correlations between clot composition and various aspects such as radiological findings, stroke etiology, and treatment outcomes.

Clots retrieved from patients experiencing AIS exhibit a heterogeneous composition, elucidated by the diversity of its constituents. These constituents include:

- distinct fibrin morphologies and various content of cellular components, most notably red blood cells (RBCs), white blood cells (WBCs), and platelets.
- protein expression profiles.
- the presence of extracellular DNA.

The intricate characterization of thrombus components is pivotal for understanding the underlying pathophysiology, and it has been proposed that thrombogenic mechanisms contribute to the formation of a core-shell structure. This structural insight holds significance in the conceptualization and design of therapeutic interventions. Substantial evidence has been gleaned from the analysis of clots retrieved from ischemic stroke patients, shedding light on the spatial distribution of thrombus components and the nuanced variations in thrombus compactness. These findings contribute to the ongoing efforts to tailor therapeutic strategies to the specific histological attributes of thrombi in AIS, ultimately enhancing treatment efficacy and patient outcomes.

2.1 CEREBRAL THROMBUS COMPOSITION

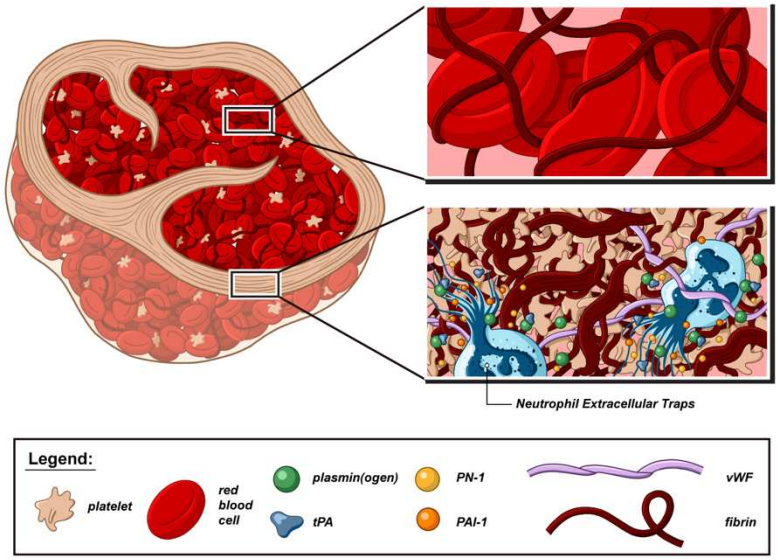

Figure 16: schematic thrombus composition (Desilles JP et al, Front. Neurol., 06 July 2022Sec. Stroke Volume 13 - 2022 https://doi.org/10.3389/fneur.2022.870331

A cerebral thrombus is a blood clot that forms within the cerebral vessels of the brain. The composition of a thrombus can vary, but generally, it consists of a meshwork of fibrin, platelets, red blood cells, and other cellular components. More in detail:

A) **Fibrin:** Fibrin stands as a pivotal fibrous protein, constituting the foundational architecture of a clot. Generated through a series of enzymatic reactions within the coagulation process, fibrin emerges from the conversion of fibrinogen—a soluble 340 kD plasma glycoprotein—into insoluble fibrin strands. These strands intricately interweave, forming a meshwork crucial for the stability and structure of the thrombus.

Fibrin significantly contributes to thrombi, and alterations in its structure wield influence over clot formation, stability, and eventual breakdown. Elevated thrombin concentrations give rise to dense fibrin networks resistant to fibrinolysis, as observed in previous in vitro studies correlating changes in fibrin clot structure, viscoelastic properties, and hypofibrinolysis with thrombotic events. However, bridging the gap between in vitro clot characteristics and the structure of in vivo thrombi remains unclear, despite a consistent association (Alkarithi G et al, 2021).

Numerous investigations underscore the variable contribution of fibrin to thrombi across different disorders, suggesting potential implications for disease progression and outcomes.

In vitro studies indicate that heightened fibrin content in clots corresponds to increased friction, implying enhanced stickiness of these thrombi. This aspect could play a crucial role in clot stability, embolization, and outcomes of thrombectomy procedures.

Recent revelations introduce a novel facet of fibrin's structural role in clots. Rather than forming traditional 3-dimensional fiber networks, fibrin molecules align to create continuous films that serve as a protective layer enveloping clot surfaces. This film-like structure not only influences clot properties but also provides defense against infections. Intriguingly, there is emerging evidence of fibrin film formation within the vasculature (Macrae FL et al, 2018). A recent study identified structures surrounding thrombi in acute ischemic stroke patients, resembling fibrin films, and exhibiting characteristics that impeded the thrombolysis process (Di Meglio L et al, 2019).

B) **Platelets:** Platelets, small disc-shaped cell fragments derived from megakaryocytes, assume a pivotal role in blood clotting and hemostasis. Upon blood vessel damage, platelets adhere to exposed surfaces and release signaling chemicals, beckoning more platelets to initiate plug formation. This plug not only staunches bleeding but forms the foundational basis of the thrombus. Platelets emerge as an enticing target for antithrombotic treatments.

Activated platelets offer negatively charged membrane surfaces crucial for assembling the prothrombinase and tenase complexes. During clot formation, platelets differentiate into distinct populations: procoagulant platelets, supporting thrombin generation and fibrin formation, and aggregating platelets, pivotal in initial clot formation and subsequent contraction. Within thrombi, intensely activated platelets concentrate in the inner core, while discoid and quiescent platelets localize to the periphery. Clot contraction hinges on aggregating platelets binding to fibrin fibers via αIIbβ3.

Procoagulant platelets adopt a balloon-like structure, exposing phosphatidylserine on the surface to generate thrombin in situ. Additionally, platelets contribute to thrombus growth and propagation by binding glycoprotein VI to fibrin. The temporal and morphological contribution of platelets to the architecture of ex vivo-obtained thrombi warrants further exploration. Understanding these intricacies is essential for unraveling the dynamic role of platelets in clot formation and devising targeted interventions to modulate thrombus architecture.

C) Red Blood Cells (RBCs): While not the primary constituent, red blood cells (erythrocytes) can integrate into the evolving thrombus, contributing to its overall mass and influencing consistency. Recent studies reveal a more intricate role for RBCs in clot structure and function than previously perceived.

Interactions between RBCs and activating platelets through FasL/FasR (CD95) receptor ligands result in phosphatidylserine exposure on both platelets and RBCs, triggering platelet degranulation and fostering thrombus formation. RBCs actively support thrombin generation via the meizothrombin pathway. Elevated hematocrit promotes platelet accumulation at vascular injury sites by displacing them from the blood vessel center to the vessel wall.

Factor XIII mediates RBC retention within venous thrombi, suggesting that targeting factor XIII to reduce RBC content could serve as a therapeutic approach in venous thrombus management, potentially limiting thrombus mass and stability. Despite their typically biconcave shape, RBCs assume an alternative structure during thrombosis referred to as polyhedrocytes. Forces exerted by platelets pulling on fibrin fibers lead to clot contraction, compressing RBCs and transforming them into a polyhedral structure.

RBCs in clots impact fibrinolysis and alter clot mechanical properties. Conditions like sickle cell disease render RBCs rigid, diminishing thrombus permeability.

RBC-rich thrombi are characterized by increased inflammatory cell presence, correlating with heightened thrombus burden and impaired reperfusion in patients with AIS. The two primary mechanisms through which RBCs influence thrombosis involve the formation of polyhedrocytes and the generation of additional thrombin.

D) White Blood Cells (WBCs): White blood cells, or leukocytes, are nucleated cells crucial to the immune system. While not typically predominant in thrombi, their presence may occur in specific situations like inflammation or infection. Their role within the thrombus is intricately connected to immune response dynamics in the clotting environment. Leukocytes significantly contribute to clot formation and are found in both arterial and venous thrombi.

Leukocytes bind fibrin via the integrin receptor αMβ2 (Mac-1), actively supporting the inflammatory response. Among leukocytes, neutrophils, the most abundant in circulation, release various substances such as matrix metalloproteinases, platelet-activating factor, cathepsin G, and elastase. These molecules exert diverse effects on coagulation, including the

activation of coagulation factors V, VIII, and X, as well as the activation and aggregation of platelets. Additionally, they contribute to the degradation of antithrombin III and proteolytic cleavage of the TF (tissue factor) pathway inhibitor.

Monocytes, significant contributors to intravascular TF expression, serve as a membrane surface for initiating coagulation in various conditions. TF expression is also detected in neutrophils in animal models. While some studies report TF expression in neutrophils and eosinophils, discrepancies exist, with other studies failing to detect TF expression in granulocytes. These variations may stem from the direct transfer of TF from monocytes to granulocytes. Understanding the nuanced roles of WBCs in thrombi provides insights into the complex interplay between immune responses and coagulation pathways, offering potential avenues for therapeutic exploration.

E) Plasma Proteins: Beyond fibrinogen, numerous plasma proteins actively participate in the clotting cascade, intricately shaping the composition and structure of thrombi. Notable factors in this complex network include:

- Von Willebrand Factor (vWF): This factor plays a pivotal role in platelet adhesion, a crucial early step in clot formation. By facilitating the binding of platelets to exposed surfaces, vWF contributes to the initiation of the clotting process.
- Factor VIII: Another key player in the clotting cascade, Factor VIII is instrumental in the stabilization of the clot. Its involvement enhances the structure and integrity of the developing thrombus.
- Factor XIII: This factor plays a crucial role in fortifying the structure of the clot. Factor XIII contributes to the cross-linking of fibrin strands, providing additional stability to the evolving thrombus.

Understanding the multifaceted contributions of these plasma proteins illuminates the intricate orchestration of events in the clotting cascade. Their involvement in platelet adhesion, clot stabilization, and structural reinforcement highlights the complexity of thrombus formation, offering potential targets for therapeutic interventions aimed at modulating specific elements of the clotting process.

F) Cellular Debris: As the clot initiation process unfolds, a noteworthy aspect emerges, the entrapment of cellular debris originating from compromised cells and various blood components. This encompasses fragments of cells that might have endured injury throughout the coagulation process. The inclusion of cellular debris introduces an

additional stratum of intricacy to the thrombus composition, potentially exerting a profound impact on its overall properties.

The incorporation of cellular debris into the developing thrombus adds diversity to its structural makeup, potentially influencing its stability, density, and responsiveness to therapeutic interventions. The amalgamation of these cellular remnants with other substances within the clot underscores the dynamic and heterogeneous nature of thrombus composition.

2.2 INSIGHTS INTO THROMBUS STRUCTURE: UNRAVELING THE IMPACT OF MULTIPLE FACTORS IN CEREBROVASCULAR PATHOPHYSIOLOGY

The specific composition of a cerebral thrombus can depend on various factors, including the underlying cause of clot formation, the presence of vascular diseases, and individual variations in clotting factors. Thrombi can form due to conditions like atherosclerosis, which leads to the buildup of plaques in blood vessels, creating a predisposition for clot formation. Additionally, conditions such as atrial fibrillation can increase the risk of clot formation in the heart, with these clots potentially traveling to the brain and causing a cerebral thrombus. Clot structure and function are influenced by genetic and environmental factors, including cigarette smoking, inflammatory status, hyperglycemia, oxidative stress, and high homocysteine levels. Many events have led to the suggestion that fibrin characteristics may represent a new risk factor for arterial and venous thromboembolism. The effects of drugs in cardiovascular prevention, particularly aspirin and statins, may also increase clot properties, and cellular and soluble factors also contribute through mechanisms that are not fully elucidated. Long-term studies aim to go to investigate how fibrin parameters may predict increased risk of thromboembolic events in the general population and also in arterial and venous disorders (Undas A. et al, 2009).

The structure of the fibrin clot varies depending on many factors with which it interacts. Understanding the intricate cellular dynamics of a cerebral thrombus is pivotal for designing targeted therapeutic strategies and interventions. It underscores the need to consider individual variations and the influence of underlying clinical conditions on the composition of these blood clots, especially in the context of conditions such as stroke.

1. MODULATORS OF FIBRIN PROPERTIES:

A) **Genetic factors:** Genetic factors play a crucial role in shaping the structure of fibrin, and specific genes associated with fibrinogen chains contribute to variations in fibrin structure. The three fibrinogen chains, FGG, FGA, and FGB, are encoded by genes located within the same region of chromosome 4, specifically at 4q28.1, 4q28.2, and 4q28.3, respectively (Weisel J.W. et al, 2017). the presence of particular polymorphisms and genetic variants influences the structure of fibrin, prominent among them:

- Polymorphisms in β-Chain: A common genetic variation occurs in the β-chain, known as the Lys448Arg polymorphism. This variation results in a structural difference in fibrinogen. Notably, the recombinant variant significantly influences the timing of clot lysis.

- Polymorphisms in α-Chain: Another frequent polymorphism involves the α-chain, specifically the Thr312Ala substitution. The presence of alanine is associated with the formation of denser fibrin fibers. This denser structure is linked to increased mortality in patients with atrial fibrillation complicated by ischemic stroke, predisposing them to atrial embolism.

- Splicing Variant in γ-Chain: One splicing variant affects the γ-chain, leading to the formation of γ'. This involves the replacement of 4 C-terminal residues containing a platelet binding site with 20 new residues containing both thrombin and Factor XIII subunit B binding sites. Clots produced with fibrinogen containing γ' exhibit thinner fibers, higher branch points, and greater resistance to lysis.

- Polymorphisms in FXIII: Polymorphisms related to Factor XIII (FXIII) are also significant. A G→T transition in codon 34 results in a Val34Leu substitution in the FXIII protein sequence.

- Effect of FXIII Activation: Thrombin, when activated by FXIII with Leu34, demonstrates greater catalytic efficiency compared to activation with Val34. Early activation of FXIII leads to clot formation with smaller pores and thinner fibers.

- Protective Role of Leu34 Allele: The allele containing Leu34 is associated with protection against myocardial infarction and venous thrombosis.

- Role of Fibrinogen Concentrations: The apparent discrepancy between increased FXIII activation and protection against myocardial infarction may be linked to different fibrinogen concentrations. At high fibrinogen concentrations, the interaction between Leu34 and FXIII leads to the formation of clots that are more permeable and susceptible to lysis. Conversely, at low fibrinogen concentrations, the opposite effect is observed (Duval C. et al, 2017).

B) Lipoprotein (a): Lp(a) is an apolipoprotein (apo (a)) that associates with particles such as low-density lipoprotein (LDL), commonly known as "bad" cholesterol, or very-low-density lipoprotein (VLDL). Elevated levels of Lp(a) are recognized as a risk factor for cardiovascular disease across various ethnic groups. The mechanisms by which high

levels of Lp(a) contribute to an increased risk of vascular disease involve multiple pathways. Delving into details of the correlation with fibrin properties:

- Fibrin Permeability: High levels of Lp(a) are correlated with decreased fibrin permeability. This suggests that Lp(a) may influence the structure of fibrin networks, potentially leading to altered clot properties.
- Fiber Formation: Increased Lp(a) levels are associated with thinner fiber formation in fibrin clots. The impact on fiber thickness suggests a direct influence on the structural characteristics of fibrin networks.
- Fibrinolysis Susceptibility: Elevated Lp(a) levels correlate with reduced susceptibility of fibrinolysis. This implies that clots formed under the influence of high Lp(a) may be more resistant to breakdown, contributing to a prothrombotic state.

C) Platelets: Platelets play a crucial role in the process of blood clotting, and their released proteins significantly impact the properties of fibrin clots.

- Platelet Factor IV and Clot Compactness: Platelets release proteins, including platelet factor IV (PF4), which plays a role in altering the properties of the clot. An increased amounts of PF4 are associated with the formation of a much more compact clot. This suggests that PF4 contributes to the overall density and structure of the fibrin network.
- Polyphosphate and Fibrin Network Alteration: Platelets secrete polyphosphate, a negatively charged inorganic phosphate polymer, from dense granules. They alter the fibrin network, and their effect is calcium-dependent. This means that the presence of calcium ions influences the interaction between polyphosphate and fibrin. Unlike some factors, polyphosphate's impact on clot structure is independent of factor XIII activation. The effect of polyphosphate on clot structure depends on factors such as polymer length and high fibrin turbidity, highlighting the sensitivity of fibrin dynamics to the specific characteristics of polyphosphate.
- Plasminogen Activator Inhibitor-1 (PAI-1) Release: Platelets release plasminogen activator inhibitor-1 (PAI-1), a protein that inhibits the activity of tissue plasminogen activator (tPA). In clot lysis, the role of PAI-1 increases as the number of platelets increases. This implies that a higher platelet count is associated with enhanced inhibition of fibrin degradation, contributing to the persistence of the clot.

D) Thrombin: Thrombin is a crucial enzyme in the blood clotting cascade, playing a central role in converting fibrinogen into fibrin, the insoluble protein that forms the basis of blood clots.

- Fibrinogen to Fibrin Conversion: Thrombin catalyzes the conversion of fibrinogen into fibrin monomers. This process involves the cleavage of specific peptide bonds in the Aα and Bβ chains of fibrinogen. Thrombin cleaves the N-terminal portions of the Aα and Bβ chains of fibrinogen, releasing fibrinopeptides A and B. This cleavage exposes binding sites on fibrin, allowing fibrin monomers to polymerize.

- Fibrin Polymerization: Fibrin monomers polymerize both linearly and laterally, forming a complex network of fibrin strands. This network creates the structural basis for a blood clot. The resulting fibrin network is highly organized and provides strength and stability to the clot.

- Factor XIII Activation: Thrombin plays a key role in the activation of Factor XIII (XIII-A), an enzyme crucial for clot stabilization. It catalyzes the hydrolysis of the activation peptide segment of Factor XIII, leading to the generation of active Factor XIII (XIII-A). Active Factor XIII (XIII-A) cross-links fibrin strands, contributing to the stability and resistance to fibrinolysis of the clot.

- Thrombin Concentration and Fibrin Structure: Thrombin concentration has a consistent impact on fibrin structure. As thrombin levels increase, the diameter of fibrin fibers decreases. Clots formed under conditions of high thrombin concentration are characterized by thin fibers and a network with small pores. This altered structure influences the overall mechanical and biochemical properties of the clot.

- Factors Influencing Thrombin Generation and Clot Structure: Recombinant Factor VII is noted for its ability to increase thrombin generation. By normalizing fibrin structure and enhancing clot stability, it contributes to the overall dynamics of blood clot formation. Thrombin generation is a dynamic and localized process. Factors such as the procoagulant activity of cells influence fibrin formation, leading to spatial heterogeneity in clot structure. The distance of fibrin from the cell surface contributes to this variability.

Stimulation of endothelial cells with cytokines induces the formation of compact fibrin networks that exhibit resistance to lysis. This highlights the dynamic interplay between cellular processes and fibrin clot characteristics.

E) Blood flow: The presence of blood flow has a significant impact on the structure of fibrin fibers within a clot. The fibers exhibit a tendency to align themselves according to the direction of blood flow. They become stronger when exposed to blood flow. This strengthening is manifested in the increased stiffness of the fibrin clot (Bonar RA et al, 2017).

F) Oxidative stress: studies in the literature suggest how oxidation alters the structure of fibrinogen. Fibrinogen can scavenge oxidants and protect other proteins from oxidation. Oxidation of fibrinogen follows exposure to oxygen, metal, and myeloperoxidase-derived oxidants and leads to a decrease in clot formation rate. Exposure to iron ascorbate and nitration of 2 β-chain tyrosines promotes fibrin formation by increasing aggregation and altering its structure (Violi F. et al, 2017).

2. PATHOLOGICAL CONDITION-RELATED MODULATION:

A) Alzheimer's disease (AD): is a severe neurodegenerative disease characterized by amyloid-β (Aβ) plaques, tau tangles, brain atrophy and vascular pathology. AD pathology involves not only neuronal changes but also profound vascular defects, including cerebrovascular dysfunction, decreased cerebral blood flow, and blood-brain barrier (BBB) rupture. Fibrinogen, a key coagulation protein circulating in the blood, emerges as a pivotal player in the hemostatic system's involvement in AD. In AD, fibrinogen is aberrantly deposited in the brain parenchyma and cerebral blood vessels, co-localizing with Aβ. The interaction between fibrinogen and Aβ leads to increased fibrinogen aggregation, Aβ fibrillation, and the formation of resilient fibrin clots resistant to breakdown. Abnormal fibrin deposition contributes to cerebrovascular complications, exacerbating cerebral amyloid angiopathy (CAA). The impact on BBB permeability is profound, implicating fibrinogen in the compromised vascular integrity observed in AD. AD is characterized by a prothrombotic state, evident in heightened clot formation, impaired fibrinolysis, and elevated levels of clotting factors and activated platelets. These factors collectively contribute to the persistence of fibrin deposits in the AD brain.

Lowering fibrinogen levels not only mitigates microglial activation associated with AD but also improves cognitive performance in murine models (Cortes-Canteli M et al, 2012). This

underscores the therapeutic potential of targeting fibrinogen to alleviate neuroinflammatory responses.

The influence of fibrinogen extends beyond AD, as seen in hyperhomocysteinemia. Elevated homocysteine levels promote the formation of denser clots, emphasizing the broader impact of systemic factors on clot structure and function.

B) Diabetes Mellitus: DM is associated with abnormal clotting dynamics, characterized by elevated fibrinogen levels in tandem with hyperglycemia. In DM, an increase in fibrinogen levels coincides with the hyperglycemic condition. The abnormal clot properties in DM are attributed to fibrinogen glycation. This process interferes with fibrin polymerization, affecting plasminogen binding, and impeding the conversion of plasminogen to plasmin. Insulin treatment, a cornerstone in DM management, introduces a dynamic element to clot formation (Undas A. et al,2011).

C) Smoking-related pathology: smoke increases thrombotic risks through multiple mechanisms, including an increase in fibrinogen levels. High exposure to smoke leads to the formation of clots that are denser and composed of thinner fibers than those found in the clots of nonsmokers. Cigarette smoking is associated with a 22% decrease in clot permeability and a 35% decrease in clot lytic capacity (Undas A. et al,2011).

3. DRUG-RELATED MODULATION:

A) Aspirin: a pharmaceutical agent involved in the regulation of clot formation, and similarly, other drugs exhibit notable effects on this process. Its administration leads to a 60% increase in clot permeability and fiber length, while acetylation of fibrinogen reduces clot stiffness by 30% and enhances lytic capacity. A noteworthy inverse relationship exists between the extent of fibrinogen acetylation and the efficacy of clot lysis. In laboratory settings, aspirin demonstrates inhibitory effects on fibrinogen oxidation, thereby contributing to an improved fibrinolytic response. Furthermore, it hinders the activation of Factor XIII, attributed to a dampening effect on thrombin generation, as elucidated by Undas and colleagues in 2003.

B) **Statins:** Statins play a crucial role in diminishing cardiovascular morbidity and mortality by mitigating coagulation processes and inducing changes in fibrin structure. Administering statins for four weeks results in heightened fibrin permeability and reduced lysis time. This effect is intricately linked to the diminished generation of thrombin, particularly through the downregulation of tissue factor.

2.3 IN-DEPTH EXPLORATION OF THROMBUS ANALYSIS AND CORRELATIONS

The wealth of study material derived from occluding clots, made available for lab bench analysis, has ushered in a unique opportunity to discern connections between thrombus characteristics and various critical aspects of stroke dynamics, treatment responses, procedural intricacies, and ultimate outcomes. (De Meyer SF et al, 2017).

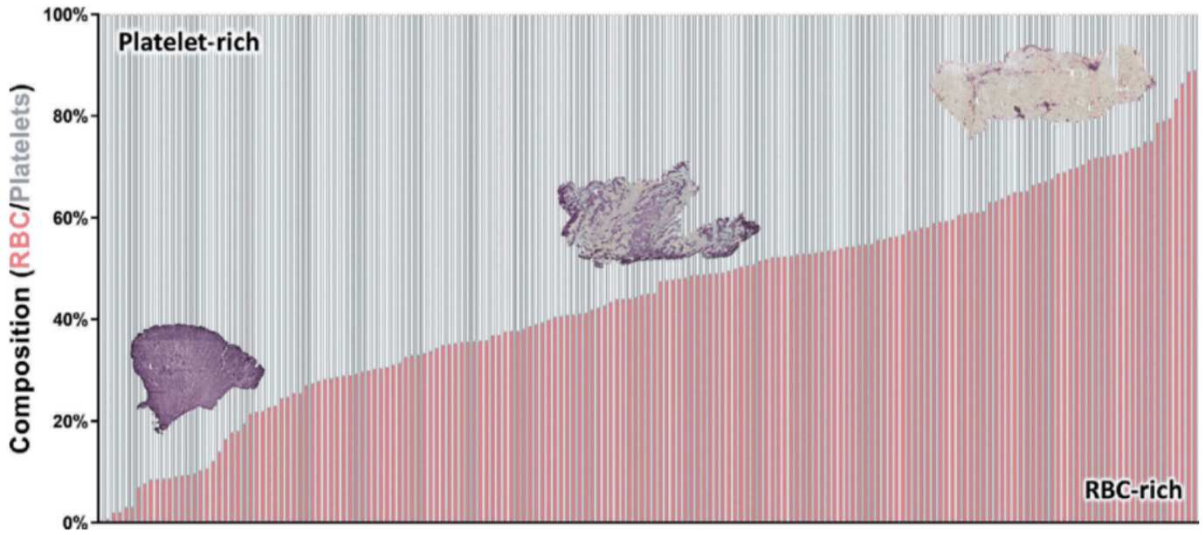

Figure 17: General stroke thrombus composition. Stroke thrombi (n=177, vertical bars) were quantitatively analyzed and the percentage of red blood cell (RBC)-rich areas (red) and platelet-rich areas (white) were determined.

In the realm of thrombus characterization, conventional histopathological assessment stands as the gold standard. Among the varied elements discerned, RBCs hold importance, with increased content often linked to heightened susceptibility to intravenous thrombolysis or mechanical thrombectomy. Conversely, a surge in fibrin/platelet content tends to correlate with treatment resistance.

Insights from Staessens et al showcase that clots from AIS patients exhibit RBC-rich areas with limited complexity, while platelet-rich areas boast intricate structures, dense fibrin aligned with vWF, and an abundance of leukocytes and extracellular DNA. This complexity potentially contributes to thrombolysis resistance.

Thrombectomy challenges were attributed to vWF and DNA, particularly from neutrophil extracellular traps (NETs), coexisting with microcalcifications at the clot core. NETs, predominantly located in fibrin-rich areas, are encircled by neutrophils, exerting a significant influence on clot dynamics.

Studies by Fitzgerald et al reveal that later thrombectomy passes are associated with higher fibrin and platelet content, suggesting increased fragility at the interface between RBC-rich and fibrin/platelet regions. Liu et al's spatial heterogeneity index (SHI) quantifies clot non-uniformity, demonstrating its impact on endovascular treatment efficacy. More heterogeneous structures, characterized by a higher SHI, are linked to lower first-pass effect (FPE) rates.

Di Meglio's study differentiates fibrin-rich and RBC-rich regions in AIS patient clots, unveiling a common fibrin shell formed through platelet-driven mechanisms. Despite challenges to the core-shell model, Rossi et al's large-scale analysis, drawing from the RESTORE registry, supports the reduction of all clot components, including RBC, fibrin, platelets, collagen, and calcifications, following thrombolysis. Mereuta et al challenge the core-shell model, presenting thrombi with interspersed RBC-rich and fibrin/platelet regions.

A multitude of studies in the scientific literature has delved into the intricate realm of deciphering correlations between the cellular components of blood clots and the underlying causes of strokes (Nicolini E et al, 2021). Key components like red blood cells (RBC), platelets (PLT), white blood cells (WBC), and fibrin constitute the common elements, but there exists a profound heterogeneity unfolds in both qualitative and quantitative histological patterns. Despite these investigations, many studies have failed to establish a consistent association, potentially due to the limitations of small sample sizes. However, understanding the connection between the composition of blood clots and the origin of strokes could have valuable implications for secondary stroke prevention, as the choice of preventive treatment depends on the specific cause of the stroke. AIS has various identified causes, with large artery atherosclerosis and cardiac embolism being the most prevalent. Both conditions can lead to the formation of thrombo-embolic blockages in the blood vessels of the brain. Notably, thrombi retrieved from cases of cardioembolic (CE) strokes exhibit a distinct composition characterized by a notably lower RBC content but an elevated presence of fibrin and platelets. In contrast, thrombi from patients with large artery atherothrombosis (LAA) show a higher RBC content. These variations underscore the complexity of thrombus composition in different stroke etiologies.

Insight from studies illuminates the unique features of CE thrombi, highlighting the presence of enlarged platelets, indicative of platelet activation when compared to LAA counterparts. Furthermore, distinctive distribution patterns emerge, with LAA strokes exhibiting peripheral platelet arrangements and CE displaying clustered patterns (Khismatullin et al,).

Moving beyond stroke etiology, a burgeoning body of research navigates the intricate interplay between thrombus composition and procedural dynamics, including time considerations, recanalization rates, and procedural complications. Noteworthy correlations surface in studies centered around successful reperfusion. Intriguingly, a higher rate of complete recanalization aligns with occlusions stemming from RBC thrombi, often referred to as red clots. Conversely, a diminished recanalization rate surfaces when platelets and fibrin components dominate, a phenomenon attributed to the frictional properties of platelets impending the retrieval process. The study conducted by Hund HM and colleagues in 2023 explored the relationship between the histopathologic composition of mechanically extracted thrombi and the etiology of strokes in patients with AIS enrolled in the Dutch MR CLEAN Registry. The researchers focused on the red blood cell and fibrin/platelets (F/P) contents of thrombi retrieved from AIS patients, with a specific emphasis on distinguishing strokes of cardioembolic and non-cardioembolic origin. The results demonstrated significant differences in the composition of thrombi between these two categories (figure 18). Differences were demonstrated also in Boeckh-Behrens study of 2016 (figure 19).

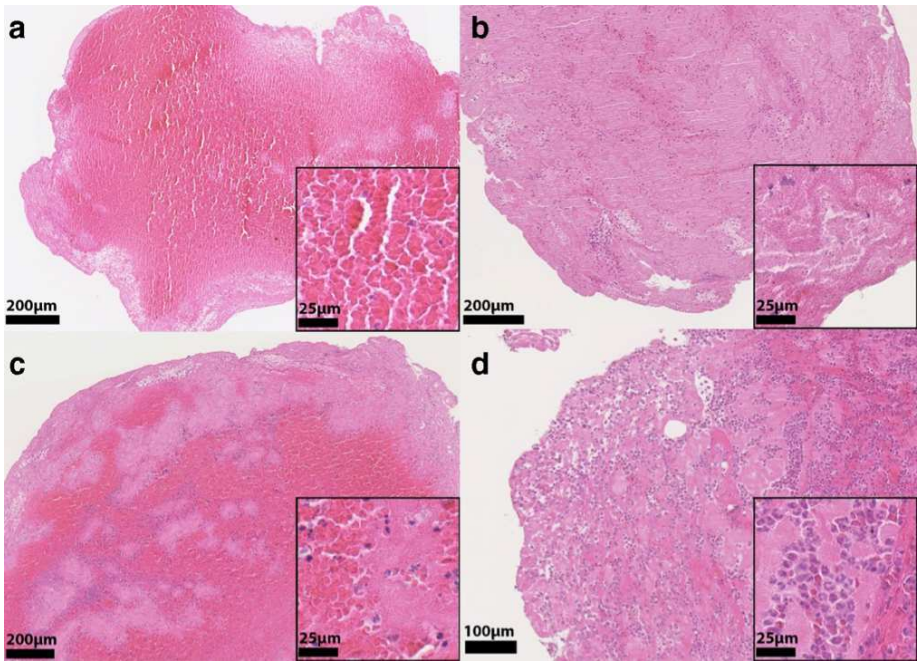

Figure 18: Examples of RBC-rich (A), F/P-rich (B), mixed (C), and leukocyte rich (D) thrombus areas. RBC are red, F/P purple, and nuclei of leukocytes blue.

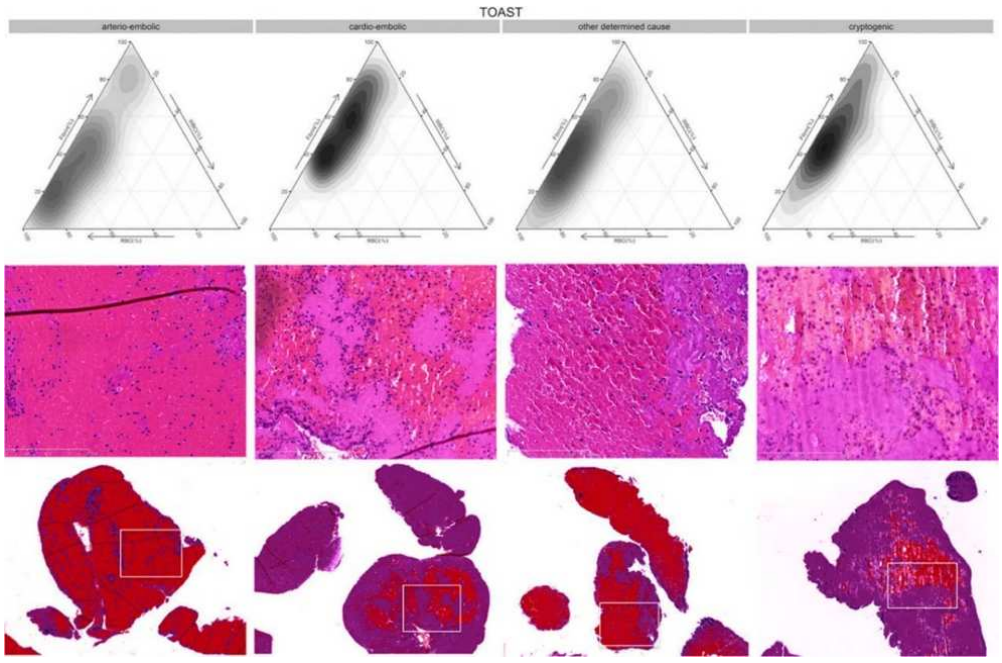

Figure 19: Top, the triangle graphs show similar distributions of the 3 main thrombus components—red blood cells (RBCs), fibrin/platelet, and white blood cells (WBCs)—in Trial of Org 10172 in Acute Stroke Treatment (TOAST) groups. Middle and bottom, the lower row shows 1 thrombus example of each of the respective TOAST. Red color represents RBCs; purple regions represent fibrin; and blue dots represent WBCs (Boeckh-Behrens, 2016).

Thrombi from patients with non-cardioembolic etiology exhibited a higher RBC content compared to those from patients with cardiac etiology and undetermined origin. Conversely, the F/P content in thrombi from patients with non-cardioembolic etiology was lower than in thrombi from patients with cardioembolic etiology and thrombi with an undetermined origin (figure 20). The results obtained in this study align with those reported by Wei L et al in 2021.

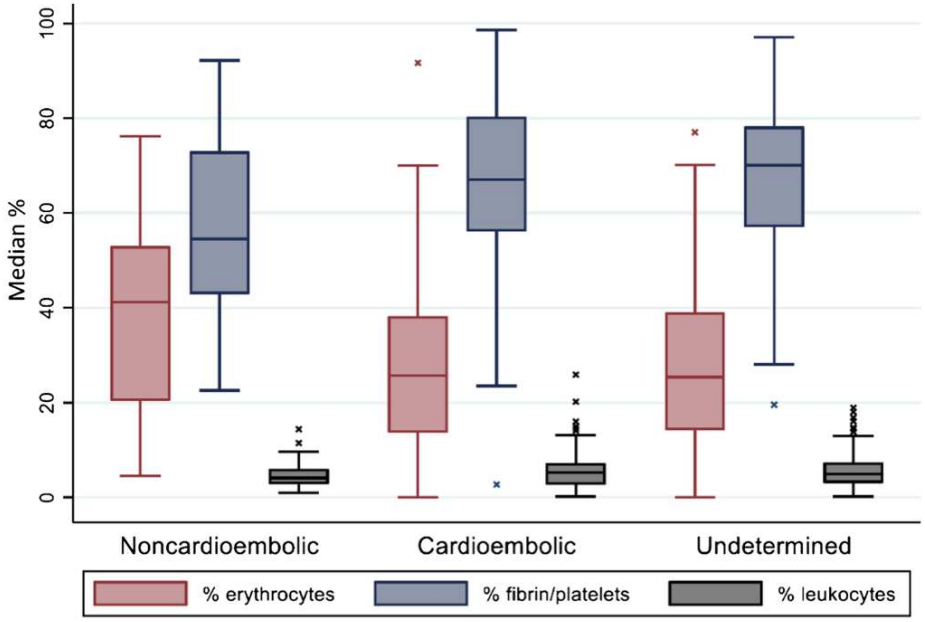

Figure 20: Bar-whisker plot of thrombus composition for the three etiologic groups. Significant differences were found for both erythrocyte content ($p < 0.001$) and fibrin/platelet content ($p = 0.002$), but not for leukocytes ($p = 0.240$) (Hund et al, Neuroradiology 65, 933–943 (2023)

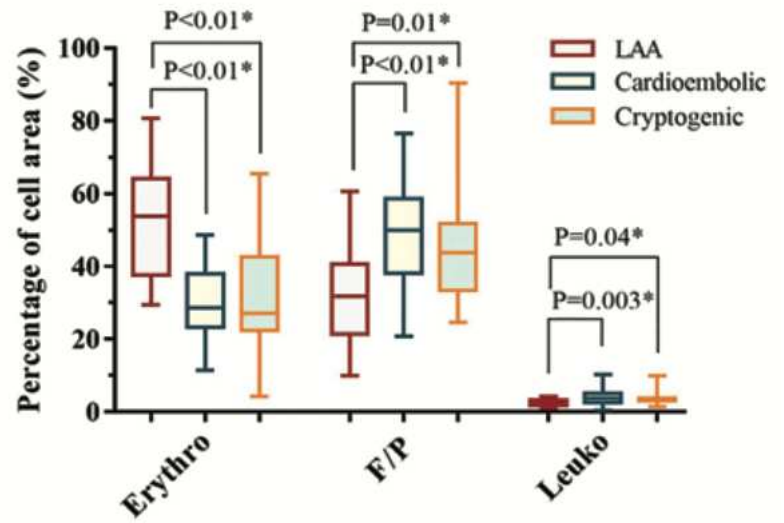

Figure 21: pathologic observations of the thrombi revealed that thrombi from large artery atherosclerosis contained larger amounts of broadly distributed erythrocytes accompanied by a smaller F/P ratio and fewer leukocytes, whereas more highly organized F/Ps and leukocytes and fewer erythrocytes appeared in the thrombi retrieved from patients with cardioembolic and cryptogenic strokes

Interestingly, the study also noted a similarity in thrombus composition between those of cardioembolic origin and those of undetermined origin. This observation led to the suggestion that patients with an undetermined stroke origin and thrombi rich in F/P may have a higher likelihood of a cardiac source. As a potential implication, these patients might benefit from more extensive monitoring for arrhythmias and extended cardiac analysis (figure 22).

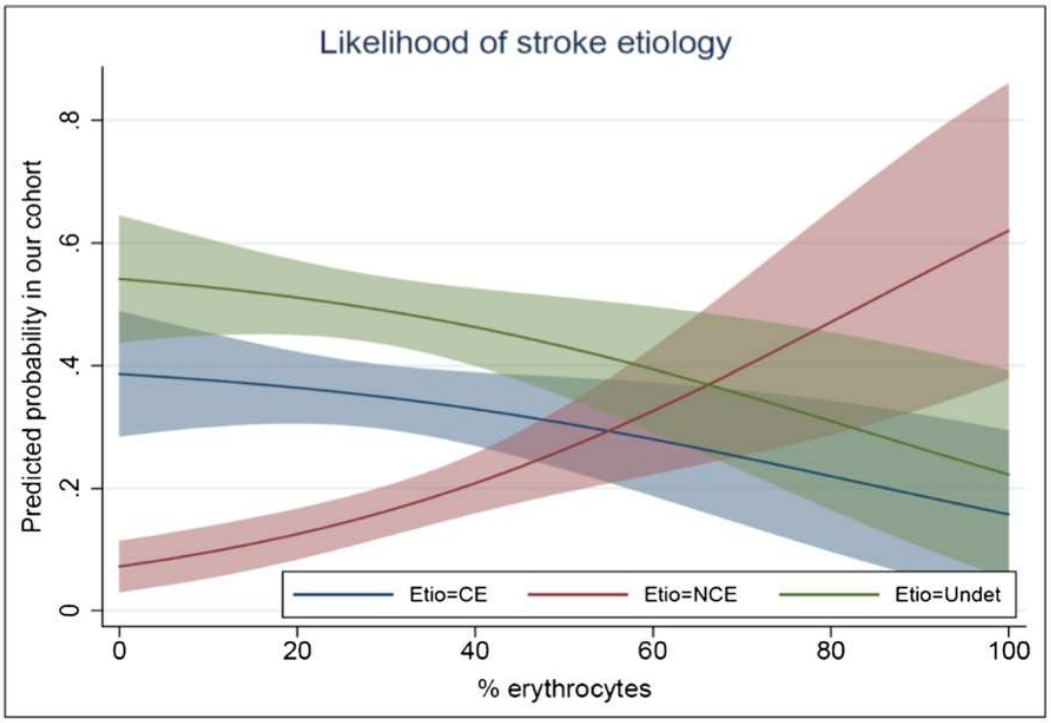

Figure 22: Likelihood of cardioembolic (CE), non-cardioembolic (NCE), and undetermined (Undet) etiology (Etio) based on erythrocyte content after univariable multinomial regression) (Hund et al, Neuroradiology 65, 933–943 (2023).

Those studies contribute to the growing body of literature exploring the nuanced relationships between thrombus characteristics and stroke dynamics. The insights gained pave the way for personalized stroke prevention and treatment strategies, acknowledging the diversity in thrombus composition across different stroke etiologies. As future research continues to unravel the complexities of thrombus dynamics, these findings offer a foundation for refining clinical approaches and improving outcomes for AIS patients.

CHAPTER 3

OMICS SCIENCES

In biology, the word “omics” refers to the sum of constituents within a cell. The omics sciences share the overarching aim of identifying, describing, and quantifying the biomolecules and molecular processes that contribute to the form and function of cells and tissues (Rogers K, 2023). Omics research is a multidisciplinary and high-throughput approach that encompasses several subfields, each focusing on a specific type of biomolecule, such as genomics (DNA), transcriptomics (RNA), proteomics (proteins), and metabolomics (metabolites). From healthcare to agriculture, these methodologies are revolutionizing the understanding of the molecular underpinnings of life. Here's a detailed exploration of the applications of omics sciences:

- PRECISION MEDICINE: Tailoring medical treatments based on individual molecular profiles, enhancing treatment efficacy, and minimizing side effects.
- DISEASE DIAGNOSIS AND BIOMARKER DISCOVERY: Early and accurate disease diagnosis, paving the way for targeted therapies and personalized medicine.
- DRUG DISCOVERY AND DEVELOPMENT: Accelerating drug discovery, predicting drug responses, and minimizing adverse effects.
- CANCER RESEARCH: Unraveling the complexity of cancer, identifying therapeutic targets, and advancing personalized cancer treatments.
- AGRICULTURAL BIOTECHNOLOGY: Enhancing crop yield, developing disease-resistant varieties, and improving agricultural sustainability.
- MICROBIOME STUDIES: Understanding the role of the microbiome in health and disease, developing microbiome-targeted therapies.
- ENVIRONMENTAL MONITORING: Monitoring ecological changes, assessing environmental health, and guiding conservation efforts.
- SYSTEM BIOLOGY: Uncovering complex interactions within biological systems, contributing to the field of systems biology.

This approach has revolutionized biological and medical research, providing a holistic and systematic understanding of biological systems at the molecular level. The interdisciplinary nature of omics fosters a more comprehensive and integrative approach, facilitating breakthroughs in various scientific fields. Each type of omics data unveils differentially expressed disease-associated molecules, acting as potential biomarkers that illuminate disease progression and offer insights into the variances in biological pathways or processes between disease and control groups (Chen C et al, 2023). The integration of diverse omics data types holds the potential to unveil the fundamental pathogenic changes associated with a disease, providing a foundation for

subsequent molecular investigations. Through the comprehensive integration of multi-omics datasets, scientists gain the ability to discern intricate associations between biomolecules and disease phenotypes. This approach enables the identification of previously undiscovered links, the delineation of relevant signaling pathways, and the establishment of detailed biomarkers for the disease. In essence, the integration of various omics data sets facilitates a more nuanced understanding, allowing for the correlation of molecular-disease associations with the influence of phenotype-environmental factors. This integrated approach enhances the depth and accuracy of insights into the molecular underpinnings of diseases, paving the way for more targeted and effective research and potentially transformative advances in medical science.

3.1 OMICS BRANCHES

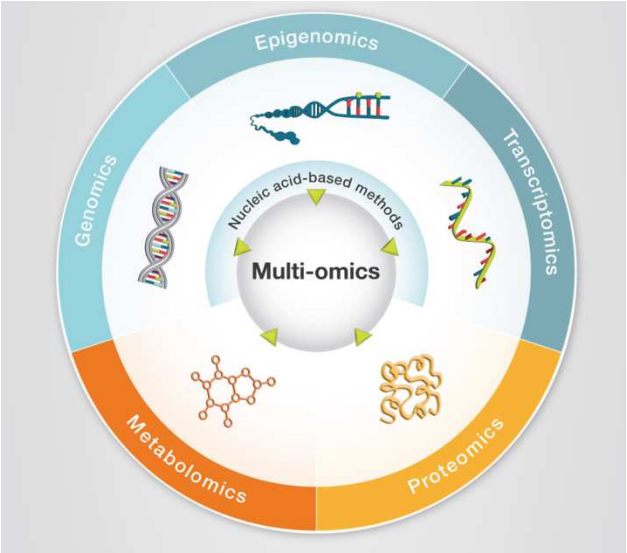

Figure 23: Omics branches

A) Genomics

Genomics, the pioneering -omics field, emerged with the development of DNA amplification techniques and automated sequencing in the 1980s and '90s. The landmark Human Genome Project followed, promising unprecedented insights into genetic diseases, and marking the advent of the omics era (Breda Genetics, 2016). While successful in mapping the human genome and those of other organisms, challenges persist in interpreting the vast amount of data, understanding the functionality of non-coding regions, and deciphering genetic responses to environmental conditions.

Next-generation sequencing technologies have revolutionized genetic analysis, significantly reducing costs and enabling comparative studies crucial for evolutionary biology and large-scale polymorphism analysis (Servushan et al, 2023). This is particularly vital for omics, where generating extensive datasets is essential for building algorithms used in various applications, such as in silico drug repurposing for cancer patients. The ability to generate large, well-annotated datasets at a reasonable cost is key to the future of omics technologies, facilitating advancements in personalized medicine through individual genome sequencing.

A limitation of genomics lies in the fact that the presence of a gene does not guarantee its influence on the phenotype. Phenotypic expression is influenced by factors such as protein synthesis and degradation rates, RNA splicing and silencing, and environmental influences on

gene products. To closely examine phenotypes, a deeper understanding of the functional products of genes is essential.

B) Epigenomics

Epigenomics, an intriguing facet of Genomics research, delves into the complex study of the complete set of epigenetic modifications present on a cell's genetic material, commonly termed the epigenome. Epigenetic modifications encompass alterations to the DNA structure or histones within cells. Despite their reversible nature, these modifications exert a significant impact on gene expression, orchestrating how genes are activated or silenced, all without directly modifying the underlying physical structure or sequence of the genes (Breda Genetics, 2016).

This field of inquiry, while relatively new, has been made accessible and feasible through the implementation of genomic high-throughput assays. These advanced assays enable researchers to scrutinize and decode the complex landscape of epigenetic modifications across the genome on a large scale. Epigenomics, therefore, stands at the forefront of unraveling the dynamic and intricate regulatory mechanisms that govern gene expression, contributing invaluable insights into the broader landscape of genomic function and regulation.

C) Proteomics

Proteomics is a scientific discipline dedicated to exploring the interactions, functions, compositions, and structures of proteins, as well as their activities within cells. In comparison to genomics, proteomics offers a more comprehensive understanding of an organism's structure and function. However, its complexity surpasses that of genomics due to the dynamic nature of protein expression, which is subject to changes influenced by factors such as time and environmental conditions (Al-Amrani S et al, 2021).

The human proteome is estimated to encompass nearly one million proteins, featuring various modifications, including post-translational modifications (PTMs). This diversity stands in contrast to the roughly 26,000 to 31,000 proteins encoded by the human genome (Chandramouli K et al, 2009). To navigate this intricate landscape, proteomics employs diverse techniques: traditional methods like one-dimensional (1D) and two-dimensional (2D) gel electrophoresis, that offer visual

representations of protein expression, and advanced gel-free high-throughput screening technologies, such as multidimensional protein identification technology.

Proteomics enables the analysis of protein expression at different levels, facilitating the assessment of specific quantitative and qualitative cellular responses associated with particular proteins. Moreover, proteomics contributes valuable insights into the molecular mechanisms of diseases and facilitates comparative studies between two groups, such as patients and healthy controls.

D) Metabolomics

Metabolomics is a dynamic field within the domain of omics sciences, with the scope of identifying and comprehending the vast array of small molecules generated as intermediates or end products in any chemical processes unfolding within the human body.

The scope of metabolomics is twofold, encapsulating the study of chemical processes involving endogenous human molecules, known as the Endogenous Metabolome, as well as processes entailing external molecules introduced into the body, termed the Exogenous Metabolome (Breda Genetics, 2016).

This division allows researchers to dissect and understand the distinct biochemical pathways shaped by molecules originating within the body and those entering from external sources. Metabolites serve as direct indicators of the biochemical activities occurring within cells and tissues. The dynamic nature of metabolites reflects the real-time status of cellular processes, making them invaluable in unraveling the complexity of biological systems. As metabolites are intricately tied to the phenotypic traits of an organism, changes in their abundance or composition can signify alterations in cellular functions and metabolic pathways. This makes metabolomics a pivotal player in the quest to understand the molecular basis of various diseases. Whether it's identifying biomarkers for early disease detection or unraveling the metabolic intricacies of complex disorders, metabolomics stands at the forefront of translational research.

E) Transcriptomics

Transcriptomics, a discipline at the forefront of molecular biology, is dedicated to the comprehensive study of an organism's transcriptome, the entirety of RNA transcripts synthesized by its genome. The genome, housing the genetic information encoded in DNA, manifests its complexity and functionality through transcription. mRNA emerges as a transient intermediary, conveying the genetic instructions for protein synthesis. Concurrently, non-coding RNAs contribute to a wide range of regulatory functions, expanding the gene regulatory hierarchy (Lowe et al, 2023).

The transcriptome, capturing a temporal snapshot, offers a dynamic portrayal of the RNA transcripts present within a cell. The genesis of transcriptomics dates back to the early 1990s, with subsequent technological advancements propelling it into a ubiquitous and transformative discipline. The contemporary landscape of transcriptomics is shaped by two primary techniques: microarrays, designed to quantify predetermined sequences, enabling a targeted exploration of gene expression profiles, and RNA sequencing (RNA-Seq), utilizing high-throughput sequencing to comprehensively capture all RNA sequences, offering an unbiased and exhaustive examination of the entire transcriptome.

Transcriptomics, through the meticulous measurement of gene expression across various conditions, tissues, or temporal points, unveils the intricate landscape of genetic regulation. It provides nuanced insights into the regulatory mechanisms governing an organism's biology, shedding light on the functions of both annotated and previously unannotated genes. Notably, the comprehensive analysis of the transcriptome has proven instrumental in elucidating the molecular underpinnings of human diseases.

This approach facilitates the identification of broad, coordinated trends that might elude more targeted assays. By adopting a holistic viewpoint, transcriptomics reveals the intricate patterns and trends underlying gene expression, offering a profound understanding of the complexity of molecular activities. Such insights hold significance for unraveling the complexities of genetic regulatory networks and their implications across diverse biological contexts (Stokes et al, 2023). From exploring gene expression patterns to uncovering novel functional elements, transcriptomics stands as a cornerstone in advancing our understanding of the molecular intricacies that govern biological systems.

3.2 TRANSCRIPTOMICS FOR GENE EXPRESSION PROFILING

The recent advancements in high-density DNA microarray technology have revolutionized the study of cellular activity at the genome-wide transcriptional level. The application of microarray technology in medical research holds significant promise for clinicians and researchers alike. This innovative technology provides invaluable support in interpreting existing medical knowledge and events. By examining gene variants and gene expression patterns in individuals, microarrays contribute to characterizing susceptibility to diseases, predicting complications, and understanding an individual's response to pharmacological treatments. The knowledge gained from microarray-based expression profiling allows researchers and clinicians to delve into the pathophysiological mechanisms that drive different molecular phenotypes. This understanding, in turn, aids in delineating the characteristics of specific clinical phenotypes. Such insights offer practical applications for prognostic assessments and therapeutic decision-making, further emphasizing the potential of microarray technology in advancing personalized and precision medicine approaches. This technology allows researchers to capture a comprehensive snapshot of cells, monitoring the expression levels of thousands, or even tens of thousands, of genes, using a single microarray chip. The primary focus of microarrays is to measure the presence of mRNA, which can be extracted from cells or tissues. Analyzing mRNA profiles provides a quantitative assessment of genetic activity at the specific location from which the mRNA was obtained.

Microarrays operate based on the principle of hybridization, the inherent ability of nucleic acids to bind to complementary sequences. This technology enables the simultaneous probing of a complex mixture of nucleic acids using an array of spatially ordered complementary sequences on a glass surface. In this process, the nucleotide sequences on the array surface, often referred to as probes, interact with sequences from the biological sample, termed targets. The hybridization process is fundamental to the functionality of microarrays, allowing for the spatially ordered analysis of nucleic acids.

The history of microarray technology traces back to the 1980s when a group led by R.P. Ekins at the University College, London, pioneered simple microspotting techniques for high-sensitivity immunoassay studies. Notable contributions in the United States came from Stephen P.A. Fodor and his colleagues at Affymetrix, Inc. (Santa Clara, California), as well as Patrick O. Brown and his team at Stanford University. Brown's group is credited with engineering the first DNA microarray

chip, while Fodor and his colleagues at Affymetrix created the first patented DNA microarray wafer chip, known as the GeneChip.

Since these early developments, numerous commercial entities and academic groups have contributed to the continuous advancements in DNA microarray technology. The exponential growth in publications related to microarray technology, especially in cancer investigations, reflects its widespread adoption and significance in biological research. In its general form, a DNA array is a chip made of materials like nylon membrane, glass, or plastic, arranged in a grid-like pattern. DNA strands are deposited or synthesized within individual grid segments. The microarray experiment involves key steps such as sample preparation and labeling, sample hybridization and washing, and microarray image scanning and processing. This technology has become an indispensable tool for unraveling the complexities of genetic activity on a global scale.

3.3 MICROARRAY CHIP MANUFACTURE

The manufacture of microarray chips involves two primary approaches: robotic spotting and in situ synthesis. Robotic deposition can occur through the deposition of PCR-amplified cDNA clones or the printing of pre-synthesized oligonucleotides. In contrast, in situ synthesis methods include photolithography, inkjet printing, and electrochemical synthesis.

In the case of in situ synthesis, there are notable distinctions from spotted arrays:

- Probe Selection: Probes are selected based on sequence information alone. This allows for the knowledge of every probe synthesized on the array. In contrast, cDNA arrays, dealing with expressed sequence tags, may have unknown functions for corresponding sequences. Additionally, this selection method avoids duplicating sequences among gene family members, enabling the quantitative monitoring of closely related genes.
- Probe Preparation: Probes are either printed (Agilent Sureprint technology) or photochemically synthesized (light direct synthesis for Affymetrix) base-by-base on the array's surface. There is no involvement of cloning or PCR processes in the preparation of these probes.

The Affymetrix GeneChip technology represents a pioneering approach in the field of genomics, particularly in the study of gene expression on a genome-wide scale. The hallmark of this technology lies in its utilization of in-situ synthesis, a process that involves the direct synthesis of probes on the array surface. The preparation of probes involves either printing or photochemical synthesis, depending on the specific technology used. Notably, this process eliminates the need for cloning or polymerase chain reaction (PCR), streamlining the preparation phase.

In the in-situ synthesis process, synthetic linkers with photochemically removable protecting groups are affixed to a glass substrate. The application of light through a photolithographic mask induces localized photo-deprotection, allowing for the precise synthesis of probes base-by-base on the array surface. This method stands in contrast to traditional approaches that rely on pre-synthesized oligonucleotides. More in detail, the support consists of a layer of silicon and is functionalized with small sequences of oligonucleotides (oligo-starter). These oligos have the characteristic of having the hydroxyl group protected by photosensitive groups and therefore, thanks to a photolithographic mask, it is possible to direct the light into specific positions of the array and free the reactive groups necessary for the sequence synthesis. Once deprotected, the hydroxyl groups can react with deoxynucleosides triphosphate (dCTP, dGTP, dATP, dTTP)

photoprotects in 5'. The lengthening of the oligonucleotide takes place one reaction at a time, making the hydroxyl group available at each deprotection cycle. The deprotection cycle takes place thanks to the application of photolithographic masks which present holes in specific positions through which UV rays pass which strike the photolabile protector.

Probe design and selection in Affymetrix GeneChips are based solely on sequence information, ensuring that every probe synthesized on the array is known. This approach is advantageous in distinguishing closely related genes and quantitatively monitoring their expression. It avoids duplicating sequences among gene family members, providing a level of specificity in gene expression studies.

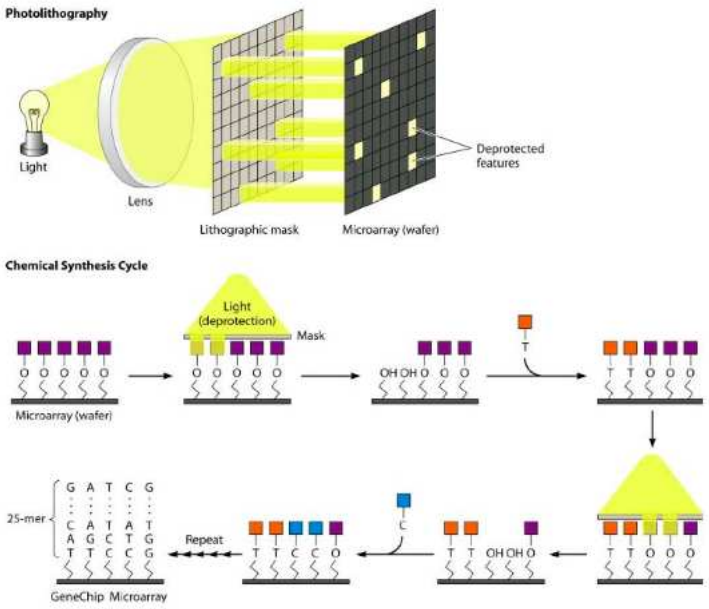

Figure 24: Affymetrix GeneChip Microarray, photolithographic process https://www.researchgate.net/figure/Affymetrix-GeneChip-oligonucleotide- microarray-Top-Photolithography-UV-light-is_fig3_26888549

3.4 AFFYMETRIX GENECHIP TECHNOLOGY

Gene expression quantification using Affymetrix technology relies on non-competitive hybridization. In this method, only one biological sample, the sample of interest, is fluorescently labeled and then hybridized to the microarray. The expression of each gene is measured by comparing the hybridization to a set of 20 probe pairs (probeset), each 25 base pairs long. An interesting feature is the inclusion of mismatch (MM) probes, intentionally designed to introduce a single mismatch at a specific position in the probe sequence. While their role is debated and controversial in some analyses, MM probes serve as a control mechanism for random variation and cross-hybridization.

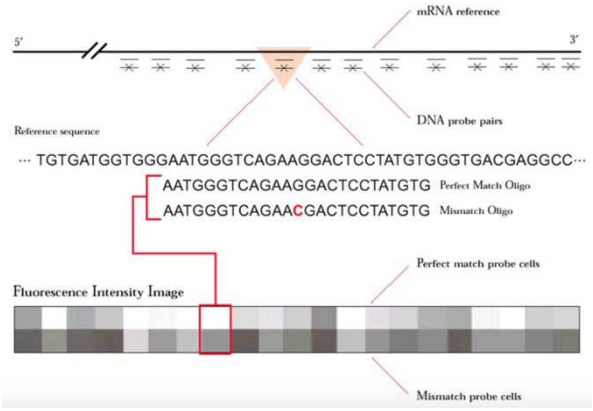

Figure 25: Perfect Match-Mismatch probe design

Applications of Affymetrix GeneChips span diverse areas, from gene expression studies on a global scale to the analysis of diseases for unraveling cellular signaling pathways and identifying potential therapeutic targets. The technology is particularly relevant in the context of personalized medicine, offering insights for diagnostic and prognostic therapy and the development of personalized therapeutic strategies.

While Affymetrix GeneChip technology has significantly contributed to genomics, it is not without its controversies, such as the debated use of MM probes in summarization processes. Nonetheless, its precision, controlled synthesis, and comprehensive approach make it a powerful tool in the realm of genomics research, addressing a spectrum of applications from basic research to clinical investigations.

The microarray-based gene expression profiling approach is valuable for understanding how gene expression patterns differ between different experimental conditions and is a widely used method in molecular biology and genomics research.

Going into more detail, the microarray analysis process can be summarized in the following steps:

a) Hybridization to Affymetrix Chips:

The process begins with the preparation of samples for hybridization. In this context, the samples used are antisense copy RNA (cRNA), which is synthesized in vitro. This synthesis is accomplished using T7 RNA polymerase in the presence of biotinylated ribonucleotides, specifically Bio-CTP and Bio-UTP. These biotinylated nucleotides serve as tags for subsequent detection steps.

The antisense cRNA is generated from double-stranded cDNA. Initially, mRNA samples are isolated from the biological material of interest. These mRNA samples act as templates for the synthesis of complementary DNA (cDNA). The resulting double-stranded cDNA then becomes the starting material to produce antisense cRNA.

Following the preparation of antisense cRNA, hybridization takes place on the Affymetrix chips. These chips are designed with an array of oligonucleotide probes that are complementary to specific sequences of the target genes. During hybridization, the biotinylated cRNA samples are allowed to bind to their complementary probes on the chip, forming cRNA: DNA hybrids.

b) Staining and Detection:

Once hybridization is complete, the next step involves staining the hybridized chip. This is achieved by using streptavidin-phycoerythrin, where streptavidin binds specifically to the biotinylated cRNA. Phycoerythrin, a fluorescent dye, serves as a detection label. This staining step is crucial for visualizing and quantifying the hybridized cRNA on the chip.

c) Confocal Scanner Reading:

After staining, the Affymetrix chip is subjected to analysis using a confocal scanner. The confocal scanner detects and measures the fluorescent signals emitted by the phycoerythrin-labeled cRNA on the chip. This step provides quantitative information about the abundance of specific RNA transcripts in the samples.

d) Comparison of Control and Experimental Samples:

It's noteworthy that control and experimental samples are hybridized to separate chips. This separation allows for a direct comparison of gene expression levels between the two conditions. The comparison is a key aspect of the analysis, as it enables the identification of differential gene expression patterns between the control and experimental samples.

CHAPTER 4

AIM OF THE STUDY

Understanding the etiologic classification of ischemic strokes is not merely beneficial but imperative, acting as a foundational pillar for precise prognosis, accurate outcome prediction, and the formulation of tailor-made event management strategies.

The primary thrust of this investigation is to delve into the intricate genetic landscape of ischemic stroke through the application of cutting-edge transcriptomic approaches. Our specific focus centers on the meticulous exploration of molecular signatures within thrombotic tissue and peripheral venous blood that are uniquely associated with distinct stroke subtypes. Through this systematic inquiry, we aim to unveil the intricate interplay between gene expression patterns and the nuanced phenotypic differences that characterize the spectrum of ischemic stroke subtypes.

In the quest to decipher these complex relationships, the overarching objective is to unearth distinctive transcriptomic signatures. This, in turn, holds the potential to provide valuable prognostic insights, facilitating the identification of predictive markers for patient outcomes across a spectrum of ischemic stroke subtypes. Beyond this, our study aspires to make substantial contributions to the evolution of personalized medicine. This paradigm shift envisions prevention and treatment strategies evolving toward increased individualization, all grounded in a profound understanding of the diverse underlying causes of ischemic events. Thus, our research endeavors to be a catalyst in shaping a more precise and personalized approach to managing and preventing ischemic strokes.

CHAPTER 5

MATERIAL AND METHODS

5.1 EXPERIMENTAL DESIGN

Reperfusion Injury after Stroke Study (RISKS study) is an observational prospective single-center hospital-based project funded by the Ministry of Health in which patients with Large Vessel Occlusion (LVO) strokes are enrolled based on specific inclusion and exclusion criteria. The study was conceptualized by Piccardi et al in 2018, under the auspices of the group coordinated by Professor Inzitari. Enrollment commenced in October 2015 and concluded in October 2018.

Inclusion criteria	Exclusion criteria
Age≥18 years	Patients transferred from an outside neurological department
Acute stroke eligible for systemic thrombolysis according to plain SITS-MOST criteria (excepting extension of the therapeutic time window to 4.5 hours and no upper age limit) or for endovascular treatment according to the local protocol	Life expectancy < 3 years
Written informed consent by patient	
	Controindication for iodine contrast medium
	Previous disability (mRs>3)

Table 1: Inclusion and exclusion criteria

In the context of this thesis, a total of 92 patients diagnosed with Acute Ischemic Stroke (AIS) and undergoing mechanical thrombectomy were recruited. These patients presented at the emergency department and received care from the Stroke Unit and Neuroradiology Unit at Careggi. Comprehensive clinical, imaging, and detailed biochemical and molecular data are available for all enrolled patients. Upon the stroke diagnosis, a baseline blood sample is collected, with blood drawn into tubes with and without anticoagulant. These samples are stored, and the plasma and serum components are preserved. Additionally, blood is collected in PAX tubes containing an RNA-stabilizing fluid and stored for subsequent analysis of gene expression profiles. Following the initial blood sampling, patients undergo treatment with recombinant tissue plasminogen activator (rtPA) and/or thrombectomy. For patients undergoing thrombectomy, the aspirated thrombus is promptly stabilized in RNA later, preserving it for subsequent global gene expression analysis. A secondary blood sample is collected 24 hours post-procedure using the same methods as the baseline sample. Furthermore, a three-month follow-up is conducted to assess the patient's condition and outcomes. For each patient, an analysis is conducted on the RNA extracted directly from the thrombus, taken from the area where the ischemic stroke developed through thrombectomy. The thrombectomy procedures adhere to the protocols outlined by Ciccone A. et al (2013) and Toni D. et al (2015).

5.2 RNA EXTRACTION FROM CEREBRAL THROMBUS AND PERIPHERAL VENOUS BLOOD

Until the extraction moment, RNA has been stored at -80°C and in RNA later, a reagent that immediately stabilizes intracellular RNA to preserve the gene expression profile. This step is crucial as RNA is a delicate molecule highly susceptible to degradation.

For thrombus extraction, the PAXgene Blood miRNA kit was utilized (https://www.qiagen.com/us/resources/resourcedetail?id=7203e2a4-99e9-4fef-8b67-3c272f1d4eb5&lang=en), and RNA was extracted following the procedure outlined below:

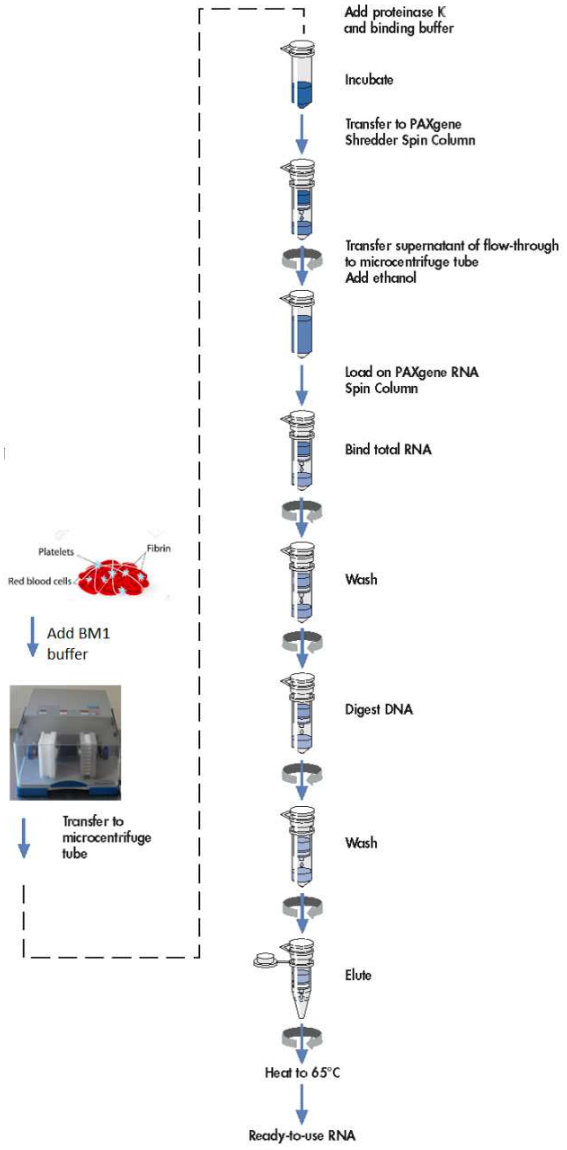

Figure 26: RNA extraction procedure

- Allow the PAXgene Tube to reach room temperature for at least 2 hours.
- Remove RNA later, add magnetic beads to the thrombus proportional to its size, and directly add 350 µl of Buffer BM1. Proceed to rupture the cell membrane using an automatic Mixer Mill homogenizer (Retsch).
- Transfer the sample to a 1.5 ml Eppendorf tube, add 300 µl of Buffer BM2 (binding buffer), and 40 µl of proteinase K. Vortex for 5 seconds and incubate for 10 minutes at 55°C.
- Transfer the sample to a Shredder spin column (lilac), insert it into a 2 ml Eppendorf, and centrifuge for 3 minutes at high speed (14000 rpm).
- Carefully transfer the entire supernatant from the column to a new 1.5 ml Eppendorf without disturbing the pellet.
- Add 700 µl of 100% Isopropanol and vortex to homogenize.
- Pipette 700 µl of the sample into the PAXgene RNA spin column (red) placed in a 2 ml Eppendorf, then centrifuge for 1 minute at 12000 rpm. Place the column in a new 2 ml Eppendorf and discard the contents of the previous Eppendorf.
- Transfer the remaining sample to the red column and centrifuge for 30 seconds at 12000 rpm. Then, place the column in a new Eppendorf and discard the previous one.
- Add 350 µl of Buffer BM3 (concentrated wash buffer with added ethanol) to the column and centrifuge for 30 seconds at 12000 rpm. Transfer the column to another Eppendorf and discard the previous one.
- Add 10 µl of DNase I stock solution to 70 µl of Buffer RDD in a 1.5 ml Eppendorf, invert the Eppendorf to homogenize, and centrifuge to collect liquid residues at the bottom. Do not homogenize using a vortex as DNase I is highly sensitive to denaturation.
- Transfer the DNase I mix (80 µl) directly to the column membrane and incubate at room temperature for 15 minutes.
- Add 350 µl of Buffer BM3 to the column and centrifuge for 30 seconds at 12000 rpm. Discard the Eppendorf containing the filtrate and transfer the column to a new Eppendorf.
- Add 500 µl of Buffer BM4 (concentrated wash buffer with added ethanol) to the column and centrifuge for 30 seconds at 12000 rpm. Then discard the filtrate and transfer the column to a new Eppendorf.
- Add another 500 µl of Buffer BM4 to the column and centrifuge for 2 minutes at 14000 rpm.
- Discard the filtrate, transfer the column again, and centrifuge at 12000 rpm for 1 minute.

- Discard the Eppendorf containing the filtrate and transfer the column again to a new 1.5 ml Eppendorf. Directly add 40 µl of Buffer BM5 (elution buffer) to the column membrane and centrifuge at 12000 rpm for 1 minute. Repeat this step once.
- Discard the red column and place the Eppendorf containing the sample (elution buffer and RNA) on ice, then proceed with the assessment of quantity and quality.

5.3 QUANTITATIVE AND QUALITATIVE ASSESSMENT

A) Nanodrop Spectrophotomer

Figure 27: Nanodrop One(www.extranet.fisher.co.uk)

To quantify our samples, we used the Nanodrop spectrophotometer. This technology allows the measurement of RNA concentration in ng/µl. To obtain a quality assessment, it is necessary to analyze the following data:

- 260/280 ratio of sample absorbance at 260 and 280 nm. The ratio of absorbance at 260 and 280 nm is used to assess the purity of RNA. A ratio of ~1.8 is generally accepted as “pure” for RNA. If the ratio is 5-2 times appreciably lower in either case, it may indicate the presence of protein, phenol, or other contaminants that absorb strongly at or near 280 nm;
- 260/230 ratio of sample absorbance at 260 and 230 nm. This is a secondary measure of nucleic acid purity. The 260/230 values for “pure” nucleic acid are often higher than the respective 260/280 values. They are commonly in the range of 1.8-2.2. If the ratio is appreciably lower, this may indicate the presence of co-purified contaminants.

The assessment of RNA degradation involved examining the sharpness of the 28S and 18S bands through denaturing electrophoresis on a 1.2% agarose gel. To further appraise the integrity of the extracted RNA, we employed the RNA Integrity Number (RIN) using the Agilent 2100 Bioanalyzer. The 2100 bioanalyzer serves as a unique analytical tool capable of handling nucleic acids, proteins, and cells on a single platform. For sample processing, the Agilent RNA 6000 Pico Kit was utilized following the manufacturer's instructions. Agilent RNA kits consist of chips and reagents

specifically designed for the analysis of RNA fragments. Each RNA Pico chip comprises an interconnected set of microchannels for the electrophoretic separation of nucleic acid fragments based on their size. The RNA 6000 Pico kit, complementary to the RNA 6000 Nano kit, is suitable for applications where the amount of RNA (or cDNA) is limited, such as in biopsy samples or samples from microdissection experiments.

B) Gel Preparation and Electrophoresis:

- In a 100 ml cylinder, add 2 ml of Tris-Acetate-EDTA (TAE) and make up the volume with water.
- Add 1.2 g of agarose to the solution and heat until completely dissolved.
- Add 5 ml of GelRed, a nucleic acid dye highly sensitive and stable, designed to replace the extremely toxic Ethidium Bromide.
- Take 2 µl of each sample and add 2 µl of bromophenol blue (BPB) dye.
- Load the samples onto the gel and run them at 70-80V for about 40 minutes.
- Observe RNA bands on a UV transilluminator.
- Capture the image using Gel Doc (BioRad).

This allows observing three bands on the gel: the first two bands represent the major and high molecular weight RNA components, namely 28S and 18S rRNA; the last band consists of smaller but abundant molecules like 5.8S and 5S rRNA or tRNA. Messenger RNAs are not visible as they are present in small quantities in the cell.

C) Agilent 2100 Protocol:

- Equilibrate reagents to room temperature for 30 minutes, protecting the dye from light.
- Add 1 µl of concentrated Pico dye to 65 µl of gel and vortex, always protecting it from light.
- Take an RNA chip and place it in the chip station.
- Pipette 9 µl of the mix at the bottom of the well and set the timer to 30 seconds, ensuring the plunger is set to 1 ml, and then close the chip preparation station. The closure of the sealing device clicks when the integrated circuit injection station is closed correctly.
- Press the syringe plunger until held by the clip.
- Wait exactly 30 seconds and release the plunger with the clip release mechanism.
- Observe that the piston moves back at least to the 0.3 ml mark and wait 5 seconds, then slowly pull back the plunger to the 1 ml position.

- Pipette 9.0 µl of the mix into each marked well.
- Load the marker and ladder and subsequently load 1 µl of the samples in each well.
- Vortex the chip and run it on the Bioanalyzer for 5 minutes.

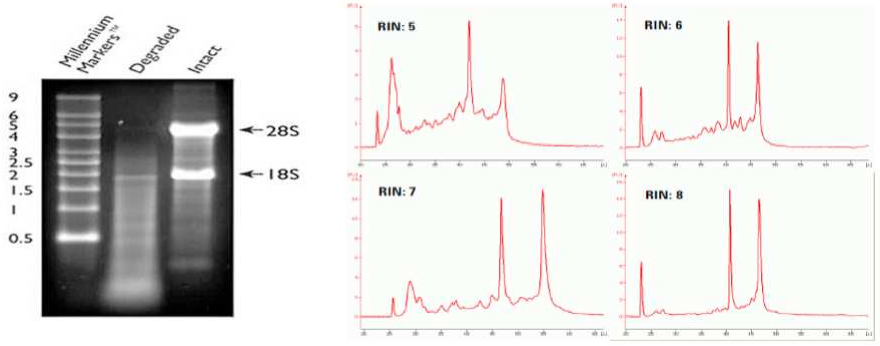

Figure 28: a) electrophoresis run b) RNA integrity number

5.4 GENE EXPRESSION PROFILE WORKFLOW

Following RNA extraction and quantitative/qualitative analyses, we employed the GeneChip WT PLUS Reagent Kit to prepare RNA samples for whole transcriptome expression analysis using the GeneChip Whole Transcript Expression Arrays (HTA 2.0). This kit generates amplified and biotinylated sense DNA strands used as targets from total RNA without the need for advanced selection or mRNA enrichment steps. The kit is optimized for use with GeneChip Sense Target Arrays. Additionally, it utilizes the Reverse Transcription method, which binds to the entire length of RNA, encompassing both poly(A)-tailed and poly(A)-lacking mRNAs, providing comprehensive and unbiased transcriptome coverage.

The GeneChip Kit provides exogenous poly-A RNA positive controls designed to monitor the entire target labeling process. These poly-A RNA controls are synthetically generated in vitro and correspond to B. subtilis genes that are absent in eukaryotic samples (Lys, Phe, Thr, and dap). The poly-A Control Stock needs to be diluted using the poly-A Control Dil Buffer. For 100 ng of total starting RNA, four serial dilutions are made: 1:20, 1:50, 1:50, and 1:10. Then, 2 µl of the final dilution is added to 3 µl of RNA sample.

The protocol provides the following steps:

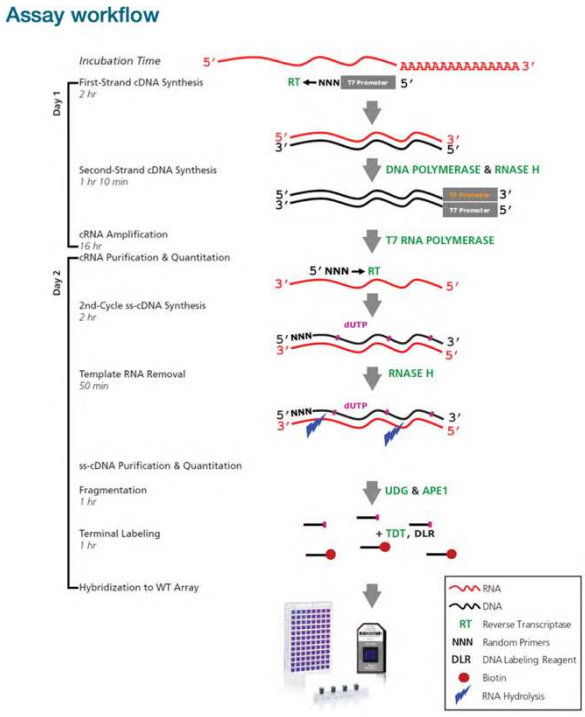

Figure 29: WT PLUS assay workflow

A) FIRST-STRAND cDNA SYNTHESIS:

In this reverse transcription procedure, total RNA is primed with primers containing a T7 promoter. The reaction synthesizes the single strand of cDNA with the T7 promoter starting from the 5' end.

- First, prepare the First-Strand Master Mix on ice using the following volumes:

REAGENT	VOLUME
First-strand buffer	4 µl
First-strand enzyme	1 µl

- Vortex to homogenize the mix and centrifuge.
- On ice, transfer 5 µl of the mix into each Eppendorf tube (one for the mic and one for the clot).
- Add 5 µl of RNA to each Eppendorf containing the mix to reach a final volume of 10 µl.
- Vortex and centrifuge.
- Incubate in a thermal cycler under the following conditions:
  1 hour at 25°C, 1 hour at 42°C, 2 minutes at 4°C
- After incubation, immediately centrifuge to collect the first cDNA strand at the bottom of the Eppendorf.

B) SECOND-STRAND cDNA SYNTHESIS:

In this procedure, the single strand is converted into double-stranded cDNA, which will serve as a template for in vitro transcription. DNA polymerase and RNase H are used to simultaneously degrade RNA and synthesize the second cDNA strand.

- Prepare the mix on ice with the following volumes:

REAGENT	VOLUME
Second-strand buffer	18 µl
Second-strand enzyme	2 µl

- Vortex and centrifuge the mix to homogenize the components.
- On ice, transfer 20 µl of the mix to each sample (10 µl) to reach a final volume of 30 µl.
- Vortex and centrifuge.
- Incubate for 1 hour at 16°C, 10 minutes at 65°C, and 2 minutes at 4°C.

C) cRNA SYNTHESIS WITH IN VITRO TRANSCRIPTION:

In this procedure, antisense RNA is synthesized and amplified using in vitro transcription (IVT) of double-stranded cDNA with T7 RNA polymerase.

- Prepare the IVT Master Mix at room temperature with the following volumes:

REAGENT	VOLUME
IVT buffer	24 µl
IVT enzyme	6 µl

- Vortex and centrifuge the mix.
- At room temperature, transfer 30 µl of the IVT Master Mix to each sample (30 µl) to reach a final volume of 60 µl.
- Vortex and centrifuge.
- Incubate for 16 hours at 40°C and then at 4°C.
- After incubation, centrifuge and proceed with the next steps.

D) cRNA PURIFICATION:

This step removes enzymes, salts, inorganic phosphates, and unincorporated nucleotides to prepare cRNA for the second round of single-strand cDNA synthesis.

- Add 100 µl of purification beads to the cRNA after centrifugation and resuspension, mixing 10 times.
- Incubate for 10 minutes to allow cRNA to adhere to the beads.
- Place the Eppendorf tubes in a magnet to capture the beads and discard the supernatant.
- Wash the beads using 200 µl of 80% ethanol and incubate for 30 seconds.
- Slowly aspirate and discard the ethanol without disturbing the beads, repeating the step for a total of 3 washes.
- Finally, remove the ethanol and air-dry completely for at least 7 minutes.
- Elute the RNA by adding 27 µl of preheated Nuclease-free Water to each sample at 65°C, incubating for 1 minute, and then pipetting 10 times.
- Place the samples in a magnetic plate, capture the beads, transfer the eluted cRNA-containing supernatant to another Eppendorf tube, and place it on ice.

DETERMINATION OF cRNA CONCENTRATION AND PURITY:

The concentration of cRNA is determined by measuring absorbance at 260 nm using Nuclease-free water as a blank. NanoDrop is used, and 1.5 µl of the sample is measured. For a good sample, the yield should be >20 µg.

E) SECOND CYCLE OF SINGLE-STRAND cDNA SYNTHESIS:

Continue with the second cycle of single-strand cDNA synthesis, where the cDNA strand is synthesized using Reverse Transcriptase with second-cycle primers. For this step, 15 µg of cRNA is required.

- Prepare 625 ng/µl of cRNA on ice, corresponding to 15 µg in a volume of 24 µl.
- Combine 24 µl of cRNA with 4 µl of 2nd-cycle Primers on ice.
- Vortex and centrifuge the mix.
- Incubate for 5 minutes at 70°C, 5 minutes at 25°C, and 2 minutes at 4°C.
- After incubation, centrifuge, put on ice, and prepare the 2nd-Cycle ss-cDNA Master Mix on ice with the following volumes:

REAGENT	VOLUME
2nd-cycle ss-cDNA buffer	8 µl
2nd-cycle ss-cDNA enzyme	4 µl

- Centrifuge the Master Mix and dispense 12 µl of the mix into each sample (28 µl), obtaining a final volume of 40 µl.
- Centrifuge and incubate for 10 minutes at 25°C, 90 minutes at 42°C, 10 minutes at 70°C, and 2 minutes at 4°C.

F) RNA HYDROLYSIS USING RNase H:

In this procedure, RNase H hydrolyzes the cRNA template, leaving the single cDNA strand.

- Add 4 µl of RNase H to the samples (40 µl), reaching a final volume of 44 µl.
- Centrifuge and incubate for 45 minutes at 37°C, 5 minutes at 95°C, and 2 minutes at 4°C.
- After incubation, centrifuge put the samples on ice, and add 11 µl of Nuclease-Free Water to each sample, reaching a volume of 55 µl.

G) PURIFICATION OF 2ND-CYCLE SINGLE-STRANDED cDNA:

After hydrolysis, the cDNA single strand is purified by removing enzymes, salts, and unincorporated dNTPs.

- Vortex and resuspend the magnetic beads, adding 100 µl of beads to each sample (final volume 155 µl).
- Add 150 µl of 100% ethanol to the 155 µl sample (ss-cDNA/Big beads) and resuspend 10 times.
- Incubate for 20 minutes to allow binding between the sample and the beads.
- Transfer the Eppendorf tubes to a magnet and wait for 5 minutes to capture the beads, then aspirate and discard the supernatant.
- Add 200 µl of 80% ethanol to each sample and proceed with washing, aspirating the supernatant, and repeating the step 2 more times.
- Remove the samples from the magnet and add 30 µl of Nuclease-Free Water preheated to 65°C.
- Pipette 10 times, then place the samples in the magnet and transfer the supernatant (eluted ss-cDNA) to another Eppendorf tube to remove the beads.

DETERMINATION OF cDNA CONCENTRATION AND PURITY:

Determine the cDNA concentration by measuring absorbance at 260 nm, using Nuclease-free water as a blank. Use NanoDrop and measure 1.5 µl of the sample. For a good sample, the yield should be >5.5 µg.

H) FRAGMENTATION AND LABELING OF ss-cDNA:

In this step, purified ss-cDNA is fragmented by Uracil-DNA glycosylase (UDG) and apurinic/apyrimidinic endonuclease 1 (APE1) at the dUTP residues, resulting in the breakage of the strand. The fragmented cDNA is labeled by terminal deoxynucleotidyl transferase (TdT) using Affymetrix reagents, covalently binding with Biotin.

- Prepare 176 ng/µl of sample on ice.
- Prepare the Fragmentation Master Mix with the following volumes:

REAGENT	VOLUME
Nuclease-Free Water	10 µl
10x cDNA Fragmentation buffer	4,8 µl
UDG 10U/µl	1 µl
APE 10U/µl	1 µl

- Centrifuge the Master Mix and transfer 16.8 µl of the mix to each fragmented ss-cDNA sample (48 µl), reaching a final volume of 48 µl.
- Centrifuge and incubate for 1 hour at 37°C, 2 minutes at 93°C, and 2 minutes at 4°C.

- After incubation, centrifuge and put the samples on ice.
- Prepare the Labeling Master Mix with the following volumes:

REAGENT	VOLUME
5x TdT buffer	12 µl
DNA Labeling Reagent 5mM	1 µl
TdT 30U/µl	2 µl

- Centrifuge the mix and transfer 15 µl to each fragmented ss-cDNA sample (45 µl), reaching a final volume of 60 µl.
- Centrifuge and incubate for 1 hour at 37°C, 10 minutes at 70°C, and 2 minutes at 4°C.
- After incubation, centrifuge.

I) HYBRIDIZATION OF HTA 2.0 CHIP:

Figure 30: GeneChip Human Transcriptome Array 2.0, Affymetrix

- Prepare the Hybridization Master Mix at room temperature with the following volumes:

REAGENT	VOLUME
Control oligo B2 3nM	3,7 µl
20x Hybridization controls	11 µl
2x Hybridization Mix	110 µl
DMSO	15,4 µl
Nuclease-Free Water	19,9 µl

- Centrifuge the Master Mix.
- Prepare the Hybridization Cocktail at room temperature:

REAGENT	VOLUME
Hybridization Master Mix	160 µl
Fragmented and labeled ss-cDNA	60 µl

- Incubate for 5 minutes at 99°C, 5 minutes at 45°C.
- After incubation, centrifuge, inject, and hybridize the array by inserting two tips at the two septa, injecting the sample (200 µl) into the array through a septum. Remove the tips and cover the chips.
- Incubate the chips in the preheated oven at 45°C for 16 hours at 60 rpm.

J) WASH AND STAIN:

- Remove the chips from the oven.
- Extract the Hybridization Cocktail Mix from the arrays.
- Load the arrays with 250 µl of Wash Buffer A.
- Place the arrays in the fluidic station and insert:
  - 600 µl of Stain Cocktail 1 into well 1
  - 600 µl of Stain Cocktail 2 into well 2
  - 800 µl of Array Holding Buffer into well 3
- Wash the arrays using protocol FS450_0001.

With this step, all elements not bound to the probes are washed away and removed. This operation takes place in the fluidic station, and commands are given using the Affymetrix GeneChip Command Console. In the fluidic station, the marking phase also takes place. This operation amplifies the hybridization signal, and subsequently, the scanner is used. Each fragment labeled with biotin binds to numerous antibodies labeled with fluorochromes, resulting in an increased intensity of the light signal.

K) MICROARRAY DATA CREATION AND ANALYSIS:

The chip analysis was carried out following the instructions provided by Affymetrix. The scanner and the computer are connected, allowing us to visualize a digital image corresponding to the chip. The chip is inserted into the scanner, and the processing begins. To facilitate the visualization of hybridized fragments, the microarray is divided into many tiny cells, each corresponding to a gene. The light intensity is directly proportional to the expression level of each gene. Visually, it is possible to perform an initial qualitative analysis and observe the presence of any artifacts, such as altered spots or global background [Figure 24]. This noise can be indirectly quantified by measuring the luminous non-uniformity within the same probe cells. The GCOS software generates a file with the extension by reprocessing the contents of the ".dat" file using the Cell Analysis Algorithm. The ".cel" extension contains the measured intensity for each probe cell. This format is compatible with all bioinformatics programs available on the market, allowing us to autonomously choose the one that we consider most suitable for each analysis. The ".report" extension contains the parameters that will allow us to perform more detailed qualitative and quantitative analyses executed through Bioconductor.

5.5 ANALYSIS PIPELINE FOR GENE EXPRESSION STUDY

In this study, we employed the GeneChip WT PLUS Reagent Kit for target preparation and the Affymetrix Transcriptome Analysis Console (TAC) software for data analysis. Quality control was ensured through internal control points, and clot quality was validated using TAC software metrics. Data processing involved the import of image files into TAC software, with the selection of microarrays meeting quality control criteria. Normalization utilized the "GeneLevel-SST-RMA" method, incorporating Signal Space Transformation (SST) and probe Guanine Cytosine Count Correction (GCCN) algorithms before applying the Robust Multichip Average method (RMA) (Affymetrix whitepaper). Differential gene expression (DEG) analysis was performed using a One-Way ANOVA comparison approach. The Benjamini-Hochberg Step-Up procedure controlled the false discovery rate (FDR) (Benjamini et al, 1995)

Genes were considered differentially expressed based on stringent criteria: p-value < 0.05, fold change (FC) > 2, and Benjamini-Hochberg adjusted p-value (FDRp-val) < 0.15. To interpret differentially expressed genes, enrichment analysis was conducted using R software (version 4.2.2) (R Core Team, 2022) and specific libraries: ClusterProfiler (v.4.6.2), DOSE (v.3.24.2), ReactomePA (v.1.42.0) (Wu T et al, 2021) (Yu G et al, 2015) (Yu G et al, 2016). This aimed to identify overrepresented or underrepresented biological processes associated with gene expression changes. Additionally, using gene expression data, CIBERSORTx, an in-silico tool, was employed to estimate the abundances of the most common immune system cells in the cohort examined (Newman AM et al, 2019).

The integration of these methods provides a comprehensive analysis of gene expression changes, contributing valuable insights into the biological processes and immune cell composition associated with the experimental conditions.

CHAPTER 6

RESULTS PART I: PROOF OF CONCEPT

For this thesis, the meticulous evaluation of RNA quality emerges as a critical initial phase crucial for the subsequent analysis of gene expression profiles. RNA, being inherently susceptible to degradation, presents a unique challenge, particularly when extracted from complex tissues like thrombus, as indicated by previous literature (Popova T et al, 2008; Fraser JF et al, 2019).

The study begins by thoroughly examining both the quantity and quality of materials extracted from thrombectomy procedures, with a specific focus on comparing them to materials obtained from peripheral venous blood. The tracking of RNA characteristics provides valuable insights into the integrity and suitability of the samples for downstream gene expression analyses, enhancing the interpretability and reliability of the study's findings.

In conducting a rigorous analysis of RNA samples, the incorporation of specific checkpoints becomes essential for assessing and ensuring the quality of the genetic material. This study employs a multifaceted approach, incorporating distinct checkpoints at various stages of the experimental workflow:

1. Pre-procedure Checks:

- Spectrophotometric Evaluation: Before proceeding with the experimental procedures, a spectrophotometric evaluation is conducted. This quantitative assessment provides insights into the concentration of RNA in the samples, offering a preliminary indication of their suitability for downstream analyses.

- RNA Integrity Number Evaluation: Another critical pre-procedure checkpoint involves evaluating the RNA Integrity Number (RIN). This qualitative measure assesses the integrity of RNA molecules, offering valuable information on their structural soundness.

2. Intraprocedural Controls:

- Pivot points in methodologies and protocols: Throughout the experimental process, intraprocedural controls are strategically placed at pivotal points within the methodologies and protocols employed. These checkpoints include spectrophotometric evaluations of cRNA and single-strand cDNA (ss_cDNA). Monitoring these parameters during the procedures ensures the reliability and consistency of the experimental steps.

3. Post-procedure Controls:

- Bioinformatics Tools Assessment: After the completion of the experimental procedures, post-procedure controls are implemented through the use of bioinformatics tools. These tools offer a comprehensive and systematic assessment of the overall quality of the experiment. They analyze various parameters, integrating data from different stages to provide a holistic view of the experimental outcome.

6.1 PRE-PROCEDURE CHECKS

The extraction of RNA is the initial step undertaken by the operator in gene expression profiling experiments, whether it involves Real-Time PCR, microarrays, or RNA sequencing. Having high-quality RNA samples is considered crucial for obtaining meaningful experimental results. Therefore, it is mandatory to assess the quality of RNA before any other analysis. The RNA Integrity Number (RIN) has become a widely accepted standard for measuring RNA quality and has proven to be a more meaningful and comprehensive method compared to previous approaches for assessing RNA samples, such as UV spectroscopy or pure ribosomal RNA ratios. The RIN was developed based on a learning algorithm that utilizes the entire capillary electrophoresis trace (Bioanalyzer), rather than just the ratio of large ribosomal peaks, although the RIN still heavily depends on this ratio. Typically, samples are deemed of good quality, meaning intact, if they have a RIN ranging from 7 to 10 (Sigurgeirsson B et al, 2014). This range signifies the integrity and suitability of RNA samples for subsequent gene expression analyses. The results revealed that the average RNA yield from thrombus samples was 1119.62 ng, with a broad range of 104-9136 ng and a median value of 536 ng. Importantly, the integrity of the RNA, assessed through the RNA Integrity Number (RIN), was found to be 5.5 ± 0.5 for thrombus samples and 9.05 ± 0.24 for peripheral venous blood samples. The significant difference in RIN indices emphasizes the distinct challenges associated with working with thrombus material compared to more accessible samples like peripheral venous blood.

6.2 INTRAPROCEDURAL CONTROLS

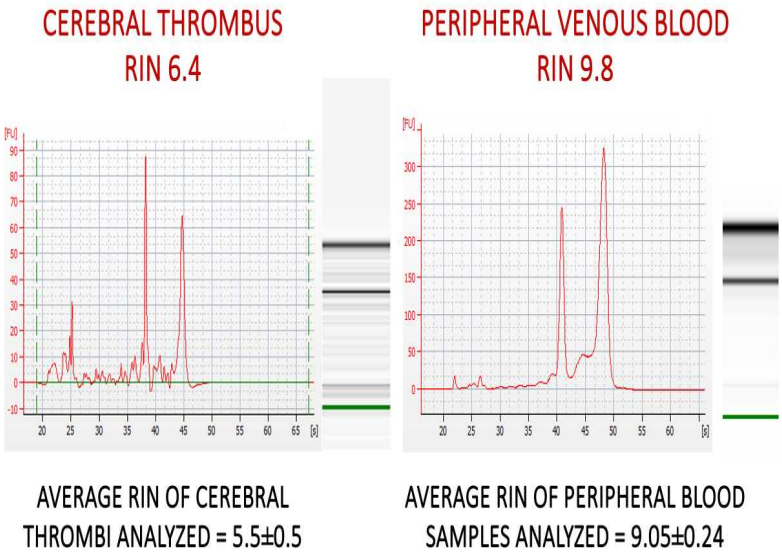

Figure 31: RIN obtain from RNA of Cerebral Thrombi and Peripheral Blood samples

To bolster confidence in the reliability of the samples, we incorporated in the quality control process the two critical phases provided by the GeneChip WT Plus protocol. These phases serve as meticulous quality control steps, scrutinizing both the sample preparation process and the intrinsic quality of the samples. The protocol involves quantifying and evaluating both cRNA and single-strand cDNA (ss-cDNA) after purification, before the fragmentation and labeling steps. These steps are not merely procedural; they are foundational to the experiment, adhering to precise protocol requirements for stringent quality assurance. The presented table serves as a comprehensive record of the concentration and purity values derived from the RNA samples obtained during various stages of the experimental workflow (total RNA extraction and at the two checkpoints of the gene expression evaluation protocol).

Samle ID	Source	Concentation ng/µl	260/280	260/230	cRNA µg (>20µg)	ss_cDNA µg (>5.5µg)
C41	Clot	41.3	1.99	1.05	23.62	11.55
C42	Clot	4.4	1.85	0.18	19	8.3
C43	Clot	9.1	1.53	0.38	19.58	8.13
C44	Clot	12.5	1.98	1.33	27	11.35
C54	Clot	17.7	1.93	0.1	21	8.7
C55	Clot	24.5	2.07	0.2	21.9	8.4
C56	Clot	11.3	2.02	0.21	21.4	8.5
C57	Clot	40.4	1.9	0.2	30.3	9.8
C58	Clot	22.6	1.8	0.39	22.8	5.4
C59	Clot	53.7	1.91	1.82	23.8	9.2
C60	Clot	13.2	1.86	0.33	19.4	8.1
C61	Clot	37.6	1.73	0.37	21.4	7.9
C62	Clot	15	2.17	0.97	30	9.8
C63	Clot	24.7	1.94	0.79	23.4	9.1
C64	Clot	1.7	2.06	0.13	17.7	8.2
C65	Clot	41.5	2.07	1.58	30.8	9.9
C66	Clot	69.6	1.95	1.25	21.2	10.8
C67	Clot	10.8	2.21	0.41	25.9	10.1
C68	Clot	13.7	2.26	0.90	18.3	9.4
C69	Clot	14.9	2.11	1.20	26.4	9.6
C70	Clot	21.9	1.93	0.11	28.3	9.5
C71	Clot	8.0	2.07	0.12	29.2	11.9
C72	Clot	16.3	2.08	0.89	30.7	10.5
C73	Clot	1.6	2.94	0.01	15.2	7.2
C74	Clot	34.9	1.95	1.19	30.7	11.5
C75	Clot	6.7	2.46	0.37	29.6	10.4
C76	Clot	3.6	2.20	0.18	18.1	8.8
C77	Clot	1.8	2.42	0.28	12.4	5.2
C78	Clot	6.2	2.15	0.47	29.2	7.1
C79	Clot	3.2	2.62	0.39	19.6	5.9
C80	Clot	14.1	2.05	1.53	21.6	5.9
C81	Clot	55.9	1.97	1.55	36.8	6.9
C82	Clot	3.4	2.81	0.73	28	5.9
C83	Clot	44.6	1.89	0.85	33.6	7
C84	Clot	3.2	1.33	0.68	16.4	4.9
C85	Clot	10.3	2.18	1.07	29.4	7
C86	Clot	25.3	1.93	1.37	34.6	11.5
C87	Clot	13.3	2.10	1.18	33	9.7
C88	Clot	15.0	1.98	1.08	27.8	9.6
C89	Clot	17.2	2.08	1.22	41.6	10.6

Sample ID	Source	Concentration ng/µl	cRNA µg (>20 µg)	ss_cDNA µg (>5.5 µg)
M22	PB	14	18.37	11
M1	PB	15.6	11.45	7.5
M4	PB	11.8	28.5	13.4
M2	PB	9.6	22.5	9.5
M5	PB	13.1	23.2	12.2
M11	PB	17.6	12	7.5
M14	PB	13.6	40.04	15.94
M15	PB	49.1	59	11.21
M17	PB	13.9	39.5	14.9
M16	PB	18.4	46.1	15
M8	PB	46.4	31.4	14.31
M12	PB	78.1	32	12.9
M13	PB	47.7	29	11.9
M9	PB	14.8	22.3	12.88
M3	PB	24.7	12.7	7.34
M10	PB	22.9	42	13
M7	PB	13	25.5	11.9
M6	PB	29.3	22.4	10.98
M34	PB	20.9	40.29	14.7
M35	PB	87.7	39.43	13.53
M36	PB	69.5	35	13.3
M37	PB	66.7	42	12.03
M38	PB	123.2	16.4	8.1
M39	PB	42.4	18.4	10.3
M40	PB	32.7	17.1	10.2
M42	PB	53.7	20.2	9.6
M43	PB	12.5	19.6	10.62
M44	PB	15	19.97	12.9
M45	PB	8.5	24.5	13.52
M46	PB	19.8	19.1	11.75
M47	PB	9.9	21.7	12.2
M48	PB	113.8	22.4	11.74
M49	PB	69.1	21.38	12.4
M41	PB	31.5	12.96	8.29

Table 2: Yields of the analyzed sample

The data derived from The GeneChip WT Plus protocol underscore the experiment's robustness, indicating satisfactory efficiency across nearly all samples. This suggests that the experimental steps, inclusive of sample preparation and operator handling, align with the stipulated criteria for quality assurance. The strategic inclusion of these rigorous quality control measures serves as a safeguard, instilling confidence in the accuracy and reproducibility of the subsequent gene expression analyses.

6.3 POST-PROCEDURE CONTROLS

Microarray data quality can be sensitive to various steps in the experimental workflow, making quality assessment a crucial component of the analysis, so the study progresses to the bioinformatic analysis of the data.

The first stage of bioinformatic preprocessing involves a comprehensive quality check across the entire dataset. This step is crucial for identifying and excluding any outliers, such as data points that deviate significantly from the norm or may be indicative of experimental artifacts (Schuchhardt J et al, 2000). The identification and removal of outliers are essential for maintaining the accuracy and reliability of the subsequent analyses.

Following the quality check, the dataset undergoes a normalization process. Normalization is employed to remove systematic variations in the data, ensuring that the gene expression measurements are comparable across different samples and conditions. After normalization, another round of quality control is performed to validate the integrity of the normalized dataset.

To carry out these bioinformatic processes, various software tools are available. The choice of software depends on factors such as the specific requirements of the analysis, the characteristics of the dataset, and the preferences of the researchers. Overall, this bioinformatic analysis is critical for extracting meaningful insights from the gene expression data and drawing accurate conclusions from the experiment.

The software Applied Biosystems Transcriptome Analysis Console (TAC) enables the rapid development of meaningful insights from transcriptomic microarray data, utilizing a variety of statistical, visualization, and quality control (QC) tools. TAC goes beyond simple identification of differential expression by providing powerful and interactive visualizations (https://tools.thermofisher.com/). The TAC software allows:

A) Array QC and Data Normalization: TAC facilitates the quality control of the array and data normalization.

B) **Statistical Tests for Differential Expression:** TAC enables the execution of statistical tests for assessing differential gene expression.

C) **Focus on Genes or Pathways of Interest:** Users can concentrate on specific genes or pathways of interest.

D) **Explore Coding and Non-Coding RNA Interactions:** TAC supports the exploration of interactions between coding and non-coding RNA.

E) **Interpret Complex Alternative Splicing Events:** Users can interpret complex alternative splicing events.

F) **Link Out to Publicly Available Annotations:** TAC allows linking out to publicly available annotations for enhanced information.

G) **Obtain Sequence Information for Experimental Design:** Users can obtain sequence information to design validation experiments.

To aid in establishing QC processes for gene expression profile analyses, many controls have been developed. It is necessary to monitor these controls to assess data quality, with many being generated as products of initial analyses by respective algorithms. To assist in monitoring these values, the TAC software provides a set of tools for visualization and graphics associated with both the array and analyses.

These metrics include:

- **Hybridization Controls:** These controls are included in the hybridization cocktail, regardless of RNA sample preparation. They are used to assess the efficiency of sample hybridization to expression gene arrays. Hybridization controls are represented by a linear graph to monitor consistency between samples and a relative signal increase.

- **Labeling Controls:** Poly-A controls are used to monitor the labeling process. Each eukaryotic probe on the GeneChip array contains a set of probes absent in eukaryotic samples. These Poly-A controls are synthesized in vitro. Poly-A controls can be inserted into a complex RNA sample, carried through the sample preparation process, and assessed as internal control genes. Labeling controls can be visualized in a linear graph.

- **Internal Control Genes (Housekeeping Genes):** Housekeeping genes are constitutively transcribed genes in the examined samples. These genes serve as internal controls and are useful for monitoring the quality of the starting sample, subject to any variability in sample labeling and array hybridization. GAPDH and β-Actin are usually used to assess RNA samples and the quality of the ongoing analysis.

- Global Array Metrics.

- Algorithmic Parameters.

It is crucial to understand the process of creating charts and tables that facilitate the evaluation of the quality of individual hybridizations within a single study. This ensures easy assessment and offers initial guidance for interpretation. As a general practice, it is advisable to establish a record that consolidates all essential parameters for monitoring quality and identifying potentially irregular samples. A useful approach in scrutinizing such QC data involves identifying outliers in comparison to other closely correlated samples.

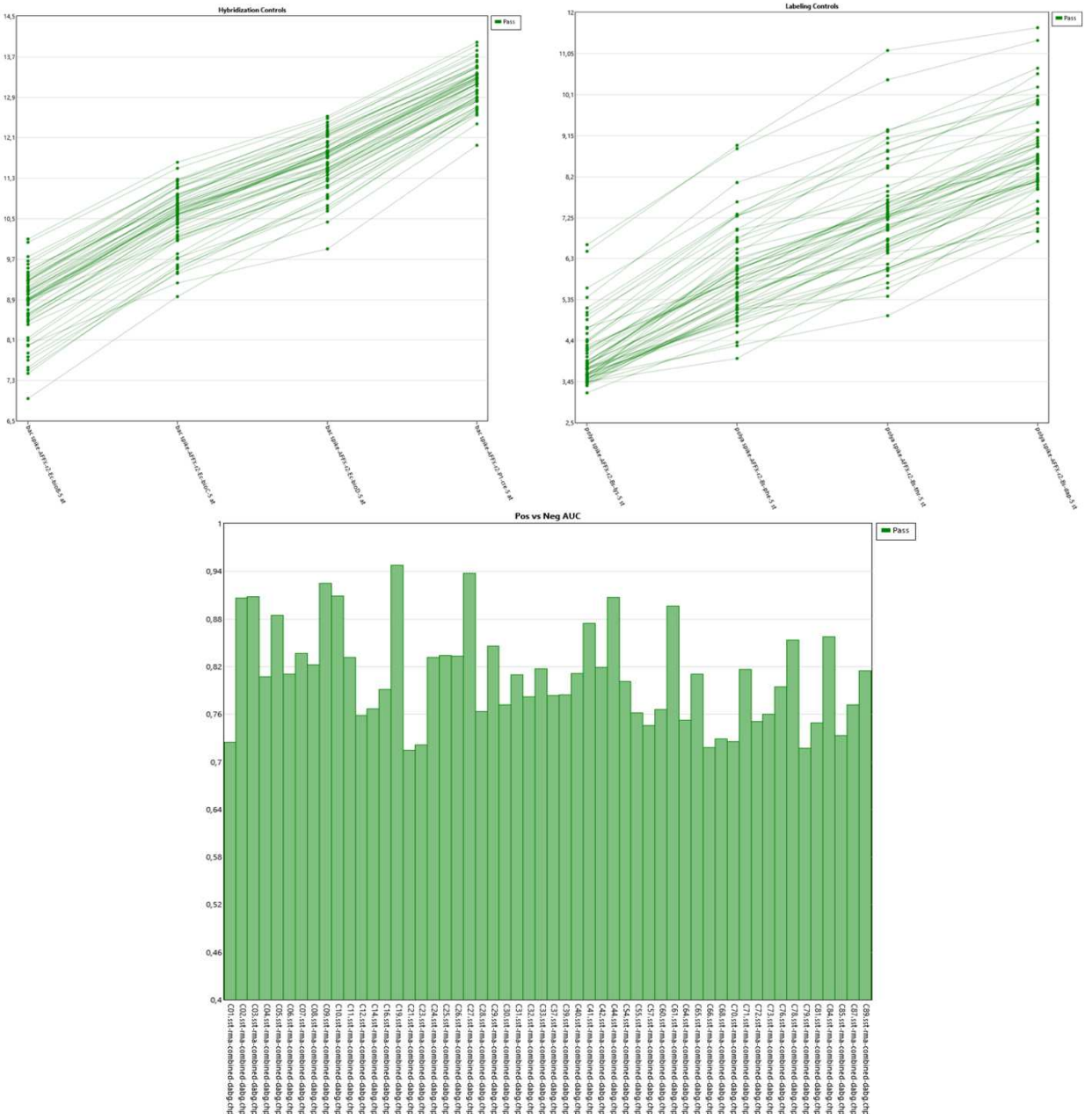

Figure 32: Post-procedural controls in Cerebral thrombi samples. A) Hybridization Controls: On the x-axis, representation of the 20x Eukaryotic Hybridization Controls B) Labeling Controls C) Positive vs. negative AUC: Shows the value of the samples analyzed.

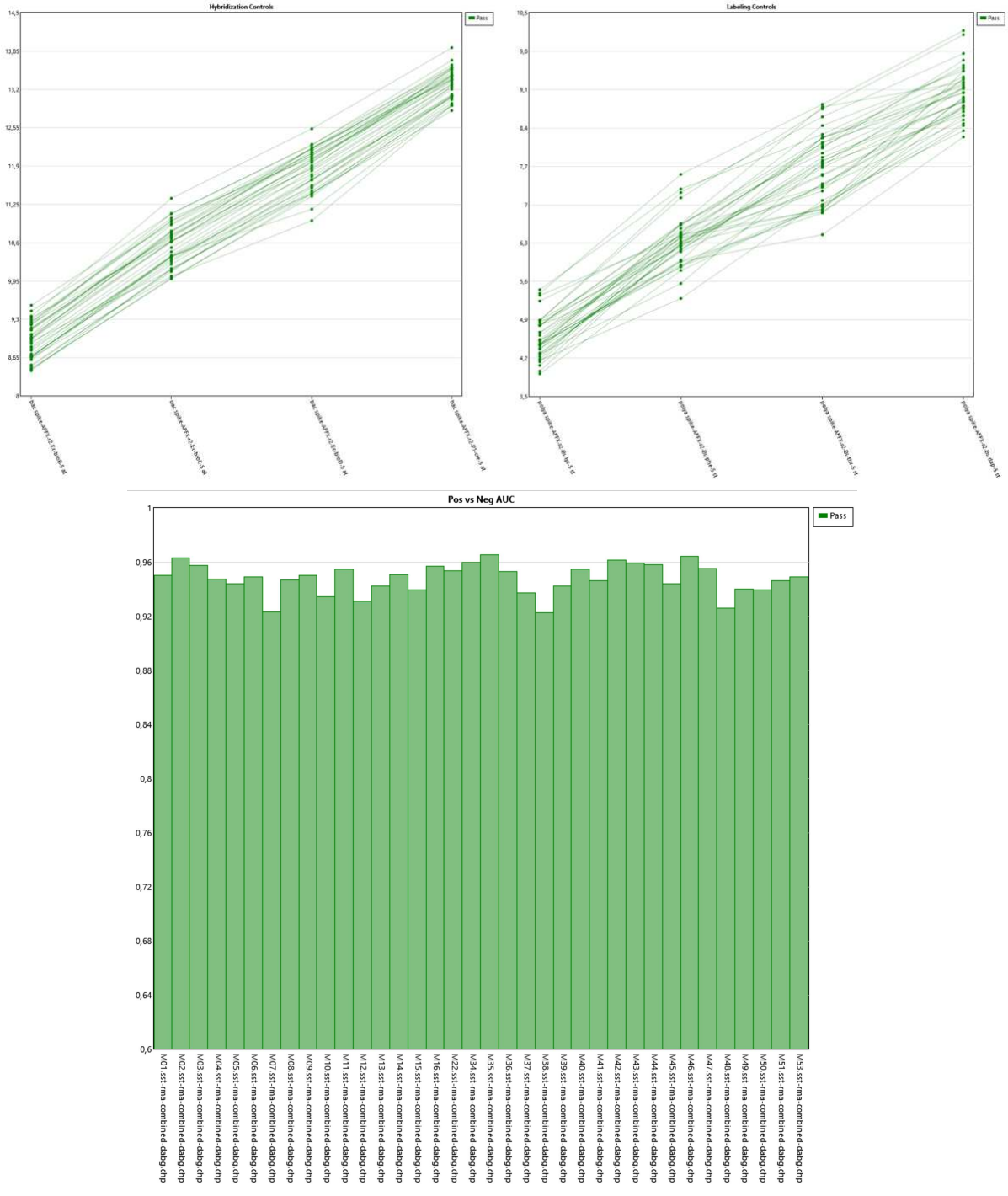

Figure 33: Post-procedural controls in Peripheral Venous Blood samples. A) Hybridization Controls: On the x-axis, representation of the 20x Eukaryotic Hybridization Controls B) Labeling Controls C) Positive vs. negative AUC: Shows the value of the samples analyzed.

TAC provides the capability to normalize data using both the RMA (Robust Multi-array Average) algorithm and its proprietary SST (Signal Space Transformation) algorithm.

The Signal Space Transformation algorithm, or SSTRMA, involves preprocessing steps applied to ".cel" files before the actual normalization and summarization with RMA. This method, known as SST-RMA, serves multiple purposes. It addresses GC4 background corrections, where GC stands for the content of guanine (G) and cytosine (C) nucleotides in a DNA or RNA sequence. The correction, known as GC Correction Version 4 (GC4), is crucial for refining the background signal. Additionally, SST-RMA performs intensity normalization using the Signal Space Transformation approach. Intensity normalization is a crucial step to ensure that the measured intensities of the probes are adjusted appropriately, providing accurate and comparable data.

The overall goal of employing these algorithms, especially SST-RMA, is to improve the quality of the data by addressing background corrections, normalization, and enhancing the fold change metric. Fold change is a vital measure indicating how much a particular quantity changes between two consecutive measurements. It is calculated as the ratio between these measurements.

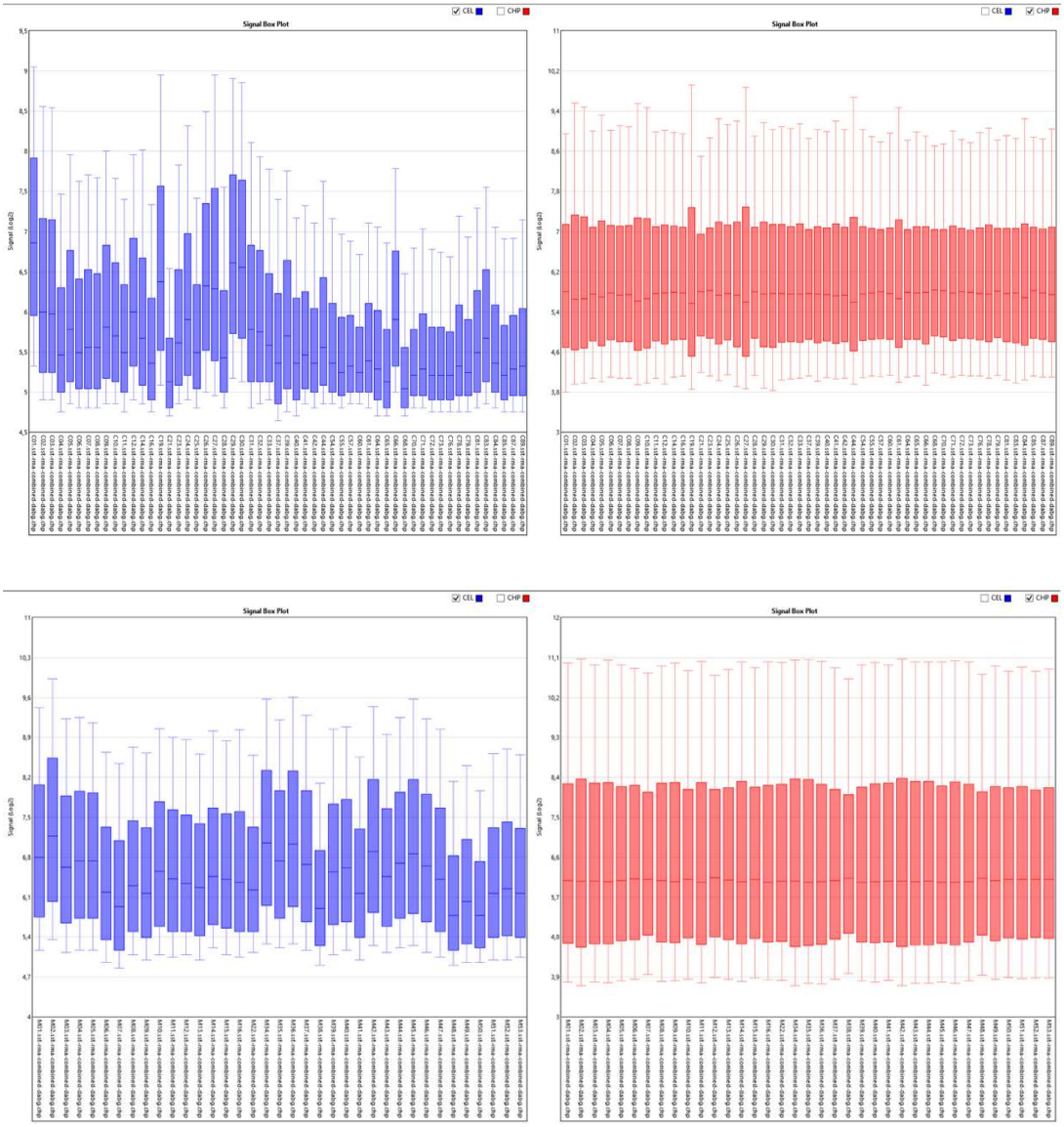

Figure 34: Box plot of expression data before and after normalization. The x-axis presents the different samples, and the y-axis presents the expression value. The black line in each box represents the expression median for each sample. A) Data obtained from cerebral thrombi samples B) Data obtained from peripheral blood samples.

CHAPTER 7

RESULTS PART II: GENE EXPRESSION PROFILING

7.1 STUDY POPULATION

We conducted gene expression profile analysis using RNA extracted from 80 cerebral thrombi (clots) and 37 samples of peripheral venous blood (mic). After performing a quality control study (discussed in Chapter 6), we found that 54 out of the 80 cerebral thrombi samples had sufficient quality for transcriptome analysis using Affymetrix technology. In the table are reported the clinical and demographic characteristics of the cohort in analysis.

Specifically, in this study we categorized the patients into different subtypes of stroke based on the nature of the blood clot. In this cohort, 5 patients were classified under the Large Artery Atherosclerotic subtype, 21 under Cardioembolic stroke, 20 under Cryptogenic (of unknown cause), and 8 had strokes of other determined causes. This categorization helps in understanding the diversity within the study group and may be relevant for further analysis and interpretation of the gene expression profiles.

Features	Acute Ischemic Stroke N=54
Age, years mean±SD	77.5±12.6
Sex, male N (%)	24 (44.0)
Hypertension, N (%)	29 (54.0)
Diabetes, N (%)	4 (7.4)
Dyslipidemia, N (%)	14 (26.0)
Current smoking, N (%)	4 (7.4)
Baseline NIHSS, median (IQR)	18 (15-24)
Heart failure, N (%)	8 (15.4)
Atrial Fibrillation N (%)	17 (31.5)
Systemic thrombolysis and endovascular treatment, N (%)	23 (42.6)
Endovascular treatment, N (%)	31 (57.4)

Table 3: clinical and demographic characteristics of the cohort in analysis

7.2 AFFYMETRIX GENE EXPRESSION PROFILING

The GeneChip HTA 2.0 Array is a specific microarray that contains 67,528 transcript clusters (TC), which represent different RNA molecules. After conducting data processing and applying filtering criteria, we excluded probes corresponding to redundant genes and those that were not annotated, that is they lacked information about their function or identity. This filtering process resulted in the identification of the expression of 24,013 genes in cerebral thrombi (CT) and 23,937 genes in peripheral venous blood (PB). Among all the genes analyzed, 2,772 are specific to CT, and 2,696 are specific to PB. In other words, these are genes that are uniquely expressed in each type of specimen.

Furthermore, when looking at the overlap or intersection of genes between CT and PB, it was found that 21,241 genes were common to both types of specimens. These common genes indicate shared gene expression patterns between CT and PB, despite the differences in the origin and nature of these samples. Understanding these shared and specific gene expressions can provide valuable insights into the molecular characteristics of the studied specimens.

7.3 CIBERSORT

In numerous studies, the most employed approach for delineating the various cell types present in the analyzed sample is through immunohistochemistry, yet gene expression data offers a broader examination of various immune cell types. Only a limited number of studies have employed gene expression signatures to quantify specific immune cell types (Craven K E et al, 2021). Furthermore, very few studies have endeavored to identify the molecular characteristics of acute ischemic stroke linked to heightened immune infiltrate or particular immune cell types (Tutino V et al, 2022). CIBERSORT (Cell-type Identification By Estimating Relative Subsets Of RNA Transcripts) serves as a deconvolution technique, delineating the cellular makeup of intricate tissues through gene expression data. This method utilizes linear support vector regression (SVR), a machine learning approach, to unravel the amalgamation of gene expression. Its outcomes have demonstrated a strong correlation with flow cytometric analysis, leading to its designation as "digital cytometry" (Newman AM et al, 2019).

We conducted the CIBERSORT analysis on both samples of cerebral thrombi and peripheral venous blood.

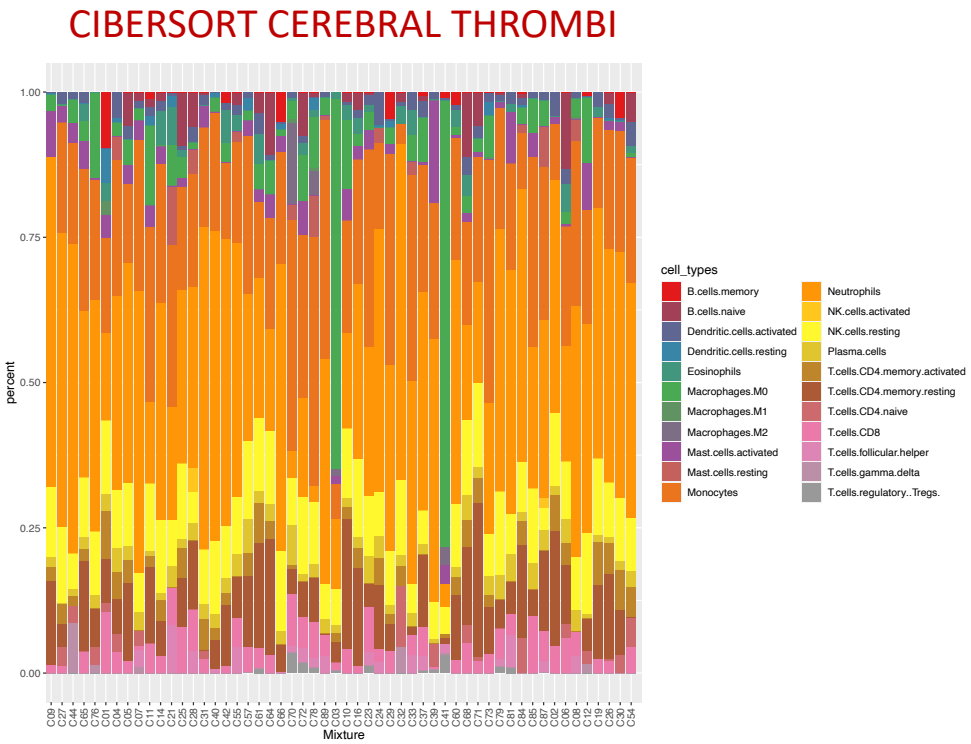

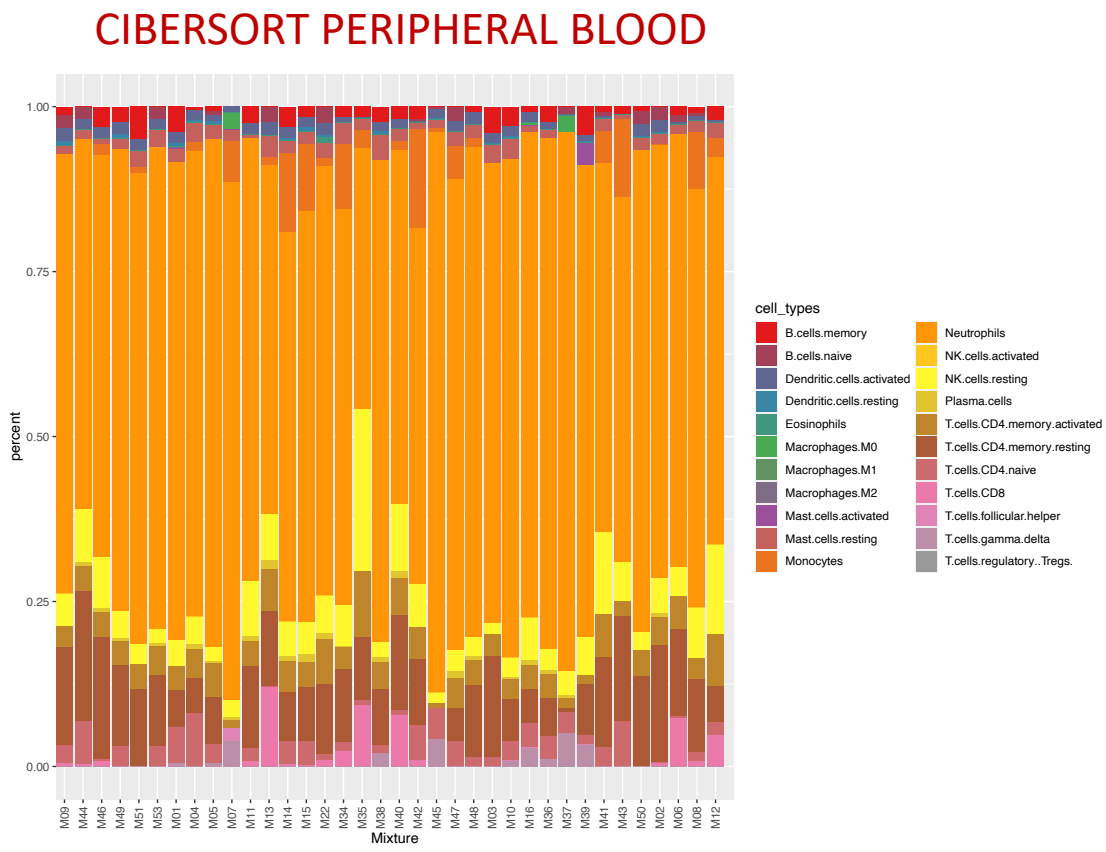

Figure 35: CIBERSORTx analysis of CT (upper) and PB (lower) samples

The results of the analysis reveal consistency and uniformity in the quantity of different types of immune cells present in the samples, suggesting a similar immune cell composition in both CT and PB. Specifically, a predominance of neutrophils, the type of white blood cell that plays a crucial role in the body's immune response, emerged in both types of analyzed material, constituting 33% and 66% of the total, respectively (In the supplementary tables 1 and 2, the data obtained from the Cibersort analysis are reported).

7.4 EXPLORING DIFFERENTIAL GENE EXPRESSION ACROSS SUBTYPES OF ACUTE ISCHEMIC STROKE

In our research, we utilized the versatility of R software to conduct a thorough analysis of differential gene expression in response to specific experimental conditions. R provided a dynamic and robust environment for processing and interpreting high-throughput data. Through the implementation of various statistical packages and bioinformatics tools, we successfully identified genes demonstrating significant expression changes across experimental conditions. This approach enabled us to compare gene expression profiles between distinct sample groups, specifically focusing on different subtypes of stroke. We examined profiles obtained from both cerebral thrombi and peripheral venous blood, aiming to pinpoint genes with a noteworthy difference in expression between conditions. To ensure robust findings, we set stringent criteria with a fold change of 2 and a significance threshold of p-value < 0.05.

A) LARGE ARTERY ATHEROSCLEROTIC vs CARDIOEMBOLIC STROKE

In our investigation of differential gene expression between Large Artery Atherosclerotic (LAA) and Cardioembolic (CE) subtypes within cerebral thrombi, we uncovered 301 genes with significant differential expression. Interestingly, a majority of these genes exhibited overexpression in LAA subtypes. Visual representation through Volcano plots highlighted the most significant differentially expressed genes, shedding light on key molecular players in this contrast.

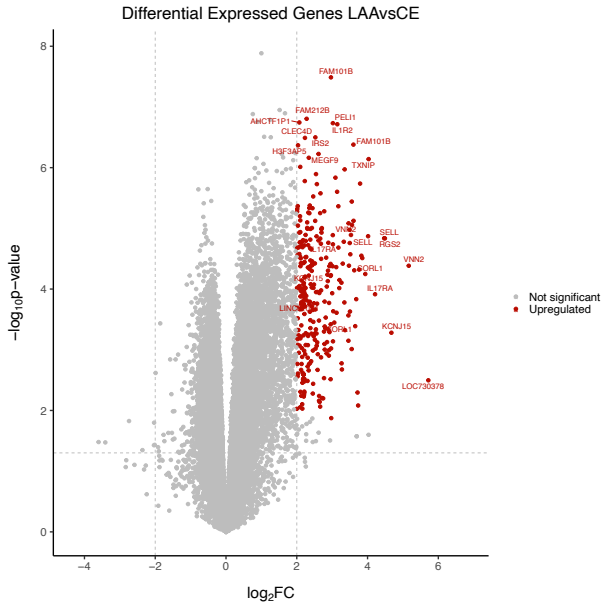

Figure 36: The volcano plots of differentially expressed genes in LAAvsCE comparison. Red dots represent up-regulated genes (fold change >2 and p-value < 0.05), Green dots represent down-regulated genes (fold change <−2 and p-value < 0.05), Grey dots represent genes with no significant difference.

In our study, we paid special attention to the overexpression of specific genes, particularly in the atherosclerotic subtype of stroke. These genes, expressed by both monocytic and non-monocytic cells, are S100A12 (logFC=3.826 p-val.adj=0,002519), S100A9 (logFC=2.8555 p-val.adj= 0,000748), and S100A8 (logFC=3.175 p-val.adj= 0,001599) and play a crucial role in inflammatory processes that are activated in response to brain damage. Additionally, they are associated with the formation and instability of atherosclerotic plaques, contributing to the underlying mechanisms of this specific subtype of stroke.

Furthermore, we observed overexpression of other genes that are involved in important processes like neutrophil degranulation and inflammation. Notable examples include MMP9 (logFC=2.3845 p-val.adj= 0,002712), IL-β (logFC=2.1035 p-val.adj= 0,004624), and VNN2 (logFC=5.1645 p-val.adj= 0,002925). These genes are significant factors that contribute to the inflammatory response and can provide valuable insights into the pathophysiology of atherosclerotic strokes.

In the realm of microRNAs (miRNAs), we highlighted the substantial overexpression of miRNA-223 (logFC=3.093 p-val.adj= 0,001225) in atherosclerotic-origin strokes. This particular miRNA has a significant role in inflammatory processes and has been linked, based on existing literature, to cardiovascular diseases.

Below is the table of genes found to be differentially expressed in the condition under consideration:

ID	gene_symbol	logFC	P.Value	adj.P.Val	diffexpressed
TC19000978.hg.1	LOC730378	5,718	0,003185	0,022555	UP
TC06003855.hg.1	VNN2	5,1645	4,13E-05	0,002925	UP
TC21000717.hg.1	KCNJ15	4,6745	0,000524	0,008968	UP
TC01001624.hg.1	RGS2	4,49	1,46E-05	0,002046	UP
TC01005928.hg.1	SELL	4,4695	1,45E-05	0,002046	UP
TC22000936.hg.1	IL17RA	4,2125	0,000122	0,004484	UP
TC01001090.hg.1	TXNIP	4,031	7,23E-07	0,000965	UP
TC01003500.hg.1	SELL	4,0155	1,35E-05	0,002013	UP
TC11002916.hg.1	SORL1	3,936	5,65E-05	0,00328	UP
TC04001809.hg.1	ACSL1	3,8515	3,09E-05	0,002638	UP
TC01003260.hg.1	S100A12	3,826	2,82E-05	0,002519	UP
TC12001178.hg.1	CLEC4E	3,7895	1,83E-06	0,001301	UP
TC01001346.hg.1	MNDA	3,762	4,78E-05	0,003104	UP
TC11002483.hg.1	IFITM2	3,7345	0,008288	0,038123	UP
TC11002392.hg.1	SNORD14D	3,717	0,005064	0,028812	UP
TC11003512.hg.1	LOC100134822	3,68	0,000147	0,004848	UP
TC18000011.hg.1	SMCHD1	3,6515	0,000409	0,007799	UP
TC16000983.hg.1	XPO6	3,624	4,91E-05	0,003104	UP
TC06001329.hg.1	FAM65B	3,605	7,51E-06	0,001706	UP
TC17002426.hg.1	FAM101B	3,601	4,17E-07	0,000807	UP
TC16001776.hg.1	GSPT1	3,56	8,75E-06	0,001763	UP
TC07000899.hg.1	MGAM	3,5545	3,62E-06	0,001595	UP
TC16000716.hg.1	LOC101929819	3,553	0,000973	0,012056	UP
TC06002121.hg.1	VNN2	3,5315	1,28E-05	0,001998	UP
TC02002767.hg.1	CXCR1	3,5135	2,68E-05	0,002435	UP
TC15000441.hg.1	AQP9	3,5035	0,000235	0,006001	UP
TC19001787.hg.1	FPR1	3,4985	1,74E-05	0,002076	UP
TC01001738.hg.1	CR1	3,492	1,06E-05	0,00188	UP
TC12000309.hg.1	LRRK2	3,4745	4,12E-05	0,002925	UP
TC01000510.hg.1	SMAP2	3,4635	8,26E-06	0,001723	UP
TC12002778.hg.1	MGP	3,46	0,000272	0,006409	UP
TC01002066.hg.1	LINC01001	3,46	0,00071	0,0103	UP
TC17000728.hg.1	MIR21	3,364	0,000475	0,008474	UP
TC01003624.hg.1	FAM129A	3,353	1,07E-06	0,001069	UP
TC01004781.hg.1	IFI16	3,3455	0,000166	0,005109	UP
TC02001292.hg.1	CXCR2	3,329	1,66E-05	0,002076	UP
TC17000727.hg.1	VMP1	3,2995	3,81E-05	0,00286	UP
TC07000399.hg.1	SNORA22	3,276	0,002111	0,018231	UP
TC0X001077.hg.1	ALAS2	3,2665	0,001674	0,016102	UP
TC05002968.hg.1	FYB	3,2625	7,85E-05	0,003739	UP
TC01002072.hg.1	LOC100288069	3,207	7,11E-05	0,003602	UP
TC07002222.hg.1	CREB5	3,2005	9,64E-05	0,004117	UP
TC17001322.hg.1	SSH2	3,177	2,08E-05	0,002194	UP
TC01003261.hg.1	S100A8	3,175	4,33E-06	0,001599	UP
TC02000619.hg.1	IL1R2	3,1455	1,93E-07	0,000562	UP
TC19000788.hg.1	FPR2	3,14	2,50E-06	0,001455	UP

TC19000976.hg.1	LINC01002	3,124	0,000246	0,006153	UP
TC07002675.hg.1	GIMAP4	3,1155	4,35E-05	0,002972	UP
TC0X000356.hg.1	MIR223	3,093	1,46E-06	0,001225	UP
TC11001107.hg.1	SORL1	3,0605	0,000357	0,007332	UP
TC22001345.hg.1	DDX17	3,03	0,000232	0,006001	UP
TC19002237.hg.1	FCAR	3,0235	0,000727	0,010409	UP
TC14000471.hg.1	FOS	3,022	1,83E-05	0,002103	UP
TC02001911.hg.1	PELI1	3,021	1,85E-07	0,000562	UP
TC04002474.hg.1	FBXL5	3,019	1,29E-05	0,002002	UP
TC09000857.hg.1	FAM157B	3,0125	4,21E-05	0,002929	UP
TC17002331.hg.1	PRKAR1A	3,001	0,000117	0,004402	UP
TC07002426.hg.1	PTPN12	2,974	0,013376	0,049812	UP
TC11002977.hg.1	LINC01001	2,9695	0,00095	0,011941	UP
TC17000965.hg.1	FAM101B	2,966	3,25E-08	0,000521	UP
TC14001124.hg.1	PYGL	2,9645	5,91E-05	0,003326	UP
TC01001640.hg.1	PTPRC	2,9595	0,00038	0,007555	UP
TC12000295.hg.1	KIAA1551	2,9565	3,85E-05	0,00286	UP
TC19002321.hg.1	MYO1F	2,9565	0,003059	0,022119	UP
TC19002275.hg.1	LINC01002	2,953	6,08E-05	0,003351	UP
TC07003026.hg.1	NCF1C	2,9255	0,000512	0,008825	UP
TC12000730.hg.1	PLXNC1	2,9235	4,20E-05	0,002929	UP
TC03003211.hg.1	TNFSF10	2,9125	0,000169	0,005161	UP
TC07002399.hg.1	NCF1B	2,9115	0,001015	0,012314	UP
TC05003443.hg.1	LINC01001	2,907	0,001251	0,013745	UP
TC22000019.hg.1	IL17RA	2,8925	1,73E-05	0,002076	UP
TC05000307.hg.1	NAIP	2,889	0,000458	0,008309	UP
TC19000470.hg.1	FFAR2	2,883	4,99E-05	0,003106	UP
TC08000383.hg.1	LYN	2,8775	7,39E-05	0,003623	UP
TC03002268.hg.1	TGFBR2	2,866	5,80E-05	0,0033	UP
TC01001254.hg.1	S100A9	2,8555	0,000748	0,010561	UP
TC12002520.hg.1	PLXNC1	2,8485	9,09E-05	0,004013	UP
TC17000349.hg.1	CPD	2,844	0,001148	0,013142	UP
TC06001152.hg.1	IGF2R	2,8315	3,04E-05	0,002624	UP
TC05001295.hg.1	FYB	2,818	0,000295	0,00669	UP
TC15000864.hg.1	IQGAP1	2,815	0,000444	0,008165	UP
TC07001516.hg.1	NCF1C	2,79	0,000994	0,012142	UP
TC12000555.hg.1	USP15	2,789	0,000413	0,007849	UP
TC06002977.hg.1	FOXO3	2,7865	0,000161	0,005045	UP
TC01000005.hg.1	LINC01001	2,784	0,000803	0,010933	UP
TC12002425.hg.1	IRAK3	2,7765	5,24E-06	0,001599	UP
TC20001234.hg.1	STK4	2,7705	0,002932	0,021707	UP
TC03002096.hg.1	BCL6	2,7695	0,000501	0,008737	UP
TC01000565.hg.1	SNORD46	2,746	0,006322	0,032538	UP
TC07001738.hg.1	NAMPT	2,7175	0,006243	0,032276	UP

TC17002657.hg.1	SLC25A39	2,7085	9,90E-06	0,001855	UP
TC06004150.hg.1	FKBP5	2,699	1,17E-05	0,001972	UP
TC04001810.hg.1	SLED1	2,697	1,03E-05	0,00188	UP
TC14001116.hg.1	SOS2	2,688	3,18E-05	0,002662	UP
TC11002344.hg.1	AMICA1	2,6875	0,000105	0,004267	UP
TC11003501.hg.1	LINC01001	2,686	0,001334	0,014287	UP
TC20000928.hg.1	B4GALT5	2,682	1,79E-05	0,002076	UP
TC02000978.hg.1	GCA	2,6705	2,65E-06	0,001489	UP
TC01000462.hg.1	38200	2,663	1,47E-05	0,002046	UP
TC05002975.hg.1	RPL37	2,6615	0,008643	0,03901	UP
TC09001028.hg.1	DCAF12	2,6605	5,61E-06	0,001599	UP
TC15000061.hg.1	SNORD116-15	2,6465	0,007247	0,035273	UP
TC20000587.hg.1	RASSF2	2,638	0,000116	0,004394	UP
TC05001589.hg.1	LUCAT1	2,631	0,005771	0,030848	UP
TC14000918.hg.1	SNORD9	2,6295	0,006909	0,034278	UP
TC10002068.hg.1	NCOA4	2,627	0,00033	0,007075	UP
TC09001537.hg.1	MEGF9	2,6155	5,94E-07	0,000958	UP
TC16000875.hg.1	GSPT1	2,615	1,58E-05	0,00206	UP
TC01005184.hg.1	LOC729737	2,595	0,001185	0,0134	UP
TC18000100.hg.1	RIOK3	2,588	0,002146	0,01838	UP
TC01001348.hg.1	IFI16	2,586	0,000112	0,00436	UP
TC13000189.hg.1	ITM2B	2,578	0,000756	0,010609	UP
TC01005067.hg.1	H3F3AP4	2,575	0,000174	0,005236	UP
TC02003767.hg.1	CASP8	2,5685	1,87E-06	0,001301	UP
TC17001341.hg.1	EVI2B	2,5645	0,000858	0,011257	UP
TC04002881.hg.1	SLED1	2,559	1,35E-05	0,002013	UP
TC11002857.hg.1	ATM	2,557	0,000539	0,009089	UP
TC12001278.hg.1	ARHGDIB	2,545	0,000112	0,00436	UP
TC02000623.hg.1	IL18RAP	2,5435	1,28E-06	0,001106	UP
TC05002988.hg.1	EMB	2,541	0,000461	0,008333	UP
TC11002165.hg.1	PICALM	2,53	0,000958	0,011987	UP
TC13000871.hg.1	IRS2	2,5255	3,17E-07	0,00069	UP
TC02004815.hg.1	CXCR2P1	2,523	0,000217	0,005815	UP
TC12000591.hg.1	IRAK3	2,52	7,53E-06	0,001706	UP
TC07002575.hg.1	LINC01000	2,517	0,000535	0,009049	UP
TC06004141.hg.1	SOD2	2,513	0,000687	0,010127	UP
TC14000429.hg.1	PCNX	2,512	3,78E-05	0,00286	UP
TC02001128.hg.1	NABP1	2,487	8,43E-05	0,003882	UP
TC01006308.hg.1	FCGR3B	2,485	0,000171	0,005186	UP
TC01000968.hg.1	CD53	2,4805	0,0006	0,00954	UP
TC12001215.hg.1	CLEC7A	2,4705	9,56E-05	0,004117	UP
TC02004161.hg.1	EIF2AK2	2,468	0,000347	0,007243	UP
TC02002637.hg.1	STK17B	2,465	2,98E-06	0,001541	UP
TC15000064.hg.1	SNORD116-18	2,4625	0,003638	0,024185	UP

TC07001546.hg.1	FGL2	2,4565	0,001031	0,012428	UP
TC15002378.hg.1	CHD2	2,453	0,005269	0,029402	UP
TC10000338.hg.1	NCOA4	2,4525	0,000221	0,005833	UP
TC19001517.hg.1	GMFG	2,4465	3,81E-05	0,00286	UP
TC19000256.hg.1	ADGRE5	2,4445	3,96E-05	0,002902	UP
TC15002174.hg.1	CCNDBP1	2,444	4,66E-06	0,001599	UP
TC01003996.hg.1	LYST	2,433	3,48E-05	0,002758	UP
TC09001287.hg.1	AGTPBP1	2,428	4,07E-05	0,002907	UP
TC01001030.hg.1	FAM46C	2,4275	9,85E-06	0,001855	UP
TC12001269.hg.1	PLBD1	2,4255	0,000194	0,005533	UP
TC15001192.hg.1	SLC12A6	2,4245	9,43E-05	0,004088	UP
TC19001241.hg.1	ADGRE3	2,4235	5,02E-05	0,003112	UP
TC20001302.hg.1	FAM210B	2,4145	0,000543	0,009101	UP
TC16000879.hg.1	CPPED1	2,41	2,21E-05	0,002258	UP
TC0X000199.hg.1	DDX3X	2,407	0,001545	0,015517	UP
TC11000027.hg.1	TALDO1	2,394	8,33E-05	0,003864	UP
TC12002416.hg.1	RASSF3	2,3855	0,00044	0,008122	UP
TC16000374.hg.1	ITGAM	2,3845	1,02E-05	0,00187	UP
TC20000363.hg.1	MMP9	2,3845	3,38E-05	0,002712	UP
TC01003638.hg.1	PTGS2	2,383	0,000326	0,007038	UP
TC11002689.hg.1	STX3	2,3825	1,53E-05	0,00205	UP
TC03003047.hg.1	GSK3B	2,3785	4,21E-05	0,002929	UP
TC10000623.hg.1	PTEN	2,3775	2,13E-05	0,002216	UP
TC01004036.hg.1	LINC01347	2,374	0,001663	0,016073	UP
TC04002095.hg.1	AFF1	2,37	0,000237	0,006035	UP
TC07001582.hg.1	STEAP4	2,368	4,20E-06	0,001599	UP
TC10001101.hg.1	PIP4K2A	2,368	0,000162	0,005058	UP
TC06001675.hg.1	STK38	2,3615	0,000163	0,005058	UP
TC11000412.hg.1	PTPRJ	2,361	4,66E-05	0,003058	UP
TC03001906.hg.1	P2RY13	2,36	0,000177	0,005272	UP
TC09000601.hg.1	TLR4	2,356	5,64E-06	0,001599	UP
TC17001311.hg.1	FLOT2	2,3535	4,62E-06	0,001599	UP
TC01006361.hg.1	GBP2	2,3475	0,001718	0,016294	UP
TC04000826.hg.1	KLHL2	2,3405	6,88E-07	0,000965	UP
TC10000293.hg.1	ALOX5	2,339	5,99E-05	0,003334	UP
TC01002512.hg.1	CSF3R	2,3365	0,002191	0,018525	UP
TC04002523.hg.1	RBM47	2,327	5,49E-06	0,001599	UP
TC02003831.hg.1	CXCR2	2,3225	1,90E-05	0,002142	UP
TC08000188.hg.1	SLC25A37	2,319	0,000592	0,009503	UP
TC20001561.hg.1	LINC00657	2,315	4,41E-05	0,002976	UP
TC07000777.hg.1	LINC01000	2,3145	0,000839	0,011168	UP
TC04000605.hg.1	LOC729218	2,314	0,000562	0,009265	UP
TC10001962.hg.1	WAC	2,3095	0,001352	0,014402	UP
TC16001773.hg.1	LITAF	2,308	0,001886	0,017118	UP

TC08002590.hg.1	DOCK5	2,304	0,003264	0,022893	UP
TC20000810.hg.1	LINC00657	2,303	1,02E-05	0,00187	UP
TC22000271.hg.1	CSF2RB	2,2945	7,97E-06	0,001723	UP
TC06000523.hg.1	MAPK14	2,2935	9,84E-06	0,001855	UP
TC01005706.hg.1	FAM212B	2,279	1,57E-07	0,000562	UP
TC06003619.hg.1	SRPK1	2,276	0,000153	0,004943	UP
TC01001685.hg.1	BTG2	2,268	2,96E-05	0,002585	UP
TC01000394.hg.1	EPB41	2,2675	0,00013	0,0046	UP
TC16000151.hg.1	C16orf72	2,2555	1,61E-05	0,002073	UP
TC0X000171.hg.1	CYBB	2,254	0,000534	0,009039	UP
TC03002349.hg.1	PRKCD	2,2535	0,000835	0,011159	UP
TC17001579.hg.1	SLC25A39	2,2495	1,28E-05	0,001998	UP
TC0X002337.hg.1	ACSL4	2,248	9,61E-05	0,004117	UP
TC11002353.hg.1	DDX6	2,2455	3,00E-05	0,002601	UP
TC19002618.hg.1	OAZ1	2,238	0,001187	0,013406	UP
TC02002624.hg.1	STAT1	2,2365	6,24E-05	0,003379	UP
TC01001741.hg.1	CD46	2,2345	0,000193	0,005528	UP
TC12000130.hg.1	CLEC4D	2,2315	3,23E-07	0,00069	UP
TC04000775.hg.1	TLR2	2,2275	1,66E-06	0,001293	UP
TC12000405.hg.1	DAZAP2	2,2275	0,00012	0,00447	UP
TC09000343.hg.1	OSTF1	2,221	3,59E-05	0,002803	UP
TC06000581.hg.1	UBR2	2,221	6,43E-05	0,003415	UP
TC18000397.hg.1	ROCK1	2,2195	9,34E-05	0,004059	UP
TC06002715.hg.1	LST1	2,2175	0,000135	0,004651	UP
TC12001227.hg.1	YBX3	2,217	1,91E-05	0,002145	UP
TC04001501.hg.1	LINC01061	2,2165	0,000257	0,00626	UP
TC14002211.hg.1	IGHA1	2,2165	0,003026	0,022026	UP
TC04001946.hg.1	RBPJ	2,2135	0,004892	0,028298	UP
TC20001560.hg.1	RBM39	2,2135	0,005088	0,028855	UP
TC11000333.hg.1	CD44	2,213	0,00333	0,023083	UP
TC02000967.hg.1	MARCH7	2,21	0,00012	0,004468	UP
TC01000990.hg.1	CAPZA1	2,2095	0,001039	0,012467	UP
TC15000067.hg.1	SNORD116-24	2,206	0,005508	0,030079	UP
TC14001030.hg.1	BAZ1A	2,2055	0,000109	0,00432	UP
TC0X000575.hg.1	IL13RA1	2,204	0,000195	0,005533	UP
TC11001818.hg.1	MPEG1	2,2005	0,000101	0,004182	UP
TC17000611.hg.1	KPNB1	2,2005	0,000176	0,005261	UP
TC12000947.hg.1	RNF10	2,2	7,95E-05	0,003774	UP
TC17002638.hg.1	STAT3	2,198	0,005903	0,031223	UP
TC03002524.hg.1	ABTB1	2,197	0,000152	0,004918	UP
TC09001547.hg.1	STOM	2,193	3,71E-05	0,00286	UP
TC06001529.hg.1	SNORD117	2,193	0,002551	0,020076	UP
TC6_apd_hap1000080.hg.1	SNORD117	2,193	0,002551	0,020076	UP
TC6_cox_hap2000158.hg.1	SNORD117	2,193	0,002551	0,020076	UP

TC6_dbb_hap3000147.hg.1	SNORD117	2,193	0,002551	0,020076	UP
TC6_mann_hap4000135.hg.1	SNORD117	2,193	0,002551	0,020076	UP
TC6_mcf_hap5000135.hg.1	SNORD117	2,193	0,002551	0,020076	UP
TC6_qbl_hap6000150.hg.1	SNORD117	2,193	0,002551	0,020076	UP
TC6_ssto_hap7000130.hg.1	SNORD117	2,193	0,002551	0,020076	UP
TC01005718.hg.1	PTPN22	2,1895	0,000579	0,009378	UP
TC21000167.hg.1	KCNJ15	2,189	8,45E-05	0,003882	UP
TC19000180.hg.1	SLC44A2	2,181	1,57E-05	0,00206	UP
TC01001382.hg.1	FCER1G	2,181	0,002982	0,021895	UP
TC12001843.hg.1	LTA4H	2,1775	0,003125	0,022346	UP
TC0X002267.hg.1	IDS	2,1685	0,000177	0,005266	UP
TC19002463.hg.1	TYROBP	2,167	0,002398	0,01952	UP
TC21001069.hg.1	SAMSN1	2,165	1,60E-05	0,00207	UP
TC20000206.hg.1	HCK	2,1625	2,05E-05	0,002194	UP
TC01005883.hg.1	TAGLN2	2,1605	0,003501	0,023725	UP
TC12003091.hg.1	RPL6	2,158	0,009331	0,040779	UP
TC09002572.hg.1	CBWD5	2,154	0,007891	0,037017	UP
TC04001355.hg.1	WDFY3	2,1525	3,78E-05	0,00286	UP
TC02002647.hg.1	SF3B1	2,152	0,001312	0,014144	UP
TC17001761.hg.1	USP32	2,148	0,000112	0,00436	UP
TC12001507.hg.1	BIN2	2,146	0,000944	0,011887	UP
TC01001414.hg.1	ATF6	2,141	1,92E-05	0,002152	UP
TC22000791.hg.1	DDX17	2,138	0,000215	0,005786	UP
TC21000938.hg.1	ATP5O	2,136	0,001713	0,016262	UP
TC15000930.hg.1	MCTP2	2,1355	7,22E-05	0,003605	UP
TC02004995.hg.1	IL18R1	2,133	1,71E-05	0,002076	UP
TC0X000052.hg.1	TLR8	2,1325	0,000131	0,004618	UP
TC19000360.hg.1	UBA52	2,129	0,000397	0,007703	UP
TC0X000112.hg.1	SAT1	2,128	0,005737	0,030746	UP
TC06003604.hg.1	TAP2	2,126	0,000166	0,005109	UP
TC07000687.hg.1	PIK3CG	2,125	0,000102	0,004182	UP
TC01006192.hg.1	EGLN1	2,122	0,002147	0,01838	UP
TC06003854.hg.1	VNN3	2,1215	0,000177	0,005266	UP
TC22000270.hg.1	NCF4	2,1165	3,75E-05	0,00286	UP
TC12000010.hg.1	WNK1	2,116	0,000207	0,005688	UP
TC17000489.hg.1	MSL1	2,114	0,000107	0,004285	UP
TC19001242.hg.1	ADGRE2	2,111	3,12E-05	0,002651	UP
TC14000605.hg.1	PAPOLA	2,1105	0,00061	0,009595	UP
TC17001882.hg.1	H3F3B	2,1045	0,004926	0,028398	UP
TC02000904.hg.1	ARHGAP15	2,104	4,20E-05	0,002929	UP
TC02002219.hg.1	IL1B	2,1035	0,000132	0,004624	UP
TC06000720.hg.1	OGFRL1	2,102	0,00065	0,009884	UP
TC0X001370.hg.1	MBNL3	2,0995	7,39E-06	0,001704	UP
TC11000316.hg.1	HIPK3	2,0995	1,15E-05	0,001964	UP

TC14000135.hg.1	LRP10	2,0985	9,71E-07	0,001069	UP
TC0X000141.hg.1	GK	2,097	0,008854	0,039526	UP
TC05000243.hg.1	MAP3K1	2,096	1,69E-05	0,002076	UP
TC14001472.hg.1	DICER1	2,0955	2,94E-05	0,002585	UP
TC02003690.hg.1	HAT1	2,0915	6,31E-06	0,001636	UP
TC19000321.hg.1	KLF2	2,09	9,54E-05	0,004117	UP
TC16000823.hg.1	CREBBP	2,088	0,000215	0,005794	UP
TC02002853.hg.1	SP110	2,085	1,71E-05	0,002076	UP
TC01001172.hg.1	FCGR1A	2,08	0,000856	0,011257	UP
TC02000432.hg.1	DYSF	2,076	8,91E-05	0,003982	UP
TC02002477.hg.1	AHCTF1P1	2,073	1,80E-07	0,000562	UP
TC06001217.hg.1	SERPINB1	2,073	1,18E-05	0,001972	UP
TC03000846.hg.1	MME	2,0725	2,65E-05	0,002422	UP
TC03002006.hg.1	TNFSF10	2,064	2,05E-05	0,002194	UP
TC01003057.hg.1	FCGR1B	2,0605	0,001121	0,012984	UP
TC09001293.hg.1	ZCCHC6	2,0545	0,000579	0,009378	UP
TC06002689.hg.1	HLA-G	2,046	0,000474	0,008457	UP
TC0X001707.hg.1	H3F3AP5	2,036	4,28E-07	0,000807	UP
TC10001160.hg.1	KIF5B	2,035	0,002472	0,019797	UP
TC12000822.hg.1	TCP11L2	2,0335	9,02E-06	0,001783	UP
TC12000817.hg.1	KIAA1033	2,03	0,000832	0,011151	UP
TC10001373.hg.1	C10orf54	2,0285	4,30E-06	0,001599	UP
TC10000360.hg.1	UBE2D1	2,028	2,74E-05	0,002462	UP
TC07000459.hg.1	NCF1	2,028	0,000303	0,006815	UP
TC19000187.hg.1	C19orf38	2,027	9,67E-05	0,004117	UP
TC10002411.hg.1	KLF6	2,027	0,000666	0,010003	UP
TC0X000353.hg.1	MSN	2,0245	0,002741	0,020857	UP
TC16000260.hg.1	PRKCB	2,0215	2,09E-05	0,002194	UP
TC03001550.hg.1	PROK2	2,018	0,001712	0,016262	UP
TC05000981.hg.1	HRH2	2,0145	4,77E-06	0,001599	UP
TC12003283.hg.1	TMBIM4	2,011	5,27E-06	0,001599	UP
TC17002755.hg.1	HELZ	2,01	0,000473	0,008447	UP
TC11002246.hg.1	CASP4	2,0075	9,58E-05	0,004117	UP
TC12001754.hg.1	OSBPL8	2,0065	0,000204	0,005679	UP
TC10000415.hg.1	SRGN	2,0015	0,0094	0,04099	UP

Table 4: DEG in the comparison LAA vs CE

B) LARGE ARTERY ATHEROSCLEROTIC vs CRYPTOGENIC

Extending our analysis to compare LAA and Cryptogenic (CRYPTO) subtypes within clot samples, we identified 209 differentially expressed genes. Similar to the LAA vs CE comparison, Volcano plots were generated to emphasize the top ten genes with the most significant differential expression in the LAA vs CRYPTO contrast.

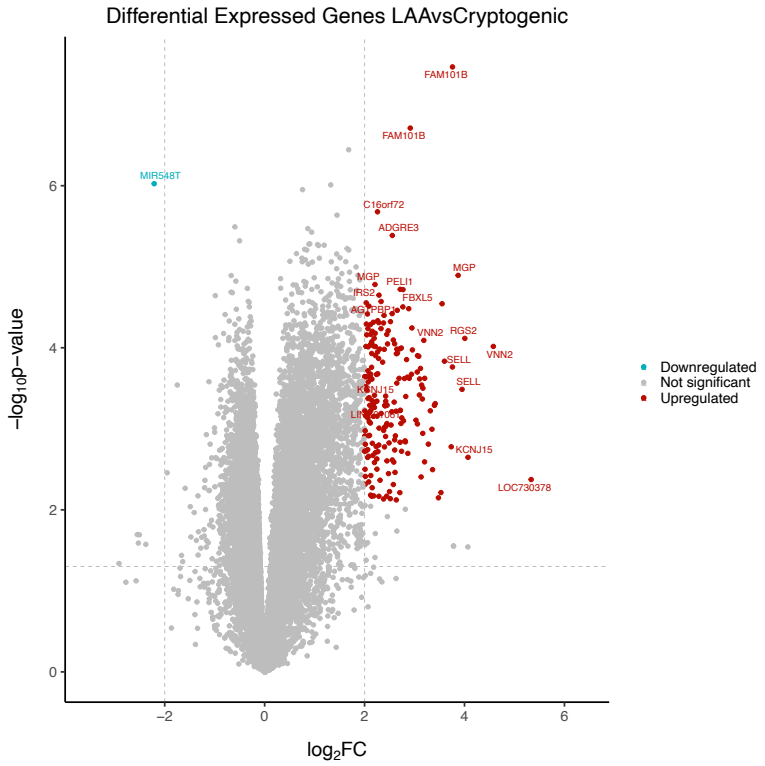

Figure 37: The volcano plots of differentially expressed genes in LAAvsCR comparison. Red dots represent up-regulated genes (fold change >2 and p-value < 0.05), Green dots represent down-regulated genes (fold change <−2 and p-value < 0.05), Grey dots represent genes with no significant difference.

Below is the table of genes found to be differentially expressed in the condition under consideration:

ID	gene_symbol	logFC	P.Value	adj.P.Val	diffexpressed
TC19000978.hg.1	LOC730378	5,334	0,004226	0,035585	UP
TC06003855.hg.1	VNN2	4,577	9,63E-05	0,009427	UP
TC21000717.hg.1	KCNJ15	4,07	0,002248	0,02663	UP
TC01001624.hg.1	RGS2	4,007	7,66E-05	0,009246	UP
TC01005928.hg.1	SELL	3,951	0,000326	0,01293	UP
TC12002778.hg.1	MGP	3,8725	1,28E-05	0,008905	UP
TC17002426.hg.1	FAM101B	3,76	3,42E-08	0,001096	UP
TC01003500.hg.1	SELL	3,7585	0,000173	0,010612	UP
TC22000936.hg.1	IL17RA	3,7345	0,001666	0,023334	UP
TC11002916.hg.1	SORL1	3,599	0,000146	0,010175	UP
TC16001776.hg.1	GSPT1	3,5515	2,86E-05	0,008905	UP
TC16001729.hg.1	HBA2	3,5285	0,006122	0,042221	UP
TC11002483.hg.1	IFITM2	3,4785	0,007105	0,045272	UP
TC18000011.hg.1	SMCHD1	3,4135	0,000489	0,01487	UP
TC01001346.hg.1	MNDA	3,399	0,000514	0,015035	UP
TC0X001077.hg.1	ALAS2	3,361	0,00319	0,031073	UP
TC12001178.hg.1	CLEC4E	3,3495	0,001012	0,019298	UP
TC01004781.hg.1	IFI16	3,3165	0,0006	0,015813	UP
TC11003512.hg.1	LOC100134822	3,277	0,001546	0,022625	UP
TC01001738.hg.1	CR1	3,203	0,000238	0,011374	UP
TC01002066.hg.1	LINC01001	3,201	0,002559	0,028061	UP
TC06002121.hg.1	VNN2	3,186	8,11E-05	0,009246	UP
TC12000309.hg.1	LRRK2	3,168	0,000315	0,012683	UP
TC01003260.hg.1	S100A12	3,165	0,001138	0,020221	UP
TC04001809.hg.1	ACSL1	3,156	0,000428	0,014078	UP
TC07000899.hg.1	MGAM	3,1425	0,000288	0,012175	UP
TC16000716.hg.1	LOC101929819	3,132	0,003925	0,034293	UP
TC05002968.hg.1	FYB	3,119	0,00018	0,010666	UP
TC07002675.hg.1	GIMAP4	3,102	0,000242	0,011431	UP
TC16000983.hg.1	XPO6	3,0975	0,000383	0,013567	UP
TC19001787.hg.1	FPR1	3,085	0,000127	0,009921	UP
TC02002767.hg.1	CXCR1	3,06	0,000125	0,009921	UP
TC01001090.hg.1	TXNIP	3,058	0,000871	0,018218	UP
TC07002222.hg.1	CREB5	3,0545	0,000199	0,011002	UP
TC06001329.hg.1	FAM65B	3,029	0,000782	0,01744	UP
TC17000727.hg.1	VMP1	2,9575	0,000106	0,009435	UP
TC01003624.hg.1	FAM129A	2,948	5,69E-05	0,009207	UP
TC07002399.hg.1	NCF1B	2,939	0,000212	0,011196	UP
TC17000965.hg.1	FAM101B	2,915	1,94E-07	0,003115	UP
TC07003026.hg.1	NCF1C	2,895	0,000238	0,011374	UP
TC12000295.hg.1	KIAA1551	2,884	3,30E-05	0,008905	UP
TC19002321.hg.1	MYO1F	2,8665	0,002011	0,025442	UP
TC02001292.hg.1	CXCR2	2,858	0,00023	0,011329	UP

TC17001322.hg.1	SSH2	2,841	0,00014	0,010175	UP
TC07001516.hg.1	NCF1C	2,8245	0,000399	0,013719	UP
TC15000441.hg.1	AQP9	2,8175	0,001449	0,022119	UP
TC01002072.hg.1	LOC100288069	2,8115	0,001409	0,021894	UP
TC19002237.hg.1	FCAR	2,798	0,00024	0,011413	UP
TC11001107.hg.1	SORL1	2,7795	0,000797	0,017572	UP
TC04002474.hg.1	FBXL5	2,769	1,91E-05	0,008905	UP
TC19000788.hg.1	FPR2	2,767	3,13E-05	0,008905	UP
TC09000857.hg.1	FAM157B	2,745	0,000732	0,017024	UP
TC01000510.hg.1	SMAP2	2,741	0,001894	0,024751	UP
TC01003261.hg.1	S100A8	2,736	0,000101	0,009427	UP
TC20001234.hg.1	STK4	2,7285	0,00086	0,018106	UP
TC17000349.hg.1	CPD	2,7175	0,000591	0,015728	UP
TC02001911.hg.1	PELI1	2,714	1,90E-05	0,008905	UP
TC03003211.hg.1	TNFSF10	2,712	0,001466	0,022205	UP
TC12002520.hg.1	PLXNC1	2,7115	0,000594	0,015765	UP
TC03002268.hg.1	TGFBR2	2,707	0,000103	0,009427	UP
TC11002977.hg.1	LINC01001	2,7065	0,006129	0,042231	UP
TC14001124.hg.1	PYGL	2,691	0,000238	0,011374	UP
TC10002068.hg.1	NCOA4	2,659	0,000116	0,009706	UP
TC06001152.hg.1	IGF2R	2,654	3,45E-05	0,008905	UP
TC17002657.hg.1	SLC25A39	2,6475	0,000104	0,009427	UP
TC12000555.hg.1	USP15	2,6455	0,000273	0,011995	UP
TC0X000356.hg.1	MIR223	2,6375	0,000118	0,009758	UP
TC05003443.hg.1	LINC01001	2,635	0,007543	0,046511	UP
TC05001295.hg.1	FYB	2,6285	0,000606	0,015903	UP
TC01001640.hg.1	PTPRC	2,617	0,001221	0,020794	UP
TC19000976.hg.1	LINC01002	2,61	0,003447	0,0323	UP
TC05001589.hg.1	LUCAT1	2,6035	0,001827	0,024339	UP
TC14000471.hg.1	FOS	2,6025	0,001369	0,021702	UP
TC08000383.hg.1	LYN	2,602	8,93E-05	0,009427	UP
TC12000730.hg.1	PLXNC1	2,593	0,000468	0,014523	UP
TC19002275.hg.1	LINC01002	2,585	0,002575	0,02811	UP
TC16000875.hg.1	GSPT1	2,576	8,02E-05	0,009246	UP
TC17002331.hg.1	PRKAR1A	2,576	0,004868	0,038011	UP
TC19001241.hg.1	ADGRE3	2,5555	4,11E-06	0,008502	UP
TC05002988.hg.1	EMB	2,5555	0,002425	0,027391	UP
TC09001028.hg.1	DCAF12	2,5515	3,79E-05	0,008905	UP
TC02000619.hg.1	IL1R2	2,545	0,000615	0,016012	UP
TC22001345.hg.1	DDX17	2,5305	0,000898	0,018411	UP
TC14001116.hg.1	SOS2	2,5185	4,76E-05	0,009207	UP
TC05000412.hg.1	VCAN	2,5145	0,007287	0,045828	UP
TC01000005.hg.1	LINC01001	2,4995	0,005952	0,041763	UP
TC15000864.hg.1	IQGAP1	2,491	0,001494	0,022381	UP

TC07001738.hg.1	NAMPT	2,4785	0,003572	0,032845	UP
TC12001215.hg.1	CLEC7A	2,4735	6,17E-05	0,009246	UP
TC01000462.hg.1	38200	2,46	8,96E-05	0,009427	UP
TC17001341.hg.1	EVI2B	2,451	0,000511	0,015028	UP
TC19000470.hg.1	FFAR2	2,448	0,002489	0,02771	UP
TC11002344.hg.1	AMICA1	2,447	0,000861	0,01811	UP
TC20000587.hg.1	RASSF2	2,445	6,84E-05	0,009246	UP
TC11003501.hg.1	LINC01001	2,4425	0,006776	0,044311	UP
TC18000100.hg.1	RIOK3	2,43	0,000923	0,018614	UP
TC11002165.hg.1	PICALM	2,424	0,000457	0,014416	UP
TC12002416.hg.1	RASSF3	2,4225	0,000394	0,013664	UP
TC20001302.hg.1	FAM210B	2,421	0,001243	0,020911	UP
TC22000019.hg.1	IL17RA	2,412	0,000522	0,015062	UP
TC01001348.hg.1	IFI16	2,404	0,000953	0,018816	UP
TC07001546.hg.1	FGL2	2,4035	0,000514	0,015035	UP
TC07002575.hg.1	LINC01000	2,3995	0,001673	0,023359	UP
TC01001030.hg.1	FAM46C	2,394	0,000105	0,009427	UP
TC01003996.hg.1	LYST	2,39	3,98E-05	0,008905	UP
TC20000928.hg.1	B4GALT5	2,382	0,001047	0,019602	UP
TC17000728.hg.1	MIR21	2,38	0,007342	0,045993	UP
TC11002689.hg.1	STX3	2,379	4,94E-05	0,009207	UP
TC09001537.hg.1	MEGF9	2,362	0,000151	0,010198	UP
TC06002977.hg.1	FOXO3	2,3315	0,000646	0,016175	UP
TC09001287.hg.1	AGTPBP1	2,331	2,68E-05	0,008905	UP
TC01000394.hg.1	EPB41	2,3295	5,80E-05	0,009207	UP
TC03002096.hg.1	BCL6	2,3105	0,004309	0,035898	UP
TC02000978.hg.1	GCA	2,3025	0,000104	0,009427	UP
TC08002590.hg.1	DOCK5	2,2905	0,000981	0,018975	UP
TC13000871.hg.1	IRS2	2,289	2,24E-05	0,008905	UP
TC01004629.hg.1	CAPZA1	2,287	0,006803	0,044378	UP
TC14000429.hg.1	PCNX	2,2855	4,90E-05	0,009207	UP
TC01002512.hg.1	CSF3R	2,285	0,001586	0,022904	UP
TC15001192.hg.1	SLC12A6	2,2805	0,000135	0,010149	UP
TC07000777.hg.1	LINC01000	2,268	0,001909	0,024858	UP
TC01005067.hg.1	H3F3AP4	2,2645	0,000209	0,011153	UP
TC02002637.hg.1	STK17B	2,2635	4,63E-05	0,009207	UP
TC06003619.hg.1	SRPK1	2,2605	0,000113	0,00956	UP
TC16000151.hg.1	C16orf72	2,259	2,10E-06	0,008502	UP
TC12001269.hg.1	PLBD1	2,25	0,000699	0,016801	UP
TC15000270.hg.1	THBS1	2,248	0,003148	0,030971	UP
TC10001101.hg.1	PIP4K2A	2,2465	0,000456	0,014416	UP
TC15002378.hg.1	CHD2	2,2465	0,002353	0,026969	UP
TC04001810.hg.1	SLED1	2,2395	0,000213	0,011196	UP
TC17002638.hg.1	STAT3	2,2335	0,001661	0,023313	UP

TC03003047.hg.1	GSK3B	2,2175	0,000125	0,009921	UP
TC17001579.hg.1	SLC25A39	2,216	9,65E-05	0,009427	UP
TC13000189.hg.1	ITM2B	2,215	0,001976	0,025226	UP
TC02003767.hg.1	CASP8	2,212	6,62E-05	0,009246	UP
TC12001276.hg.1	MGP	2,209	1,66E-05	0,008905	UP
TC01005718.hg.1	PTPN22	2,201	0,000472	0,014612	UP
TC12001843.hg.1	LTA4H	2,199	0,000385	0,013567	UP
TC10001962.hg.1	WAC	2,198	0,000545	0,01532	UP
TC02004161.hg.1	EIF2AK2	2,1975	0,002608	0,028289	UP
TC12001227.hg.1	YBX3	2,1925	7,62E-05	0,009246	UP
TC06004150.hg.1	FKBP5	2,1825	0,006727	0,044218	UP
TC06002715.hg.1	LST1	2,181	9,51E-05	0,009427	UP
TC01006308.hg.1	FCGR3B	2,176	0,000702	0,016838	UP
TC11001818.hg.1	MPEG1	2,1755	4,84E-05	0,009207	UP
TC06003604.hg.1	TAP2	2,1755	6,51E-05	0,009246	UP
TC04000605.hg.1	LOC729218	2,1655	0,002134	0,025992	UP
TC06001675.hg.1	STK38	2,16	0,000509	0,015017	UP
TC01000968.hg.1	CD53	2,156	0,001508	0,022459	UP
TC09000601.hg.1	TLR4	2,1545	6,26E-05	0,009246	UP
TC01004036.hg.1	LINC01347	2,1525	0,005337	0,039714	UP
TC16001773.hg.1	LITAF	2,152	0,000525	0,015091	UP
TC11000027.hg.1	TALDO1	2,147	0,000244	0,011431	UP
TC02000623.hg.1	IL18RAP	2,146	0,000446	0,014323	UP
TC02000967.hg.1	MARCH7	2,144	8,43E-05	0,009409	UP
TC12000405.hg.1	DAZAP2	2,143	0,000118	0,009758	UP
TC11002857.hg.1	ATM	2,1425	0,006789	0,044342	UP
TC10000623.hg.1	PTEN	2,1405	9,17E-05	0,009427	UP
TC04002881.hg.1	SLED1	2,1405	0,000174	0,010612	UP
TC12000010.hg.1	WNK1	2,1325	0,000243	0,011431	UP
TC07001582.hg.1	STEAP4	2,1285	8,96E-05	0,009427	UP
TC08000188.hg.1	SLC25A37	2,1265	0,000592	0,015742	UP
TC06004141.hg.1	SOD2	2,125	0,003776	0,03377	UP
TC11000412.hg.1	PTPRJ	2,123	0,000212	0,011196	UP
TC10000293.hg.1	ALOX5	2,122	6,82E-05	0,009246	UP
TC01006361.hg.1	GBP2	2,121	0,006575	0,043668	UP
TC04002523.hg.1	RBM47	2,118	5,16E-05	0,009207	UP
TC10000338.hg.1	NCOA4	2,1165	0,000849	0,018002	UP
TC06000720.hg.1	OGFRL1	2,113	0,000233	0,011329	UP
TC02001128.hg.1	NABP1	2,104	0,000513	0,015035	UP
TC16000879.hg.1	CPPED1	2,0995	0,001205	0,020707	UP
TC03002349.hg.1	PRKCD	2,096	0,000628	0,016136	UP
TC04001501.hg.1	LINC01061	2,0955	0,000819	0,017776	UP
TC21000167.hg.1	KCNJ15	2,091	0,000413	0,013913	UP
TC15002174.hg.1	CCNDBP1	2,087	3,06E-05	0,008905	UP

TC12002425.hg.1	IRAK3	2,0835	0,004519	0,036657	UP
TC0X000199.hg.1	DDX3X	2,0805	0,002183	0,02628	UP
TC06003854.hg.1	VNN3	2,08	0,000651	0,016279	UP
TC01000990.hg.1	CAPZA1	2,0785	0,00122	0,02079	UP
TC12000947.hg.1	RNF10	2,073	0,000264	0,011916	UP
TC06000581.hg.1	UBR2	2,0715	9,74E-05	0,009427	UP
TC02002624.hg.1	STAT1	2,07	0,000423	0,013998	UP
TC11002353.hg.1	DDX6	2,069	0,000192	0,01083	UP
TC17001761.hg.1	USP32	2,0685	5,80E-05	0,009207	UP
TC01001741.hg.1	CD46	2,067	0,000222	0,01131	UP
TC12000591.hg.1	IRAK3	2,064	0,000736	0,017076	UP
TC03001906.hg.1	P2RY13	2,063	0,001805	0,024234	UP
TC12001278.hg.1	ARHGDIB	2,0605	0,002257	0,026667	UP
TC19001517.hg.1	GMFG	2,058	3,83E-05	0,008905	UP
TC17001311.hg.1	FLOT2	2,0485	0,000331	0,012981	UP
TC04001355.hg.1	WDFY3	2,0425	6,94E-05	0,009246	UP
TC14000605.hg.1	PAPOLA	2,04	0,000662	0,016379	UP
TC04000826.hg.1	KLHL2	2,036	5,09E-05	0,009207	UP
TC12000130.hg.1	CLEC4D	2,034	2,79E-05	0,008905	UP
TC04002095.hg.1	AFF1	2,0295	0,001872	0,024576	UP
TC09000343.hg.1	OSTF1	2,028	9,61E-05	0,009427	UP
TC22000270.hg.1	NCF4	2,027	0,000302	0,012473	UP
TC01005706.hg.1	FAM212B	2,025	0,000229	0,011329	UP
TC16000374.hg.1	ITGAM	2,0205	0,000689	0,016702	UP
TC19002463.hg.1	TYROBP	2,016	0,003866	0,034059	UP
TC01001254.hg.1	S100A9	2,0155	0,00155	0,022639	UP
TC10002673.hg.1	JMJD1C	2,0125	0,001059	0,019666	UP
TC20001560.hg.1	RBM39	2,012	0,004838	0,037897	UP
TC05003330.hg.1	SLU7	2,0095	0,003156	0,030987	UP
TC22000271.hg.1	CSF2RB	2,008	0,000602	0,01582	UP
TC19000360.hg.1	UBA52	2,005	0,001227	0,020799	UP
TC16000823.hg.1	CREBBP	2,0025	0,000227	0,01131	UP
TC19000256.hg.1	ADGRE5	2,001	0,001892	0,024751	UP
TC07000965.hg.1	MIR548T	-2,211	9,45E-07	0,005977	DOWN

Table5 : DEG in the comparison LAA vs Cryptogenic

C) OTHER COMPARISONS

Despite thorough exploration, no significant differences in gene expression were detected in comparisons beyond other subtypes. This underscores a unique molecular landscape within the identified subtypes, emphasizing the necessity for a nuanced understanding of the underlying biology.

Contrastingly, gene expression analysis across multiple comparison levels within PB samples did not reveal any significant differences. This null finding highlights the homogeneity in gene expression patterns within MIC and prompts intriguing questions about the biological implications of such uniformity.

7.5 UNVEILING BIOLOGICAL SIGNIFICANCE: ENRICHMENT ANALYSIS OF DIFFERENTIALLY EXPRESSED GENES

In addition to the identification of differentially expressed genes within distinct subtypes of AIS, our investigation extended to elucidating their functional implications through sophisticated enrichment analyses. This entailed a meticulous examination of the enrichment of genes within the Gene Ontology (GO) and Reactome databases, thereby shedding light on the underlying biological processes, pathways, and potential disease correlations within the examined conditions.

- Gene Ontology (GO) Enrichment Analysis: Gene Ontology serves as a structured repository categorizing genes based on their involvement in Biological Processes (BP), Molecular Functions (MF), and Cellular Components (CC). The enrichment analysis methodically assesses the differential gene expression data within each subtype of AIS, evaluating whether specific GO terms exhibit statistical overrepresentation or underrepresentation compared to random expectations. This analytical approach unveils nuanced insights into the functional themes characterizing the identified genes, offering a comprehensive understanding of their regulatory roles.
- Reactome Pathway Enrichment Analysis: Reactome, a specialized biological pathway database, offers a detailed depiction of molecular reactions and interactions within cellular processes. The enrichment analysis within Reactome scrutinizes the differential expression patterns of genes across AIS subtypes, determining their statistically significant associations with specific biological pathways. This analytical undertaking unveils the intricate interconnectedness of molecular processes influenced by the observed gene expression changes, unraveling the mechanistic underpinnings of the identified genetic perturbations.

The outcomes of the enrichment analyses in both GO and Reactome databases provide a granular view of the pathways influenced by the differentially expressed genes. These pathways encompass diverse cellular functions, including signaling pathways, metabolic cascades, and other molecular networks that intricately contribute to cellular homeostasis and response.

By comprehending the functional implications of the identified differentially expressed genes, we can delve into potential associations with diseases or pathological conditions. Certain pathways or biological processes may exhibit links to specific diseases, thereby facilitating the establishment

of meaningful connections between the observed gene expression changes and their potential relevance to pathological states.

A) LARGE ARTERY ATHEROSCLEROTIC vs CARDIOEMBOLIC STROKE

In the context of LAA clot samples compared to CE, a meticulous analysis revealed a total of 220 biological processes that exhibited a statistically significant enrichment. Within this enriched repertoire, prominent emphasis was placed on processes intricately associated with the inflammatory response and neuronal apoptotic cascades. Notably, sub-processes such as neutrophil degranulation, a complex cellular event involving the release of intracellular contents by neutrophils, and cytokine production, the synthesis and release of signaling molecules integral to immune responses, featured prominently among the most enriched processes. Below is the table with the thirty most enriched biological processes in the condition examined (Supplementary Tables 3 and 4 of all the biological processes and pathways enriched are reported in the supplementary materials). These observations not only signify a robust molecular landscape within the LAA clot samples but also underscore the pivotal role of inflammatory and apoptotic processes, including specific events such as neutrophil degranulation and cytokine production, in elucidating the nuanced gene expression differences observed within distinct clot subtypes. This detailed insight into the enriched biological processes enhances our understanding of the underlying molecular mechanisms contributing to the observed variations in gene expression patterns between LAA and CE clot subtypes.

ID	Description	GeneRatio	BgRatio	p.adjust
GO:0001819	positive regulation of cytokine production	34/226	460/16686	2,254E-12
GO:0002764	immune response-regulating signaling pathway	32/226	441/16686	1,481E-11
GO:0031349	positive regulation of defense response	26/226	285/16686	1,912E-11
GO:1902532	negative regulation of intracellular signal transduction	33/226	492/16686	2,578E-11
GO:0032103	positive regulation of response to external stimulus	30/226	438/16686	1,997E-10
GO:0042554	superoxide anion generation	11/226	42/16686	3,54E-09
GO:0046651	lymphocyte proliferation	23/226	288/16686	4,109E-09
GO:0032943	mononuclear cell proliferation	23/226	295/16686	5,373E-09
GO:0045088	regulation of innate immune response	20/226	221/16686	6,986E-09
GO:0050670	regulation of lymphocyte proliferation	20/226	225/16686	8,946E-09
GO:0070663	regulation of leukocyte proliferation	21/226	255/16686	1,068E-08
GO:0032944	regulation of mononuclear cell proliferation	20/226	229/16686	1,068E-08
GO:0002831	regulation of response to biotic stimulus	23/226	334/16686	3,844E-08
GO:0019221	cytokine-mediated signaling pathway	27/226	469/16686	4,977E-08
GO:1901652	response to peptide	27/226	486/16686	9,001E-08
GO:0002683	negative regulation of immune system process	25/226	418/16686	9,001E-08
GO:0045730	respiratory burst	9/226	35/16686	1,076E-07
GO:0007159	leukocyte cell-cell adhesion	24/226	393/16686	1,184E-07
GO:0043065	positive regulation of apoptotic process	27/226	498/16686	1,294E-07
GO:0030595	leukocyte chemotaxis	18/226	217/16686	1,339E-07
GO:0050900	leukocyte migration	23/226	369/16686	1,643E-07
GO:0030099	myeloid cell differentiation	23/226	376/16686	2,132E-07
GO:0002274	myeloid leukocyte activation	18/226	228/16686	2,425E-07
GO:1903706	regulation of hemopoiesis	23/226	385/16686	2,972E-07
GO:0071900	regulation of protein serine/threonine kinase activity	22/226	353/16686	2,997E-07
GO:0051250	negative regulation of lymphocyte activation	15/226	155/16686	3,108E-07
GO:0006909	phagocytosis	19/226	274/16686	5,784E-07
GO:0051092	positive regulation of NF-kappaB transcription factor activity	14/226	144/16686	8,384E-07
GO:0042742	defense response to bacterium	20/226	315/16686	9,342E-07
GO:0002443	leukocyte mediated immunity	23/226	415/16686	9,342E-07

Table 6: 30 most significative biological processes enriched in the comparison LAA vs CE

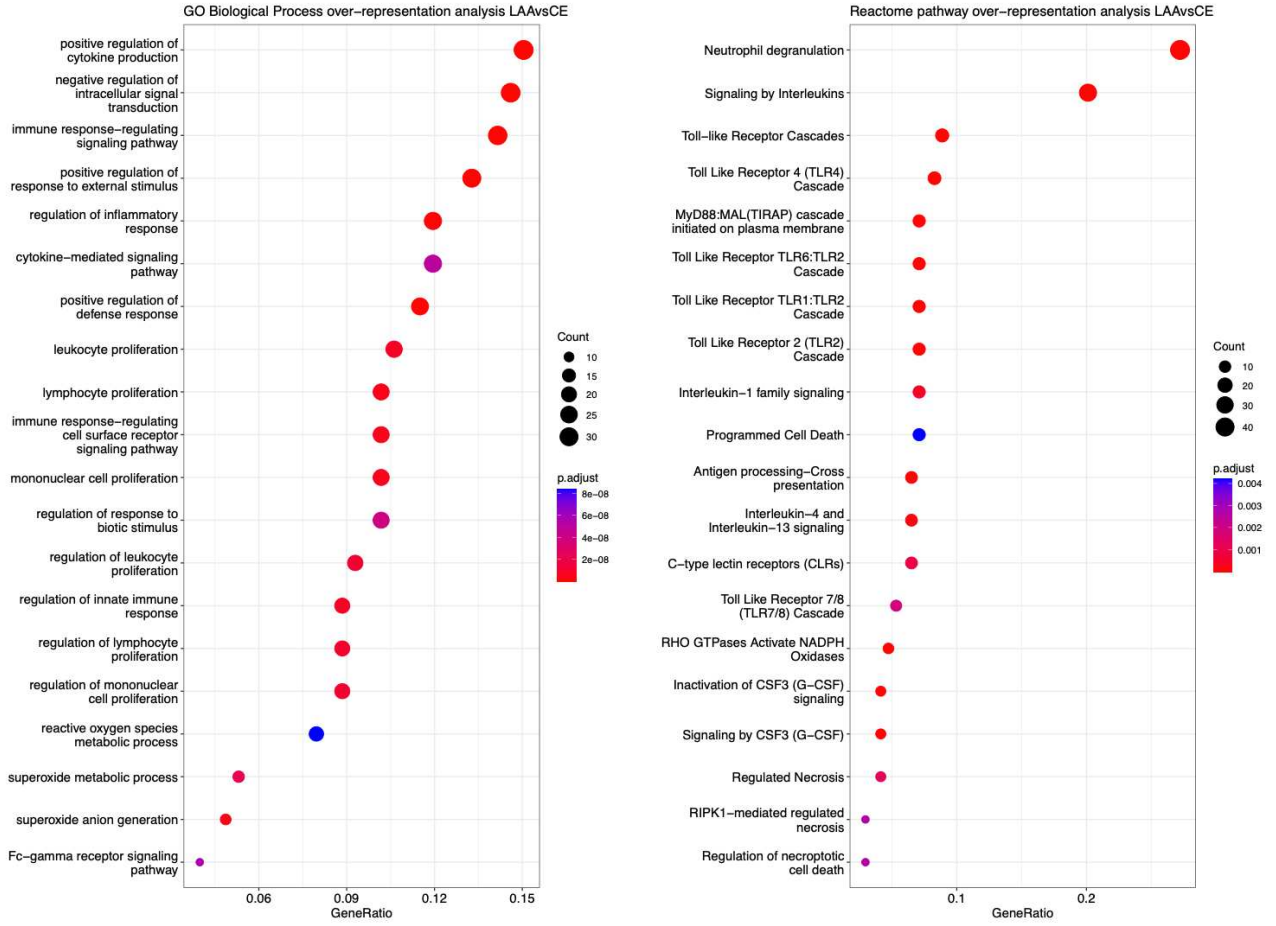

Figure 38: Dotplots of the gene ontology-biological process terms (GO-BP) and Reactome terms overrepresented in LAA vs CE comparison. The y-axis represents the significant GO terms with the higher proportion of DEG of the set involved, and the gene ratio in the x-axis represents these proportions (number of DEG involved in each GO term or Reactome term over the total number of DEG in the set). The size of each dot or gene cluster depends on the gene count that contributes to the enrichment of that pathway, and the adjusted p-value obtained for the terms with the Fisher's exact test in ORA determines the color of the dots.

The application of the Netplot function within the ClusterProfiler package has emerged as a pivotal tool for visualizing enriched term networks derived from Gene Ontology (GO) and Reactome analysis. This sophisticated function is meticulously designed to generate visually informative network plots, providing an intuitive representation of intricate relationships among enriched terms. Netplot operates by creating network plots wherein each node signifies a distinct biological term, and edges establish connections between terms sharing common genes. This graph-based representation enables the identification of clusters comprising closely related terms, facilitating the discernment of overarching thematic associations. The function serves as a powerful tool for translating complex enrichment results into visually accessible representations Enriched terms were organized into a network with edges connecting overlapping gene sets. In this way, mutually overlapping gene sets tend to cluster together, making it easy to identify functional modules. The category net plot depicts the linkages of genes and GO terms and

Reactome terms as a network, which is helpful to see which genes are involved in enriched pathways and genes that may belong to multiple annotation categories (Tzeng CM et al, 2016).

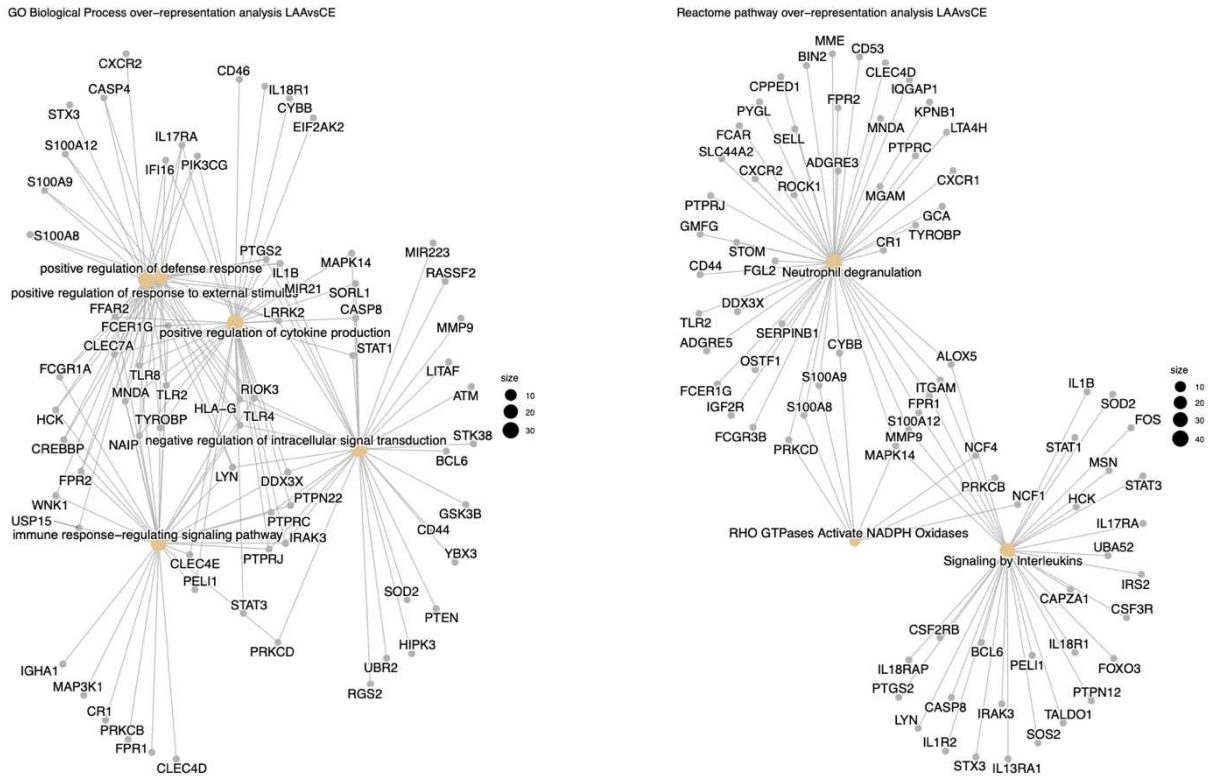

Figure 39: Gene-concept network (cnetplot) of overlapping DEG. It shows the enriched concepts, GO biological processes and Reactome pathways in LAA vs CE comparison and the relation between them when genes are involved in more than one process. The size of the concept nodes depends on the gene count involved in that pathway or process.

B) LARGE ARTERY ATHEROSCLEROTIC vs CRYPTOGENIC STROKE

In the comparative analysis between LAA and CRYPTO, a discerning examination revealed a total of 188 biological processes that demonstrated statistically significant enrichment (table below and Table 5 and 6 in supplementary materials). Significantly, a noteworthy overlap in enriched processes emerged, observed both in the LAA vs CRYPTO comparison and the previously mentioned comparison with CE. Identical processes exhibited significant enrichment in both scenarios, indicating a consistent pattern. This exceptional consistency across multiple comparative analyses attests to the robustness and reproducibility of the identified enriched biological processes. The recurrent observation of these enriched processes across distinct comparisons not only substantiates their statistical significance but also underscores their potential functional importance in distinguishing molecular signatures between LAA and CRYPTO. This reaffirms the reliability and validity of the analytical outcomes, providing a foundation for confident interpretations in the broader context of stroke subtypes.

ID	Description	GeneRatio	BgRatio	p. adjust
GO:1902532	negative regulation of intracellular signal transduction	27/155	492/16686	2,77E-10
GO:0070663	regulation of leukocyte proliferation	19/155	255/16686	3,64E-09
GO:0050670	regulation of lymphocyte proliferation	18/155	225/16686	3,64E-09
GO:0001819	positive regulation of cytokine production	24/155	460/16686	4,52E-09
GO:0072593	reactive oxygen species metabolic process	17/155	207/16686	4,95E-09
GO:0046651	lymphocyte proliferation	19/155	288/16686	1,12E-08
GO:0070661	leukocyte proliferation	20/155	330/16686	1,19E-08
GO:0043065	positive regulation of apoptotic process	24/155	498/16686	1,19E-08
GO:0032943	mononuclear cell proliferation	19/155	295/16686	1,19E-08
GO:0002683	negative regulation of immune system process	22/155	418/16686	1,43E-08
GO:1903706	regulation of hemopoiesis	21/155	385/16686	1,94E-08
GO:0071900	regulation of protein serine/threonine kinase activity	20/155	353/16686	2,69E-08
GO:0002764	immune response-regulating signaling pathway	22/155	441/16686	3,14E-08
GO:0045088	regulation of innate immune response	16/155	221/16686	5,19E-08
GO:2000379	positive regulation of reactive oxygen species metabolic process	10/155	64/16686	6,65E-08
GO:0032103	positive regulation of response to external stimulus	21/155	438/16686	1,23E-07
GO:0050866	negative regulation of cell activation	15/155	208/16686	1,56E-07
GO:0030595	leukocyte chemotaxis	15/155	217/16686	2,68E-07
GO:0002831	regulation of response to biotic stimulus	18/155	334/16686	2,77E-07
GO:0007159	leukocyte cell-cell adhesion	19/155	393/16686	5,31E-07
GO:0009620	response to fungus	9/155	61/16686	5,31E-07
GO:0002696	positive regulation of leukocyte activation	19/155	406/16686	8,15E-07
GO:0031349	positive regulation of defense response	16/155	285/16686	1,01E-06
GO:0030099	myeloid cell differentiation	18/155	376/16686	1,23E-06
GO:0010950	positive regulation of endopeptidase activity	12/155	160/16686	2,46E-06
GO:0045936	negative regulation of phosphate metabolic process	18/155	406/16686	3,07E-06
GO:0051348	negative regulation of transferase activity	14/155	245/16686	4,42E-06
GO:0019221	cytokine-mediated signaling pathway	19/155	469/16686	4,67E-06
GO:1901216	positive regulation of neuron death	9/155	89/16686	8,07E-06
GO:0002274	myeloid leukocyte activation	13/155	228/16686	1,14E-05
GO:1903037	regulation of leukocyte cell-cell adhesion	16/155	358/16686	1,22E-05

Table 7: 30 most significative biological processes enriched in the comparison LAA vs Cryptogenic

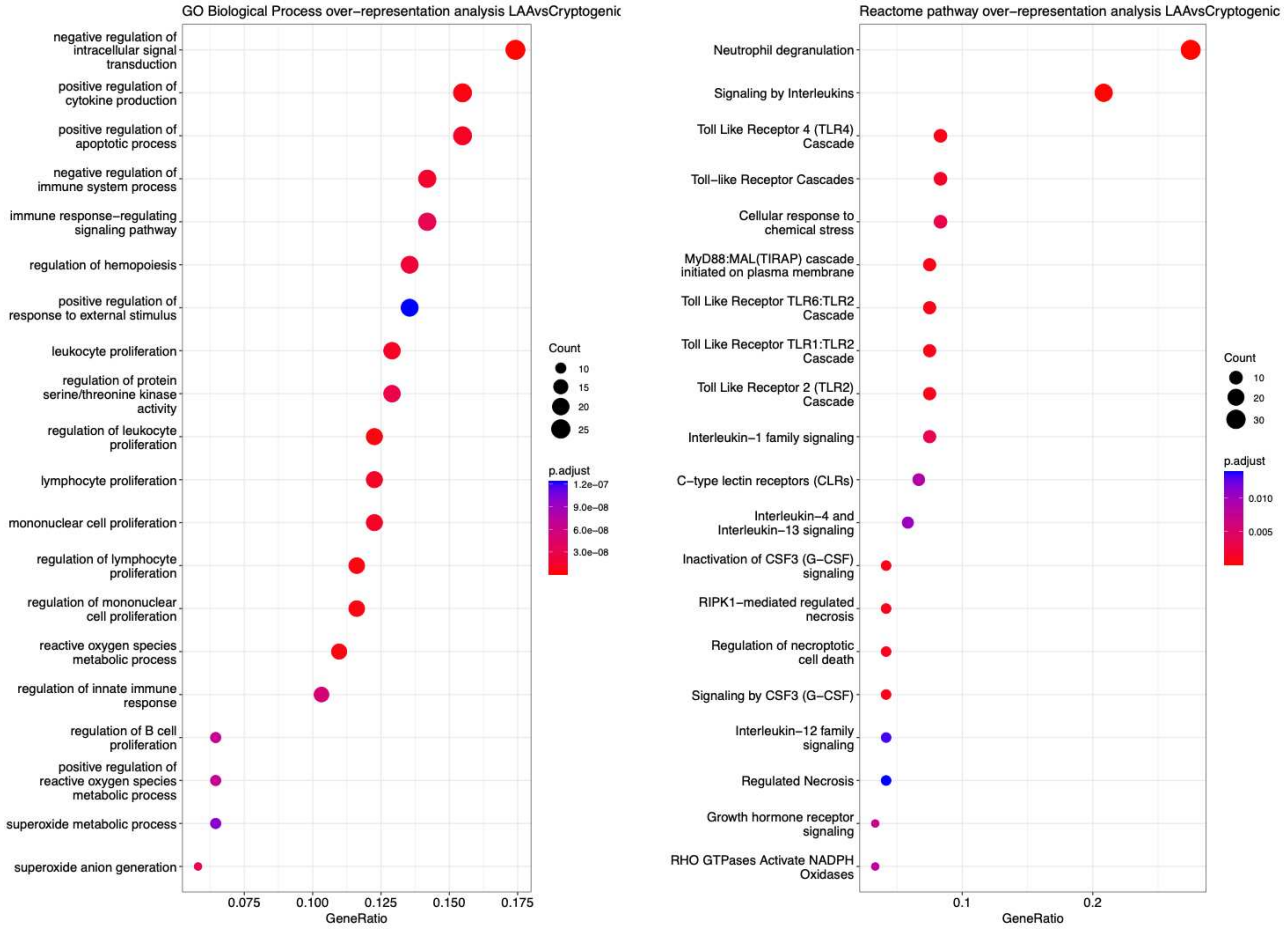

Figure 40: Dotplots of the gene ontology-biological process terms (GO-BP) and Reactome terms overrepresented in LAA vs CRYPTO comparison. The y-axis represents the significant GO terms with the higher proportion of DEG of the set involved, and the gene ratio in the x-axis represents these proportions (number of DEG involved in each GO term or Reactome term over the total number of DEG in the set). The size of each dot or gene cluster depends on the gene count that contributes to the enrichment of that pathway, and the adjusted p-value obtained for the terms with the Fisher's exact test in ORA determines the color of the dots.

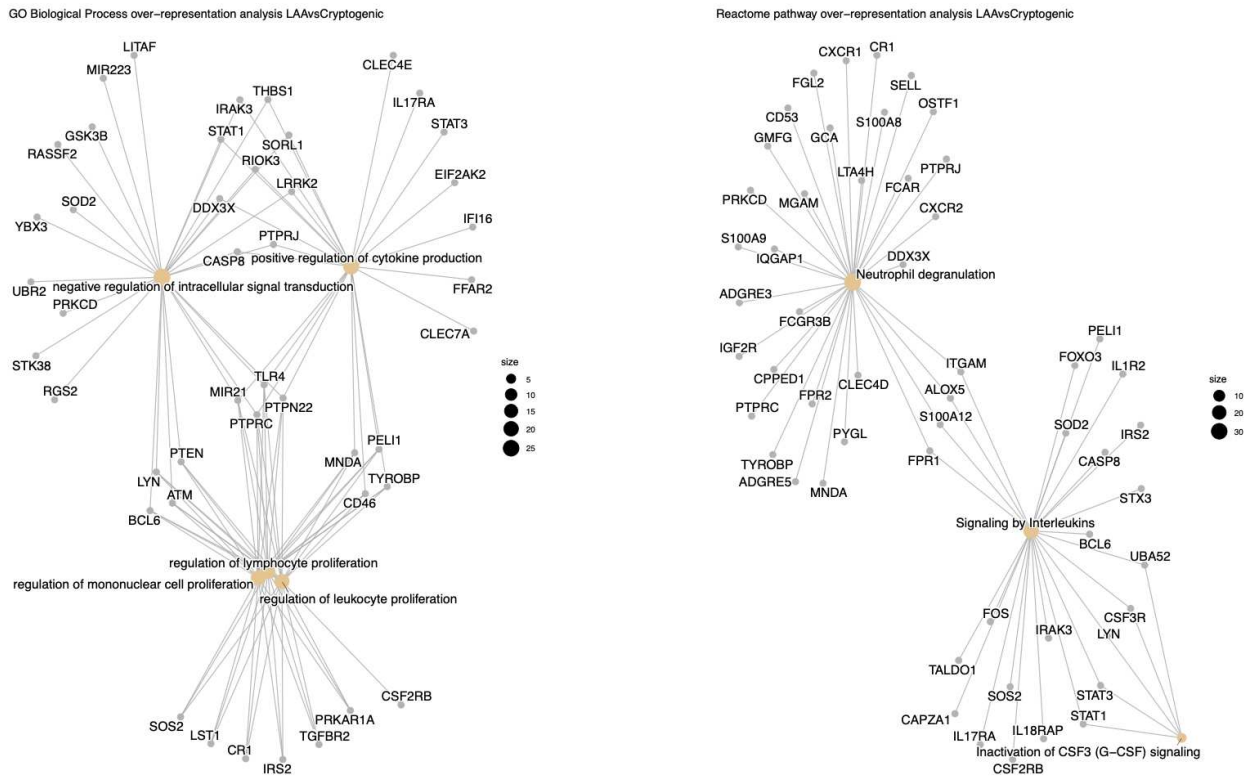

Figure 41:Gene-concept network (cnetplot) of overlapping DEG. It shows the enriched concepts, GO biological processes and Reactome pathways in LAA vs CRYPTO comparison and the relation between them when genes are involved in more than one process. The size of the concept nodes depends on the gene count involved in that pathway or process.

C) OTHER COMPARISONS

Following a meticulous examination, gene expression profiling analysis in PB did not reveal any significant differences based on the TOAST classification or other clinical endpoints. The absence of noteworthy findings accentuates the distinctiveness of molecular signatures associated with clot subtypes and prompts inquiries into the distinctive regulatory mechanisms orchestrating gene expression within varied blood compartments.

CHAPTER 8

DISCUSSION AND CONCLUSIONS

Mechanical thrombectomy (MT) stands out as a powerful and immediate avenue for the analysis of numerous aspects of cerebral thrombus, in particular in situ RNA analyses, offering a real-time opportunity to delve into the intricate processes of ischemia in the brain. This procedure provides researchers with a unique window to directly observe and capture the ongoing molecular changes associated with AIS. The immediate and direct retrieval of intracranial thrombus during MT is particularly crucial, as it allows for the extraction of RNA from the exact location affected by the stroke without any delays. This capability provides a snapshot of the dynamic molecular alterations occurring in real-time, offering researchers an unprecedented opportunity to focus specifically on the RNA expression profile within the region affected by the stroke. This precision is essential for a comprehensive understanding of the molecular events at the site of injury.

In contrast to post-mortem tissue analysis, which may be influenced by various factors, MT preserves the integrity of the tissue. This preservation ensures that the obtained RNA is a faithful reflection of the actual in vivo conditions during the acute phase of ischemia. Our research group, along with others, has been motivated to explore the characteristics of CT to deepen our understanding of the pathophysiological mechanisms underlying ischemic stroke. Furthermore, our research endeavors aim to highlight specific transcriptomic traits associated with different stroke subtypes. By meticulously analyzing the RNA expression profiles obtained CT, we seek to discern unique molecular signatures linked to distinct ischemic stroke subtypes. This detailed transcriptomic analysis is anticipated to provide valuable insights that can facilitate the accurate diagnosis of specific stroke subtypes, predict patient outcomes, and inform the selection of tailored therapeutic strategies.

The identification of subtype-specific transcriptomic traits holds the potential to revolutionize our approach to ischemic stroke management. It can contribute to a more precise and personalized understanding of the underlying molecular mechanisms driving each subtype. This, in turn, may enable clinicians to make informed decisions regarding the most effective therapeutic interventions for individual patients based on the molecular characteristics of their stroke. Ultimately, our research aims to advance the field by offering a foundation for the development of targeted therapies and improved prognostic tools, thereby enhancing patient care in the realm of ischemic stroke.

Notably, only two groups, including Fraser and colleagues (2019) and Tutino VM and team (2022), have applied a similar approach in humans. Fraser's group developed a tissue banking protocol using MT to capture thrombus samples along with arterial blood both proximal and distal to it.

Their protocol yielded sufficient tissue for subsequent gene expression and proteomics analyses. Tutino VM's group conducted a gene expression analysis from CT scans obtained from patients with AIS, utilizing RNA sequencing (RNAseq) technology. This concerted effort represents a pioneering approach to gaining comprehensive insights into the molecular landscape of ischemic stroke, paving the way for potential breakthroughs in therapeutic interventions.

Despite facing challenges posed by the critical nature of the study material, including RNA with a highly unstable structure prone to degradation and the presence of advanced necrosis and apoptosis in the cerebral thrombus due to ischemic damage, we successfully conducted a comprehensive analysis of global gene expression profiles. We achieved this through the use of Affymetrix microarray technology, chosen for its ability to deliver optimal and suitable results for advanced bioinformatic analyses, even when dealing with materials that are typically hard to analyze.

In our study project, our main goal was to identify genes that exhibit differential expression when comparing the transcriptomic profiles of two distinct conditions, specifically related to different stroke subtypes. This approach allowed us to draw attention to and emphasize those genes that experience a more pronounced impact during the occurrence of the ischemic event. Additionally, these genes may be linked to unique mechanisms characteristic of a particular subtype of stroke. In this specific analysis, we compared the gene expression profiles derived from RNA samples collected from 5 patients with LAA stroke subtypes to those from 21 patients with CE stroke. The results revealed a notable overexpression of 301 genes specifically in the atherosclerotic stroke condition.

The initial observation from our analysis, reinforced by the Cibersort analysis, spotlights a robust activation of the immune response in the aftermath of the ischemic event. The standout observation is the marked surge in neutrophil percentages across all examined samples, underscoring the pivotal and nuanced role of neutrophils in the immune milieu during ischemia. This observation offers nuanced insights into the temporal dynamics and functions of neutrophils in the context of AIS. Neutrophils, also known as polymorphonuclear leukocytes, constitute a substantial portion of human white blood cells, ranging from 50% to 70% of leukocytes. These cells play a crucial role in the innate immune response and are continuously produced in the bone marrow through granulopoiesis, serving as the first line of defense under normal conditions. Neutrophils are short-lived, surviving approximately 10–18 hours in the bloodstream, during

which they actively engage in immune functions such as phagocytosis, granule production, degranulation, release of NETs, and generation of reactive species.

During their development in the bone marrow, neutrophils accumulate secretory and antimicrobial granules to be released upon encountering pathogens. They are also capable of forming NETs, which are extracellular fibers composed of DNA-histone complexes and antimicrobial granule proteins.

In the context of AIS, neutrophils play a dual role, exhibiting both beneficial and detrimental effects. While they are among the first responders to ischemic brain tissue, their functions, effective against pathogens, can also cause significant bystander tissue damage. Neutrophils increase in circulation as early as 4–6 hours after IS, migrating into the brain parenchyma after 6–8 hours. NETs are detected 2–3 days after a stroke, and neutrophils continue to circulate, peaking at 1–3 days, with expression still detectable after 7–15 days before declining (Zhang X et al, 2023). Post-ischemia, an influx of neutrophils could potentially lead to microcirculatory failure due to factors such as microvascular plugging, elevated blood viscosity, and increased vascular resistance. Neutrophil adhesion to the endothelium emerges as a potential contributor to stalls and blockage of erythrocyte movement, influencing infarct expansion. Higher neutrophil counts correlate with larger infarct volumes and poor clinical outcomes. Activated neutrophils release pro-inflammatory factors in and around the penumbra, destabilizing the BBB, damaging vasculature, and causing secondary tissue damage. Neutrophils can also contribute to hemorrhagic transformation through the overproduction of MMPs. The activation of neutrophils produces various factors, including prostaglandins and platelet-activating factors, leading to platelet aggregation, vasoconstriction, and flow stagnation. Infiltration of neutrophils into the parenchyma further amplifies the inflammatory response, perpetuating tissue damage through the continuous release of additional factors like ROS, cytokines, and proteases (An Bui T. et al, 2022).

Zooming into the mechanism of atherosclerosis and the potential role of neutrophils, existing studies emphasize the involvement of various cell types, including endothelial cells, smooth muscle cells, monocytes, macrophages, and T cells. Despite their crucial functions in immune responses, neutrophils have been relatively understudied in the context of atherosclerosis. Challenges in detection methods, the transient nature of neutrophils, and their ability to undergo phenotypic changes contribute to this research gap. Critically, neutrophil adhesion across

endothelial cells is identified as a key player in endothelial dysfunction, a reversible stage considered pivotal in the progression of atherosclerosis (Amini H et al, 2023).

Our data confirming and enlarging the role of neutrophils-mediated immunity and activation as determinants/markers of poor outcome and disability in our cohort open significant further work to improve knowledge on suggested mechanisms by the present work.

Our analysis reveals a robust association between the atherosclerotic subtype and distinctive gene expressions. The enriched processes are particularly notable, focusing on key aspects such as neutrophil degranulation and the initiation of the immune response. Going beyond this, a thorough scrutiny of individual genes exhibiting differential expression unravels a noteworthy overexpression pattern. Specifically, genes like MMP-9, IL-1β, S100A12, S100A8, and S100A9 demonstrate higher expression levels in the atherosclerotic subtype as opposed to the cardioembolic subtype.

In a more nuanced context, MMP-9 is notable for its involvement in the remodeling of the extracellular matrix, a process intricately linked to the progression of atherosclerosis. Numerous studies conducted on murine stroke models have consistently revealed heightened MMP9 expression, serving as an early indicator of injury and correlating with changes in the blood-brain barrier (BBB) and the onset of early vasogenic edema following transient focal cerebral ischemia. MMP9 plays a pivotal role in breaking down the basal lamina and components of the extracellular matrix (Turner RJ et al, 2016).

Significantly, MMP-9 levels in the peripheral blood of stroke patients peak 24 hours after admission. Substantiating this, another study has shown a correlation between MMP-9 levels and infarct volume, stroke severity, and functional outcomes. The expression of MMP-9 (within 3 hours) was up-regulated by 2.4-fold in participants with poor 90-day outcomes. This discovery aligns with other studies illustrating that elevated blood MMP-9 levels are associated with unfavorable outcomes 90 days after ischemic stroke (Turner RJ et al, 2016).

Moreover, MMP-9, abundantly present in neutrophil secondary and tertiary granules, plays crucial roles in matrix remodeling and is found in plaque shoulders and regions of foam cell deposition. These enzymes are released from activated neutrophils and cleave intact, nonfibrillar, and fragmented interstitial collagen, essential components of the subendothelial basement membrane. MMP9 has been widely acknowledged for its contribution to promoting plaque instability. Specifically, MMP-9 cleaves and enhances the chemotactic activity of CXCL1 and CXCL8, thereby amplifying leukocyte tissue infiltration. Additionally, neutrophil elastase activates MMP-

9, potentiating its activity. The overexpression of auto-activating pro-MMP-9 significantly diminishes plaque stability (Yang Y et al, 2015).

IL-1β, a pro-inflammatory cytokine associated with immune responses and inflammation, indicates a heightened immune reaction in the atherosclerotic subtype. The IL-1 superfamily, consisting of 11 cytokines and 10 receptors, tightly regulates immunity and inflammation. The chronic accumulation of lipids and immune cells in vessel walls leads to the formation of fibrolipidic plaques.

Within the IL-1 family, IL-1β and IL-18 play a crucial role in driving the athero-inflammatory process. IL-1α and IL-1β are involved in emergency hematopoiesis, responding to situations requiring increased production of hematopoietic cells. Unlike IL-1α, IL-1β is not constitutively expressed and is produced by specific cell types, including monocytes/macrophages and dendritic cells (Gonzàlez L et al, 2023).

IL-1β is expressed as an inactive precursor, activated in response to insults through a process called priming. Caspase-1, activated by the inflammasome, triggers the processing of the IL-1β precursor. Mature IL-1β, released through vesicles or pyroptosis, activates the IRAK pathway, leading to the production of downstream inflammatory mediators like IL-6.

IL-1 cytokines are implicated in the development of atherosclerosis, expressed in atherosclerotic plaques, mainly by macrophages. Local production of IL-1 cytokines impairs endothelial cell function, inducing oxidative stress and promoting atherothrombosis. Various mediators of atherosclerosis induce IL-1 cytokine expression, including oxidized LDL, necrosis, and apoptosis. Animal models support the role of IL-1α and IL-1β in atherogenesis. Mice lacking IL-1β develop smaller lesions, and neutralizing antibodies against IL-1β reduce lesion size. IL-1β directly activates endothelial cells, promoting leucocyte adherence and recruitment in atherosclerotic lesions. Disruption of IL-1β signaling decreases adhesion molecule and/or chemokine levels, indicating dampened leucocyte recruitment (Hettwer J et al, 2022).

Our study findings indicate the overexpression of interleukins, specifically IL-1β, in patients who have experienced LAA strokes. This supports the hypothesis that an increased expression of this pro-inflammatory cytokine is linked to a higher occurrence and instability of atherosclerotic plaques.

Our research findings revealed an increased expression of three specific genes, S100A12, S100A9 and S100A8. These genes have been previously linked in various studies to inflammatory

processes and activities associated with atherosclerosis mechanisms. This additional information serves to reinforce and validate the outcomes obtained in our study.

Calgranulins, including S100A12, S100A8, and S100A9, are members of the S100 protein family, known for their calcium-binding properties. These proteins are typically expressed in myeloid-derived cells like neutrophils, monocytes, and dendritic cells. However, recent studies indicate that these proteins may also be induced in non-myeloid cells such as endothelial cells and vascular smooth muscle cells (Zhang X et al 2020).

These calgranulins play crucial roles in inflammatory processes, and their increased expression is associated with heightened immune activity seen in atherosclerosis. In patients with carotid atherosclerosis, those experiencing recent symptoms exhibited elevated mRNA levels of S100A8, S100A9, and S100A12 within plaques compared to asymptomatic patients. Moreover, plasma levels of S100A12 were linked to clinically determined plaque instability.

S100A12 has multifaceted effects, including antimicrobial properties, and plays a vital role in the host's defense mechanisms. It activates receptors such as RAGE (receptor for advanced glycation end products) and toll-like receptor 4 (TLR4), initiating downstream signals involving NFκB, ERK1/2, MAPK, IL-1β, and IL-6. This intricate signaling cascade modulates immune responses and inflammation (Farokhzadian J et al, 2019) (Singh P et al, 2023).

Epidemiological data suggests a potential role for S100A12 in mediating plaque instability or acute myocardial infarction. Its upregulation in macrophages and smooth muscle cells was observed in ruptured atherosclerotic plaques, indicating involvement in sudden cardiac death. S100A12 remained associated with acute myocardial infarction and cardiovascular mortality, emphasizing its role in athero-thrombosis.

In a study conducted by Zhang X. et al in 2020, an ischemia/reperfusion (I/R) model was used to simulate interrupted blood flow and subsequent restoration. In this model, S100A12 expression significantly increased. Knockdown of S100A12 inhibited, while overexpression enhanced, the activation of the ERK1/2 protein. The ERK pathway, known for its role in cell proliferation, survival, and inflammation, was influenced by S100A12 modulation. Inhibition of ERK counteracted the effects of S100A12 overexpression, suggesting a potential regulatory role of S100A12 in inflammation and oxidative stress triggered by I/R, particularly through the ERK signaling pathway. Despite the complexity of calgranulin actions, the study supports their role as reliable markers of inflammation. Notably, S100A12 appears to reflect a broader spectrum of inflammatory pathways compared to its counterparts, S100A8 and S100A9. These findings suggest that S100A12 could be

investigated as a potential biomarker for atherosclerotic disease and plaque instability, providing valuable insights into the intricate mechanisms underlying these conditions.

Our focus turns towards the intricate world of MicroRNAs (miRNAs), a class of non-coding RNAs comprising approximately 20–25 nucleotides. Their profound impact on cellular remodeling processes is underscored by their unique ability to regulate gene expression at the post-transcriptional level. A pivotal study by Liu XS et al in 2013 unraveled the complexities of miRNA-mediated gene modulation, providing a foundational understanding of their regulatory prowess.

In the aftermath of ischemic events, a profound reshaping occurs within the cerebral miRNA landscape. Several studies led by Dharap A et al (2009) and Jeyaseelan K et al (2008) have illuminated these dynamic alterations, collectively known as the "miRNA-ome." Importantly, these modifications transcend being mere consequences; they are recognized as integral contributors to fundamental biological processes such as neurogenesis, angiogenesis, and neural plasticity. Further substantiating the potential of miRNAs, studies by Sun Y et al (2015) and Yang J et al (2017) suggest their innovative candidacy in gene therapy, particularly in the context of cerebral processes.

Expanding our exploration beyond cerebral functions, miRNAs have been implicated in the intricate tapestry of atherosclerosis. Their endogenous nature, coupled with their modest length, positions them as potent regulators of gene expression. Within the vascular domain, their critical role unfolds, exerting post-transcriptional repression and thereby influencing key aspects of vascular functions and the progression of atherosclerosis.

Crucially, miRNAs emerge as significant orchestrators in perpetuating chronic inflammation and activating macrophages—a hallmark of atherosclerosis. These intrinsic regulators contribute to a nuanced and highly regulated network underpinning the complex pathophysiology of atherosclerosis. Evidence indicating the intricate link between miRNA target genes and chronic inflammation and macrophage activation underscores the multifaceted roles these molecules play in the intricate tapestry of atherosclerotic processes.

In our investigation, a notable overexpression of miR-223 was observed in patients with LAA stroke. A retrospective case-control study by Chen Y et al (2017) delved into the detection of exosomal miR-223 expression levels in stroke patients and non-stroke subjects. The results suggest that circulating exosomal miR-223 expression may serve as a potential risk factor for stroke. In particular, the overexpression of miR-223 in lesional areas is associated with decreased foam cell formation, lipid accumulation, and proinflammatory cytokine production—indicating

that miR-223 plays a role in reducing atherosclerosis through multiple pathways. The underlying mechanism of these functions may involve the activation of the PI3K/AKT pathway, thereby attenuating inflammation (Jiang Q et al, 2022).

While the intricate mechanisms of miRNA action in atherosclerosis warrant further investigation, they serve as a valuable starting point for understanding the complex interplay, particularly in the context of ischemic events and cerebral processes. The multifaceted roles of miRNAs in regulating gene expression, influencing vascular functions, and modulating the intricate pathophysiology of atherosclerosis make them intriguing candidates for future therapeutic interventions and a deeper comprehension of disease processes.

In comparing the list of genes found to be overexpressed in patients with significant differences in expression, what stood out was that there was a notable overlap in the biological processes that were enriched (activated or heightened) in LAA patients compared to both CE and cryptogenic stroke patients. This overlap pointed to a strong association between processes related to an increased immune response mediated by neutrophils and the presence of atherosclerotic conditions. This finding aligns with existing evidence in scientific literature and suggests a clear link between immune response, neutrophils, and atherosclerosis. However, this observation requires further detailed studies for a more comprehensive understanding.

In contrast, looking at other comparisons, such as between other stroke subtypes, or in peripheral blood samples, there were no significant differences in gene expression. This lack of difference could be attributed to the relatively small size of the patient group and the uneven distribution of patients among different stroke categories.

It's important to note that the gene expression analysis was performed on samples of PB taken during the acute phase of the stroke event. This timing is crucial because it's likely that various mechanisms responding to ischemic damage might not have fully activated yet at this early stage. To deepen our understanding, we could extend the study to investigate gene expression differences at various time points after the acute event. This extended analysis could reveal significant variations in gene expression related to different stroke subtypes, potentially leading to the identification of new and specific biomarkers associated with distinct stroke types and outcomes.

AIS remains an intricate, multifactorial disorder that demands a comprehensive exploration of its underlying mechanisms. Despite existing therapeutic modalities, the need persists for tailored

interventions, nuanced to individual patients, considering their unique clinical histories and characteristics.

The advent of MT has ushered in a new era in stroke research, enabling a more profound investigation of this condition. The adoption of a transcriptomic approach, unraveling the gene expression profiles of patients, emerges as a significant resource. This methodology offers the potential to elucidate the intricate interplay between gene patterns and the complex pathophysiology of AIS.

By scrutinizing these gene expressions, we have identified specific genes whose dysregulation is intricately linked to ischemic events. These genes serve as promising starting points for further exploration, as they may harbor the potential to function as diagnostic biomarkers, revolutionizing our approach to stroke diagnostics.

However, our scientific inquiry extends beyond mere identification; it involves a meticulous examination of stroke subtypes. Recognizing the distinctive features of each subtype becomes paramount, paving the way for the development of innovative, tailored therapeutic interventions. This envisioning of therapies customized for specific stroke categories marks a paradigm shift in stroke management.

In essence, the AIS narrative unfolds as an ongoing scientific saga. Each exploration of its molecular intricacies and the discernment of subtype-specific characteristics propels us closer to groundbreaking therapeutic strategies and a more profound comprehension of this complex cerebrovascular event.

BIBLIOGRAPHY

Abbas, Azhar, Pål Aukrust, Tuva B. Dahl, Vigdis Bjerkeli, Ellen B. Lund Sagen, Annika Michelsen, David Russell, et al 2012. “High Levels of S100A12 Are Associated With Recent Plaque Symptomatology in Patients With Carotid Atherosclerosis.” Stroke 43 (5): 1347–53. https://doi.org/10.1161/STROKEAHA.111.642256.

Adams, H P, B H Bendixen, L J Kappelle, J Biller, B B Love, D L Gordon, and E E Marsh. 1993. “Classification of Subtype of Acute Ischemic Stroke. Definitions for Use in a Multicenter Clinical Trial. TOAST. Trial of Org 10172 in Acute Stroke Treatment.” Stroke 24 (1): 35–41. https://doi.org/10.1161/01.STR.24.1.35.

Ai, Yong, Xudong Zhang, Xudong Hu, Jinte Gao, Jiyuan Liu, Shaowu Ou, and Jun Wang. 2023. “Role of the Voltage-gated Sodium Channel Nav1.6 in Glioma and Candidate Drugs Screening.” International Journal of Molecular Medicine 51 (6): 46. https://doi.org/10.3892/ijmm.2023.5249.

Al-Amrani, Safa, Zaaima Al-Jabri, Adhari Al-Zaabi, Jalila Alshekaili, and Murtadha Al-Khabori. 2021. “Proteomics: Concepts and Applications in Human Medicine.” World Journal of Biological Chemistry 12 (5): 57–69. https://doi.org/10.4331/wjbc.v12.i5.57.

Aliena-Valero, Alicia, Júlia Baixauli-Martín, Germán Torregrosa, José I. Tembl, and Juan B. Salom. 2021. “Clot Composition Analysis as a Diagnostic Tool to Gain Insight into Ischemic Stroke Etiology: A Systematic Review.” Journal of Stroke 23 (3): 327–42. https://doi.org/10.5853 /jos.2021.02306.

Alkarithi, Ghadir, Cédric Duval, Yu Shi, Fraser L. Macrae, and Robert A.S. Ariëns. 2021. “Thrombus Structural Composition in Cardiovascular Disease.” Arteriosclerosis, Thrombosis, and Vascular Biology 41 (9): 2370–83. https://doi.org/10.1161/ATVBAHA.120.315754.

Amini, Hajar. 2023. “Early Peripheral Blood Gene Expression Associated with Good and Poor 90-Day Ischemic Stroke Outcomes.”

Baysoy, Alev, Zhiliang Bai, Rahul Satija, and Rong Fan. 2023. “The Technological Landscape and Applications of Single-Cell Multi-Omics.” Nature Reviews Molecular Cell Biology 24 (10): 695–713. https://doi.org/10.1038/s41580-023-00615-w.

Benjamini, Yoav, and Yosef Hochberg. 1995. “Controlling the False Discovery Rate: A Practical and Powerful Approach to Multiple Testing.” Journal of the Royal Statistical Society. Series B (Methodological) 57 (1): 289–300.

Boehme, Amelia K., Charles Esenwa, and Mitchell S.V. Elkind. 2017. “Stroke Risk Factors, Genetics, and Prevention.” Circulation Research 120 (3): 472–95. https://doi.org/10.1161 /CIRCRESAHA.116.308398.

Bui, Truong An, Glen C. Jickling, and Ian R. Winship. 2022. “Neutrophil Dynamics and Inflammaging in Acute Ischemic Stroke: A Transcriptomic Review.” Frontiers in Aging Neuroscience 14 (December): 1041333. https://doi.org/10.3389/fnagi.2022.1041333.

Chellan, Bijoy, Nadia R. Sutton, and Marion A. Hofmann Bowman. 2018. “S100/RAGE-Mediated Inflammation and Modified Cholesterol Lipoproteins as Mediators of Osteoblastic Differentiation of Vascular Smooth Muscle Cells.” Frontiers in Cardiovascular Medicine 5 (November): 163. https://doi.org/10.3389/fcvm.2018.00163.

Chen, Chongyang, Jing Wang, Donghui Pan, Xinyu Wang, Yuping Xu, Junjie Yan, Lizhen Wang, Xifei Yang, Min Yang, and Gong-Ping Liu. 2023. “Applications of Multi-omics Analysis in Human Diseases.” MedComm 4 (4): e315. https://doi.org/10.1002/mco2.315.

Chen, Shiyu, Liuwang Zeng, and Zhiping Hu. 2014. “Progressing Haemorrhagic Stroke: Categories, Causes, Mechanisms and Managements.” Journal of Neurology 261 (11): 2061–78. https://doi.org/10.1007/s00415-014-7291-1.

Chen, Yajing, Yaying Song, Jun Huang, Meijie Qu, Yu Zhang, Jieli Geng, Zhijun Zhang, Jianrong Liu, and Guo-Yuan Yang. 2017. “Increased Circulating Exosomal miRNA-223 Is Associated with Acute Ischemic Stroke.” Frontiers in Neurology 8 (February). https://doi.org/10.3389 /fneur.2017.00057.

Christiansen, Spencer D. n.d. “Ischemic Stroke Thrombus Characterization through Quantitative Magnetic Resonance Imaging.”

Ciarambino, Tiziana, Pietro Crispino, Erika Mastrolorenzo, Antonello Viceconti, and Mauro Giordano. 2022. “Stroke and Etiopathogenesis: What Is Known?” Genes 13 (6): 978. https://doi.org/10.3390/genes13060978.

Coelho, Luís Guilherme Bastos Silva Aguiar, José Manuel Dias Costa, and Elsa Irene Peixoto Azevedo Silva. 2016. “Non-Aneurysmal Spontaneous Subarachnoid Hemorrhage: Perimesencephalic versus Non-Perimesencephalic.” Revista Brasileira de Terapia Intensiva 28 (2). https://doi.org/10.5935/0103-507X.20160028.

Colliot, Olivier, ed. 2023. Machine Learning for Brain Disorders. Vol. 197. Neuromethods. New York, NY: Springer US. https://doi.org/10.1007/978-1-0716-3195-9.

Costamagna, Gianluca, Sara Bonato, Stefania Corti, and Megi Meneri. 2023. “Advancing Stroke Research on Cerebral Thrombi with Omic Technologies.” International Journal of Molecular Sciences 24 (4): 3419. https://doi.org/10.3390/ijms24043419.

Craven, Kelly E., Yesim Gökmen-Polar, and Sunil S. Badve. 2021. “CIBERSORT Analysis of TCGA and METABRIC Identifies Subgroups with Better Outcomes in Triple Negative Breast Cancer.” Scientific Reports 11 (1): 4691. https://doi.org/10.1038/s41598-021-83913-7.

Dai, Xiaofeng, and Li Shen. 2022. “Advances and Trends in Omics Technology Development.” Frontiers in Medicine 9 (July): 911861. https://doi.org/10.3389/fmed.2022.911861.

DeLong, Jonathan Howard, Sarah Naomi Ohashi, Kevin Charles O’Connor, and Lauren Hachmann Sansing. 2022. “Inflammatory Responses After Ischemic Stroke.” Seminars in Immunopathology 44 (5): 625–48. https://doi.org/10.1007/s00281-022-00943-7.

Desilles, Jean-Philippe, Lucas Di Meglio, Francois Delvoye, Benjamin Maïer, Michel Piotin, Benoît Ho-Tin-Noé, and Mikael Mazighi. 2022. “Composition and Organization of Acute Ischemic Stroke Thrombus: A Wealth of Information for Future Thrombolytic Strategies.” Frontiers in Neurology 13 (July): 870331. https://doi.org/10.3389/fneur.2022.870331.

Di Meglio, Lucas, Jean-Philippe Desilles, Véronique Ollivier, Mialitiana Solo Nomenjanahary, Sara Di Meglio, Catherine Deschildre, Stéphane Loyau, et al 2019. “Acute Ischemic Stroke Thrombi Have an Outer Shell That Impairs Fibrinolysis.” Neurology 93 (18). https://doi.org/10.1212/WNL.0000000000008395.

Dumitriu LaGrange, Daniela, Philippe Reymond, Olivier Brina, Robert Zboray, Antonia Neels, Isabel Wanke, and Karl-Olof Lövblad. 2023. “Spatial Heterogeneity of Occlusive Thrombus in Acute Ischemic

Stroke: A Systematic Review." Journal of Neuroradiology 50 (3): 352–60. https://doi.org/10.1016/j.neurad.2023.01.004.

Endres, Matthias, Maria A. Moro, Christian H. Nolte, Claudia Dames, Marion S. Buckwalter, and Andreas Meisel. 2022. "Immune Pathways in Etiology, Acute Phase, and Chronic Sequelae of Ischemic Stroke." Circulation Research 130 (8): 1167–86. https://doi.org/10.1161 /CIRCRESAHA.121.319994.

Fitzgerald, Seán, Rosanna Rossi, Oana Madalina Mereuta, Duaa Jabrah, Adaobi Okolo, Andrew Douglas, Sara Molina Gil, et al 2021. "Per-Pass Analysis of Acute Ischemic Stroke Clots: Impact of Stroke Etiology on Extracted Clot Area and Histological Composition." Journal of NeuroInterventional Surgery 13 (12): 1111–16. https://doi.org/10.1136/neurintsurg-2020-016966.

Fitzgerald, Seán, Rosanna Rossi, Oana Madalina Mereuta, Sara Molina, Adaobi Okolo, Andrew Douglas, Duaa Jabrah, et al 2021. "Large Artery Atherosclerotic Clots Are Larger than Clots of Other Stroke Etiologies and Have Poorer Recanalization Rates." Journal of Stroke and Cerebrovascular Diseases 30 (1): 105463. https://doi.org/10.1016 /j.jstrokecerebrovasdis.2020.105463.

Ghozy, Sherief, Abdullah Reda, Joseph Varney, Ahmed Sallam Elhawary, Jaffer Shah, Kimberly Murry, Mohamed Gomaa Sobeeh, et al 2022. "Neuroprotection in Acute Ischemic Stroke: A Battle Against the Biology of Nature." Frontiers in Neurology 13 (May): 870141. https://doi.org /10.3389/fneur.2022.870141.

Gigliotti, Michael J., Shwetha Srikanth, and Kevin M. Cockroft. 2022. "Patterns of Prophylactic Anticonvulsant Use in Spontaneous Intracerebral and Subarachnoid Hemorrhage: Results of a Practitioner Survey." Neurological Sciences 43 (3): 1873–77. https://doi.org/10.1007 /s10072-021-05588-2.

González, Leticia, Katherine Rivera, Marcelo E. Andia, and Gonzalo Martínez Rodriguez. 2022. "The IL-1 Family and Its Role in Atherosclerosis." International Journal of Molecular Sciences 24 (1): 17. https://doi.org/10.3390/ijms24010017.

Greco, Antonio, Giovanni Occhipinti, Daniele Giacoppo, Federica Agnello, Claudio Laudani, Marco Spagnolo, Maria Sara Mauro, et al 2023. "Antithrombotic Therapy for Primary and Secondary Prevention of Ischemic Stroke." Journal of the American College of Cardiology 82 (15): 1538–57. https://doi.org/10.1016/j.jacc.2023.07.025.

"Guidelines for the Management of Spontaneous Intracerebral Hemorrhage." n.d. Hettwer, Jan, Julia Hinterdobler, Benedikt Miritsch, Marcus-André Deutsch, Xinghai Li, Carina

Mauersberger, Aldo Moggio, et al 2022. "Interleukin-1β Suppression Dampens Inflammatory Leucocyte Production and Uptake in Atherosclerosis." Edited by Ziad Mallat. Cardiovascular Research 118 (13): 2778–91. https://doi.org/10.1093/cvr/cvab337.

Huang, Joanna C., and Sonu M. M. Bhaskar. 2022. "Clot Morphology in Acute Ischemic Stroke Decision Making." International Journal of Molecular Sciences 23 (20): 12373. https://doi.org /10.3390/ijms232012373.

Hund, Hajo M., Nikki Boodt, Daniel Hansen, Willem A. Haffmans, Geert J. Lycklama À Nijeholt, Jeannette Hofmeijer, Diederik W. J. Dippel, et al 2023. "Association between Thrombus Composition and Stroke Etiology in the MR CLEAN Registry Biobank." Neuroradiology 65 (5): 933–43. https://doi.org/10.1007/s00234-023-03115-y.

Imran, Rajeel, Ghada A Mohamed, and Fadi Nahab. 2021. "Acute Reperfusion Therapies for Acute Ischemic Stroke." Journal of Clinical Medicine 10 (16): 3677. https://doi.org/10.3390 /jcm10163677.

Karenberg, Axel. 2020. "Historic Review: Select Chapters of a History of Stroke." Neurological Research and Practice 2 (1): 34. https://doi.org/10.1186/s42466-020-00082-0.

Khoshnam, Seyed Esmaeil, William Winlow, Maryam Farzaneh, Yaghoob Farbood, and Hadi Fathi Moghaddam. 2017. "Pathogenic Mechanisms Following Ischemic Stroke." Neurological Sciences 38 (7): 1167–86. https://doi.org/10.1007/s10072-017-2938-1.

Lapchak, Paul A, and Dalia M Araujo. 2007. "Advances in Hemorrhagic Stroke Therapy: Conventional and Novel Approaches." Expert Opinion on Emerging Drugs 12 (3): 389–406. https://doi.org/10.1517/14728214.12.3.389.

Laskowitz, Daniel T., and Brad J. Kolls. 2010. "Neuroprotection in Subarachnoid Hemorrhage." Stroke 41 (10_suppl_1). https://doi.org/10.1161/STROKEAHA.110.595090.

Lee, Eun Chae, Tae Won Ha, Dong-Hun Lee, Dong-Yong Hong, Sang-Won Park, Ji Young Lee, Man Ryul Lee, and Jae Sang Oh. 2022. "Utility of Exosomes in Ischemic and Hemorrhagic Stroke Diagnosis and Treatment." International Journal of Molecular Sciences 23 (15): 8367.

https://doi.org/10.3390/ijms23158367.

Li, Wentao, Chongyu Shao, Huifen Zhou, Haixia Du, Haiyang Chen, Haitong Wan, and Yu He. 2022. “Multi-Omics Research Strategies in Ischemic Stroke: A Multidimensional Perspective.” Ageing Research Reviews 81 (November): 101730. https://doi.org/10.1016/j.arr.2022.101730. Lowe,

Rohan, Neil Shirley, Mark Bleackley, Stephen Dolan, and Thomas Shafee. 2017. “Transcriptomics Technologies.” PLOS Computational Biology 13 (5): e1005457. https://doi.org /10.1371/journal.pcbi.1005457.

Macrae, Fraser L., Cédric Duval, Praveen Papareddy, Stephen R. Baker, Nadira Yuldasheva, Katherine J. Kearney, Helen R. McPherson, et al 2018. “A Fibrin Biofilm Covers Blood Clots and Protects from Microbial Invasion.” Journal of Clinical Investigation 128 (8): 3356–68. https://doi.org /10.1172/JCI98734.

Magid-Bernstein, Jessica, Romuald Girard, Sean Polster, Abhinav Srinath, Sharbel Romanos, Issam A. Awad, and Lauren H. Sansing. 2022. “Cerebral Hemorrhage: Pathophysiology, Treatment, and Future Directions.” Circulation Research 130 (8): 1204–29. https://doi.org/10.1161 /CIRCRESAHA.121.319949.

Miceli, Giuseppe, Maria Grazia Basso, Giuliana Rizzo, Chiara Pintus, Elena Cocciola, Andrea Roberta Pennacchio, and Antonino Tuttolomondo. 2023. “Artificial Intelligence in Acute Ischemic Stroke Subtypes According to Toast Classification: A Comprehensive Narrative Review.” Biomedicines 11 (4): 1138. https://doi.org/10.3390/biomedicines11041138.

Mosconi, Maria Giulia, and Maurizio Paciaroni. 2022. “Treatments in Ischemic Stroke: Current and Future.” European Neurology 85 (5): 349–66. https://doi.org/10.1159/000525822.

Newman, Aaron M., Chloé B. Steen, Chih Long Liu, Andrew J. Gentles, Aadel A. Chaudhuri, Florian Scherer, Michael S. Khodadoust, et al 2019. “Determining Cell Type Abundance and Expression from Bulk Tissues with Digital Cytometry.” Nature Biotechnology 37 (7): 773–82. https://doi.org /10.1038/s41587-019-0114-2.

O'Connell, Grant C., and Julia H.C. Chang. 2018. "Analysis of Early Stroke-Induced Changes in Circulating Leukocyte Counts Using Transcriptomic Deconvolution." Translational Neuroscience 9 (1): 161–66. https://doi.org/10.1515/tnsci-2018-0024.

Ojaghihaghighi, Seyedhossein, Samad Shams Vahdati, Akram Mikaeilpour, and Ali Ramouz. 2017. "Comparison of Neurological Clinical Manifestation in Patients with Hemorrhagic and Ischemic Stroke." World Journal of Emergency Medicine 8 (1): 34. https://doi.org/10.5847 /wjem.j.1920-8642.2017.01.006.

Potter, Thomas B. H., Jonika Tannous, and Farhaan S. Vahidy. 2022. "A Contemporary Review of Epidemiology, Risk Factors, Etiology, and Outcomes of Premature Stroke." Current Atherosclerosis Reports 24 (12): 939–48. https://doi.org/10.1007/s11883-022-01067-x.

Pu, Liyuan, Li Wang, Ruijie Zhang, Tian Zhao, Yannan Jiang, and Liyuan Han. 2023. "Projected Global Trends in Ischemic Stroke Incidence, Deaths and Disability-Adjusted Life Years From 2020 to 2030." Stroke 54 (5): 1330–39. https://doi.org/10.1161/STROKEAHA.122.040073.

Qian, Yu. 2020. "Emerging Role of microRNAs in Ischemic Stroke with Comorbidities." Experimental Neurology.

Qin, Chuan, Sheng Yang, Yun-Hui Chu, Hang Zhang, Xiao-Wei Pang, Lian Chen, Luo-Qi Zhou, Man Chen, Dai-Shi Tian, and Wei Wang. 2022. "Signaling Pathways Involved in Ischemic Stroke: Molecular Mechanisms and Therapeutic Interventions." Signal Transduction and Targeted Therapy 7 (1): 215. https://doi.org/10.1038/s41392-022-01064-1.

Schlunk, Frieder, Johannes Kuthe, Peter Harmel, Heinrich Audebert, Uta Hanning, Georg Bohner, Michael Scheel, Justus Kleine, and Jawed Nawabi. 2022. "Volumetric Accuracy of Different Imaging Modalities in Acute Intracerebral Hemorrhage." BMC Medical Imaging 22 (1): 9. https://doi.org/10.1186/s12880-022-00735-3.

Servushan, Pasderhsh. 2023. "Next-Generation Sequencing Technologies: Revolutionizing Genomic Analysis." Preprint. Open Science Framework. https://doi.org/10.31219/osf.io/4q8c9.

Siniscalchi, Antonio. 2022. “Use of Stroke Scales in Clinical Practice: Current Concepts.” Turkish Journal of Emergency Medicine 22 (3): 119. https://doi.org/10.4103/2452-2473.348440. Stokes, Tanner, Haoning Howard Cen, Philipp Kapranov, Iain J Gallagher, Andrew A. Pitsillides,

Claude-Henry Volmar, William E Kraus, et al 2023. “Transcriptomics for Clinical and Experimental Biology Research: Hang on a Seq.” Advanced Genetics 4 (2): 2200024. https://doi.org/10.1002/ggn2.202200024.

Tutino, Vincent M, Sarah Fricano, Aichi Chien, Tatsat R Patel, Andre Monteiro, Hamid H Rai, Adam A Dmytriw, et al 2023. “Gene Expression Profiles of Ischemic Stroke Clots Retrieved by Mechanical Thrombectomy Are Associated with Disease Etiology.” Journal of NeuroInterventional Surgery 15 (e1): e33–40. https://doi.org/10.1136/neurintsurg-2022-018898.

Tutino, Vincent M., Sarah Fricano, Kirsten Frauens, Tatsat R. Patel, Andre Monteiro, Hamid H. Rai, Muhammad Waqas, Lee Chaves, Kerry E. Poppenberg, and Adnan H. Siddiqui. 2021. “Isolation of RNA from Acute Ischemic Stroke Clots Retrieved by Mechanical Thrombectomy.” Genes 12 (10): 1617. https://doi.org/10.3390/genes12101617.

Wei, Liming, Yueqi Zhu, Jiangshan Deng, Yuehua Li, Minghua Li, Haitao Lu, and Yuwu Zhao. 2021. “Visualization of Thrombus Enhancement on Thin-Slab Maximum Intensity Projection of CT Angiography: An Imaging Sign for Predicting Stroke Source and Thrombus Compositions.” Radiology 298 (2): 374–81. https://doi.org/10.1148/radiol.2020201548.

Wolf, M. E., T. Sauer, A. Alonso, and M. G. Hennerici. 2012. “Comparison of the New ASCO Classification with the TOAST Classification in a Population with Acute Ischemic Stroke.” Journal of Neurology 259 (7): 1284–89. https://doi.org/10.1007/s00415-011-6325-1.

Wu, Tianzhi, Erqiang Hu, Shuangbin Xu, Meijun Chen, Pingfan Guo, Zehan Dai, Tingze Feng, et al 2021. “clusterProfiler 4.0: A Universal Enrichment Tool for Interpreting Omics Data.” The Innovation 2 (3): 100141. https://doi.org/10.1016/j.xinn.2021.100141.

Xiong, Yunyun, Ajay K. Wakhloo, and Marc Fisher. 2022. “Advances in Acute Ischemic Stroke Therapy.” Circulation Research 130 (8): 1230–51. https://doi.org/10.1161 /CIRCRESAHA.121.319948.

Yan, Honglin, Wenxian Huang, Jie Rao, and Jingping Yuan. n.d. “miR-21 Regulates Ischemic Neuronal Injury via the P53/Bcl-2/Bax Signaling Pathway.”

Yang, Xiao-Li, De-Sheng Zhu, Hui-Hui Lv, Xin-Xin Huang, Yan Han, Shuai Wu, and Yang-Tai Guan. 2019. “Etiological Classification of Cerebral Ischemic Stroke by the TOAST, SSS-TOAST, and ASCOD Systems: The Impact of Observer’s Experience on Reliability.” The Neurologist 24 (4): 111–14. https://doi.org/10.1097/NRL.0000000000000236.

Yang, Xitong, Pengyu Wang, Shanquan Yan, and Guangming Wang. 2022. “Study on Potential Differentially Expressed Genes in Stroke by Bioinformatics Analysis.” Neurological Sciences 43 (2): 1155–66. https://doi.org/10.1007/s10072-021-05470-1.

Yu, Guangchuang, Li-Gen Wang, Guang-Rong Yan, and Qing-Yu He. 2015. “DOSE: An R/Bioconductor Package for Disease Ontology Semantic and Enrichment Analysis.” Bioinformatics 31 (4): 608–9. https://doi.org/10.1093/bioinformatics/btu684.

Yuan, Mei, Yi-Sha Guo, Xin-Xin Zhang, Zhen-Kun Gao, Xin-Ya Shen, Yu Han, and Xia Bi. n.d. “Diagnostic Performance of miR-21, miR-124, miR-132, and miR-200b Serums in Post-Stroke Cognitive Impairment Patients.” Folia Neuropathologica.

Zhai, Hu, Chunyan Peng, and Tong Li. 2022. “Human Plasma Transcriptome Implicates Dysregulated S100A12 Expression: A Strong, Early-Stage Prognostic Factor in ST-Segment Elevated Myocardial Infarction: Bioinformatics Analysis and Experimental Verification.” Frontiers in Cardiovascular Medicine 9.

Zhang, Xiang, Rui Shen, Zhongwen Shu, Quanbin Zhang, and Zuoquan Chen. 2020. “S100A12 Promotes Inflammation and Apoptosis in Ischemia/Reperfusion Injury via ERK Signaling in Vitro Study Using PC12 Cells.” Pathology International 70 (7): 403–12. https://doi.org/10.1111 /pin.12924.

Zhou, Yue, Yiwen Zha, Yongqi Yang, Tan Ma, Hongliang Li, and Jingyan Liang. 2023. “S100 Proteins in Cardiovascular Diseases.” Molecular Medicine 29 (1): 68. https://doi.org/10.1186 /s10020-023-00662-1.